METHODS IN THE MEASUREMENT OF BIOMECHANICAL RESPONSE TO MODIFICATIONS IN FOOTWEAR DESIGN

By

Jerrod E. Braman

A THESIS

Submitted to
Michigan State University
in partial fulfillment of the requirements
for the degree of

MASTER OF SCIENCE

Engineering Mechanics

2010

ABSTRACT

METHODS FOR MEASURING BIOMECHANICAL CHANGES DUE TO MODIFICATIONS IN FOOTWEAR MIDSOLE CHARACTERISTICS

By

Jerrod E. Braman

Orthopaedic problems can be caused or accentuated by both normal and abnormal gait characteristics. Traditionally, footwear modifications and orthotic interventions have been limited to internal and external wedges and other assorted orthotics. This thesis will discuss various methods to measure biomechanical responses of human subjects in response to changes in footwear design. Chapter 1 provides an overview of what is currently known regarding interventions in relation to providing medial compartment knee osteoarthritis relief as well as limiting excessive rear-foot motion. Chapter 2 discusses a method for measuring the center of pressure in multiple steps using an insole pressure measurement system and evaluating the effect that varying midsole stiffness has on the center of pressure. Chapter 3 presents a dynamic segmental model for knee adduction moment measurements and how a full lateral stiffened shoe and five other prototype shoes with varying midsole stiffness change that moment in healthy subjects. Chapter 4 presents a method for measuring rear-foot motion and evaluates a new footwear technology designed to reduce excessive rear-foot motion. Chapter 5 is a summation of the thesis and recommendations for future studies. The information in this thesis could be helpful in providing strategies for changing location and stiffness values of footwear midsoles to elicit positive biomechanical responses in human subjects during gait.

ACKNOWLEDGMENTS

I would first like to thank Dr. Roger C. Haut for direction, support, and patience through the past five years. I would not be where I am now without his help. I would also like to thank Dr. Dianne Ulibarri for guiding me to the field of biomechanics. This research would not be possible without the technical help from Clifford Beckett. In addition, I would like to thank Dr. John Powell for his guidance and Dr. Tamara Reid-Bush for sitting on my committee. I also want to thank my wife, Leah, for her support and being so understanding and patient throughout this whole process. My family also deserves thanks, as they have always given their support through the good times and the tough times. In addition, I would like to thank Wolverine World Wide, Inc. for providing the footwear used for this research. Last but not least, I would like to thank all of my friends and fellow students that have helped me through this journey.

TABLE OF CONTENTS

LIST OF TABLES

LIST OF FIGURES

CHAPTER 1 – INTRODUCTION

Gait is the pattern of movement of the limbs during locomotion. Orthopaedic problems can be caused or accentuated due to both abnormal and normal gait. The knee is an especially susceptible joint where injury and other orthopaedic problems can manifest due to gait characteristics. Specifically, the knee joint is susceptible to degeneration of cartilage, commonly referred to as osteoarthritis. Other lower limb problems have been linked to the problem of excessive pronation, a common gait abnormality. Traditionally, footwear modifications have been limited to internal and external wedges and other assorted orthotics. This introduction will discuss methods that have been used to delay the onset or slow the progression of osteoarthritis by attempting to modify knee adduction moments. There will also be a discussion of some of the issues related to excessive foot pronation and the methods used in an attempt to limit such rotations.

Knee Joint

Osteoarthritis of the knee joint can be caused or accelerated by gait. According to Mow and Huiskes, osteoarthritis is characterized by a breakdown of articular cartilage (Mow and Huiskes 2005). The knee can be divided into medial and lateral compartments, which are on the inside and outside of the knee, respectively. Knee osteoarthritis occurs in about 10% of adults after the age of 55 (Davis 1988). Within this group, osteoarthritis occurs in the medial compartment almost 10 times as frequent as in the lateral compartment (Ahlback 1968). One mechanism that is associated with the onset or progression of osteoarthritis is that of an abnormally large adduction moment (Fisher, Dyrby et al. 2007). Approximately 60% to 80% of the load transmitted to the knee goes through the medial compartment and is largely due to this moment (Crenshaw, Pollo et al. 2000). It has also been suggested that there is a correlation between the intensity of the knee adduction moment and the severity of medial compartment disease (Ueda, Dyrby et al. 2003). The severity of osteoarthritis can be measured several different ways, but the Kellgren-Lawrence scale is the most common method. The Kellgren-Lawrence scale has five separate descriptive categories of a joint based on radiological features that help quantify the severity of osteoarthritis. These five radiological features are listed below (Kellgren and Lawrence 1957).

1) The formation of osteophytes on the joint margins or, in the case of the knee joint, on tibial spines.
2) Periarticular ossicles; these are found largely in relation to the distal and proximal interphalangeal joints.
3) Narrowing of joint cartilage associated with sclerosis of subchondral bone.
4) Small pseudocystic areas with sclerotic walls situated usually in the subchondral bone.
5) Altered shape of the bone ends, particularly in the head of the femur.

The five categories of osteoarthritis based on these features are as follows: (0) None; (1) Doubtful; (2) Minimal; (3) Moderate; (4) Severe. A radiologist would classify an individual into one of these five categories based on an x-ray of the affected area.

A knee adduction moment is centered at the knee joint and oriented in the coronal plane. This concept is illustrated in Figure 1.1. There have been numerous studies to investigate the efficacy of different adduction moment reducing techniques for either placating existing medial compartment osteoarthritis or delaying its onset. These methods include surgical and non-surgical interventions. The surgical methods include a high-tibial osteotomy or total knee replacement. The high-tibial osteotomy is an invasive surgery in which a wedge of bone is taken out of the tibia in order to redistribute the forces through the knee. Due to the nature of the surgery, a long recovery period ensues following this operation. Bracing devices, such as canes or crutches, may be necessary for up to 10 weeks post-surgery. This bracing is in addition to the rehabilitation that is necessary. A total knee replacement is used in cases where there is little or no cartilage left on the end of the bones.

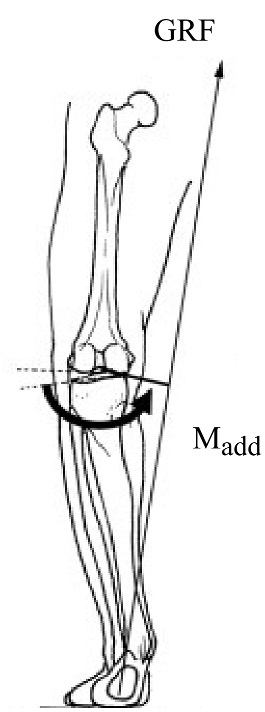

Figure 1.1 – Illustration of the orientation of a knee adduction moment. View is of a left leg in a posterior orientation. GRF stands for ground reaction force and M_{add} stands for the adduction moment.

Less invasive methods have been proposed, primarily in the last 20 years, to provide an alternative to the surgical approaches such as a high-tibial osteotomy or knee replacement. The use of orthotics and other non-surgical interventions have been shown to decrease the knee adduction moments. For example, Yasuda and Sasaki measured the change in position of the center of gravity between barefoot and with a wooden lateral wedge with an incline of 5 degrees placed under the entire foot (Yasuda and Sasaki 1987). The findings of this study suggest a more conservative method of decreasing static medial knee compressive loads. The explanation for this effect was that the calcaneus becomes more valgus when the lateral wedge is used. This is in addition to a more vertical angle of the lower limb mechanical axis. This change in mechanical axis would cause a decrease in the adduction moment at the knee due to a shorter moment arm between the knee joint center and the ground reactive force vector. Figure 1.2 describes this change in spatial relation of the "extended mechanical axis of the lower limb" with and without the use of the lateral wedge. The extended mechanical axis is the line drawn from the center of the femoral head to the point of heel strike contact on the calcaneus. It should be noted that the angle between the femur and the tibia and fibula complex does not change – only the angle of the calcaneus becomes more valgus to impart the change in angle.

Yasuda and Sasaki (1987) also noted that a change in the tibiofemoral angle does not need to occur in order for a decrease in adduction moment. The other suggested method for a reduction in adduction moment occurs with a lateral shift in the origin of the ground reaction force, causing the force to pass closer to the center of the knee joint.

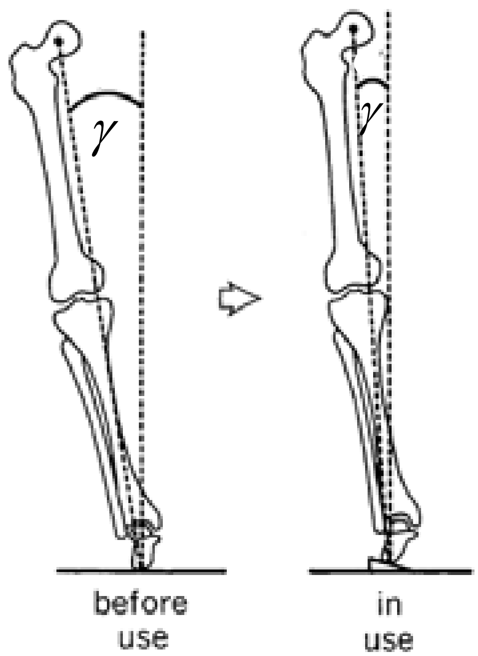

Figure 1.2 – Yasuda and Sasaki diagram for spatial changes in the calcaneus leading to an angular decrease in the extended mechanical axis due to orthotic use

There have been several studies trying to quantify the effect of the lateral wedge orthotic. The experiments have largely been designed to quantify the benefits of the lateral wedge orthotic for people who already have knee osteoarthritis (Kerrigan, Lelas et al. 2002). Yet, there have also been studies on people who do not have any symptoms of knee osteoarthritis (Crenshaw, Pollo et al. 2000; Kakihana, Akai et al. 2004; Fisher, Dyrby et al. 2007). There has also been reseach investigating the role of orthotics during running and other sporting activities in healthy subjects (Nigg, Nurse et al. 1999; Mundermann, Nigg et al. 2003; Nigg, Stergiou et al. 2003) or injured subjects (Kakihana, Torii et al. 2005). Kakihana et. al. (2005) “assessed the biomechanic effects of wearing a lateral wedge on the subtalar joint movement during gait in athletes with and without an unstable lateral ankle.” The focus of the study was to find the joint kinematic effects of a 6 degree full lateral wedge with the stable and unstable ankle. The authors document a decrease in knee adduction moment in the 50 male athletes studied, regardless of their subtalar stability status. In addition, they also made note of a lateral shift in the center of pressure. It was noted that the origin of the ground reaction force vector was shifted lateral when using the 6 degree full lateral wedge as compared to a zero degree platform during dynamic walking trials. This lateral center of pressure shift coupled with a decrease in adduction moment is important to note because it supports the method of adduction moment reduction put forth by Yasuda and Sasaki (1987).

Nigg et. al. also performed experiments to find kinematic, center of pressure, and leg joint moment responses to flat, half- and full-medial and half- and full-lateral orthotics (Nigg, Stergiou et al. 2003). Data were collected from 15 healthy male subjects with no knee osteoarthritis. For the lateral wedge condition, the lateral height of the orthotic was 4.5 mm higher than the medial border. The opposite was true for the medial wedge. The authors document that the full lateral orthotics generated a statistically significant lateral shift in the center of pressure but not a consistent change in the adduction moment at the knee. In addition, no other insert condition significantly and consistently changed the center of pressure. The only significant finding with the full medial insole was an increase in the knee external rotation moment. The COP finding is consistent with Kakihana et al. (2004), but the authors suggested that the lateral COP shift using partial length orthotics was not highly correlated to a reduction in the knee adduction moment. They also state that the overall reactions to orthotics are often subject-specific effects and cannot be related to the general population.

The effectiveness of lateral wedged insoles has also been evaluated in people with knee osteoarthritis. One group tested the biomechanical efficacy of 5 and 10 degree lateral wedges in patients with at least a category 3 knee on the Kellgren-Lawrence scale (Kerrigan, Lelas et al. 2002). The authors document that the 10 degree lateral wedge decreases the peak adduction moment by 8%, while the 5 degree lateral wedge decreases the peak moment by 6%. In addition to these measurable changes, a comfort questionnaire was also given to the subjects. They found that even though the 10 degree lateral wedge was more effective at reducing peak knee adduction moment, the insert also provided a significant amount of discomfort. In essence, the subjects were trading discomfort at the knee for discomfort in the shoe. If the patient is unwilling to wear the orthotic, the benefit of decreasing the adduction moment is lost. This implies that in order for an orthotic intervention to be successful, it also must be comfortable.

In addition to studies being performed on athletes and persons with osteoarthritis, studies quantifying the effect of a lateral wedge in the general population have been documented in current literature. Crenshaw et al (2000) studied the effects of a lateral wedged insole in 17 healthy subjects. The study used a 5 degree full lateral orthotic in a velocity-controlled walking experiment. The results of their study suggest no change in joint angles at the ankle, knee, or hip and also no change in kinetics at the hip or ankle. The study documents a significant reduction in the external adduction moment at the knee joint. This study is important because it was the first to document the reduction of knee adduction moment in a healthy, non-athletic population with the use of a full lateral wedge orthotic.

Following Crenshaw et al (2000), Kakihana et al (2004) performed a study on healthy adults using full lateral wedged insoles. The authors' aim was to try and find a correlation between the decrease in knee adduction moment and the change in moment at the subtalar joint. The authors used 3 and 6 degree lateral wedged insoles on 10 healthy adults (5 male, 5 female). They document that the larger, 6 degree wedged insole intervention significantly decreases the knee adduction moment. The authors indicate that the decrease in knee adduction moment was most likely due to a lateral shift in the center of pressure. The lateral shift in pressure was found by measuring the increase in the length of the moment arm at the subtalar joint. From this finding, it was assumed that the more lateral location of the center of pressure caused a smaller distance of the moment arm at the knee joint in the adduction/abduction plane and subsequent reduction of the knee adduction moment.

Fisher et al (2007) also addressed the issue of reducing the knee adduction moment in healthy subjects with the use of an in-shoe intervention. In addition to the traditional lateral wedge, the authors proposed the use of a dual-density mid-sole with the lateral component of the mid-sole being stiffer than the medial half of the insole. A total of 14 subjects (9 male and 5 female) were used in the study. The intervention conditions tested in the study were a 4 degree full lateral wedge orthotic, an 8 degree full lateral wedge orthotic, a 120% lateral stiffness shoe (a shoe that is 20% stiffer in the lateral half than the medial half), and a 150% lateral stiffness shoe (a shoe that is 50% stiffer in the lateral half than the medial half). These four intervention conditions were compared to the personal walking shoes of each study participant. The authors report that there was a significant decrease in the knee adduction moment when using the 150% stiffness shoes, as well as the 4 and 8 degree full lateral wedge orthotics. The investigators also indicated that the 120% stiffness shoes show a statistical trend towards decreasing the moment. When the methods of reduction were compared, they document that the 8 degree full lateral wedge provides the largest reduction in adduction moment. As seen in a previous study, full lateral wedges with high degree values provide the most reduction in adduction moment, but they can also be uncomfortable. While the 150% stiffness shoe did not provide as much relief as the two wedged conditions, it may be a more effective way to decrease the knee adduction moment in patients without osteoarthritis because of the minimal impact on the subject. This use of variable density mid-sole characteristics is intriguing, but the tests in this study did not use production model shoes.

A second study was performed by this group using variable density midsole technology using subjects with medial compartment knee osteoarthritis (Erhart, Mundermann et al. 2008). Using a constant-stiffness shoe and a variable-stiffness intervention shoe, 79 subjects were tested at three different paces of walking gait – slow, self-selected, and fast. The variable stiffness shoe had a lateral half that was 1.3-1.5 times stiffer than the medial half. The Asker C values – a measure of material stiffness – for the medial half were 55$\pm$2, and the lateral half had values between 70-76$\pm$2. Subjects who were bilaterally affected with osteoarthritis were evaluated on the limb with the most pain, as subjectively determined by the subject. An inverse dynamics model was used with a six marker set and a force plate in order to determine kinetic and kinematic parameters. It was shown that the peak knee adduction moment was reduced at all speeds of walking, and the largest reduction in moment was found with an increase in gait velocity.

Lower Limb Problems Caused by Excessive Pronation

There are many possible problems throughout the body that originate at or around the ankle joint during gait. The focus of the studies here will be to discuss the role of excessive pronation as it relates to injury mechanisms. Excessive foot pronation has been proposed to increase the possibility for patellofemoral pain syndromes, shin splints, Achilles tendinitis, plantar fasciitis, and stress fractures (Nigg 2001). For purposes of this thesis, pronation and eversion motions were considered to be the same. In actuality, pronation is a complicated tri-planar motion that includes motion of the individual bones in the foot, while eversion is often considered to be only the rotation of the foot about its long axis. There have been several strategies proposed to change the degree of foot pronation.

One excessive pronation reduction method is taping. The low-dye arch support is one taping technique that is employed by athletic trainers as a method to reduce the amount of foot pronation (Schulthies and Draper 1995). Another commonly used method to control inversion or eversion of the foot is by the use of posting an insole or creating a custom-molded insole, making it biomechanically difficult for the wearer to pronate or supinate past a certain point of rotation. These in-shoe modifications are described in many articles (Stacoff, Reinschmidt et al. 2000; Mundermann, Nigg et al. 2003; Nigg, Stergiou et al. 2003; Kakihana, Akai et al. 2005; Kakihana, Torii et al. 2005).

In the Stacoff, et. al. (2000) study, five male subjects were outfitted with intracortical bone pins and tested in running sandals with different medial foot orthoses in an attempt to accurately measure skeletal motion during running. Reflective marker triads were attached to the pins for motion analysis as subjects ran across a forceplate. The three conditions tested were a neutral orthotic, a posterior medial orthotic, and an anterior medial orthotic. The posterior orthotic was designed to support the foot from the calcaneus to the medial malleolus, while the anterior orthotic supported the arch region of the foot. In each condition, support was created by posting or by a raised area in the orthotic. There was no difference in the reduction of eversion between the two insole conditions or between the posterior orthotic, the anterior orthotic, and the control insole. However, four of the five subjects did show a decrease in maximum foot eversion between 1 and 3 degrees, but because of only having a small subject pool the difference was not statistical.

Mundermann et. al. (2003) performed a study also using running sandals, but not bone pin arrays. Instead, 21 subjects (12 female, 9 male) had markers attached to the skin surrounding the calcaneus. Kinematic data were collected using a motion capture system and evaluated using a software program developed by the University of Calgary. Four different insole conditions were tested – a control insole, a full medial posted insole, a neutral custom-made shell, and a custom shell with full medial posting. They document that posting alone significantly reduces the amount of maximum eversion, while molding and posting and molding changes the amount of tibia rotation, but not the degree of foot eversion.

In addition to measuring moment and center of pressure data, the 2003 Nigg et. al. study evaluated 15 healthy male subjects while running in five different shoe configurations in terms of their capability to change the amount of foot inversion and eversion. One shoe insert was the unaltered insert that arrived with the shoe. The test conditions were full lateral, full medial, half lateral, and half medial posting. The half inserts were placed at the metatarsal region. Posting was 4.5 mm either medial or lateral. Kinetic and kinematic data were captured using a motion capture system and a force plate. An inverse dynamics method was used to calculate resultant joint moments. It was found that the full lateral insert condition increased the amount of initial foot inversion (1.8 $\pm$ 2.1 degrees), and the full medial insert condition decreased the maximum eversion position (-1.5 $\pm$ 1.3 degrees). In addition, the total eversion motion was larger in the full lateral (2.1 $\pm$ 1.7 degrees) and smaller in the full medial condition (-2.0 $\pm$ 1.5 degrees).

The first of two Kakihana et. al. studies (2004) assessed the kinetics and kinematics of 10 subjects (5 men, 5 women) while they walked in three different insole conditions – no wedge, a 3-degree lateral angle wedge, and a 6-degree lateral angle wedge. This study was unable to find a significant difference in the average pronation angle during the stance phase when comparing the 6-degree wedge with the no wedge condition.

The second Kakihana et. al. study (2005) was conducted with 50 males in the no wedge and 6-degree lateral wedge condition. In the subject population, 25 subjects were considered to have an unstable lateral ankle while the other 25 subjects were considered to be healthy controls. Once again, the amount of rotation was not significantly different between subject groups or between insole conditions. What the researchers did find, however, was that the subtalar joint moment in the frontal plane was different between the two different insole conditions for both subject populations.

Most of the studies mentioned above have had similar experimental designs and have used similar equipment. In general, a motion analysis system coupled with a force plate is used to properly calculate joint kinetics and kinematics. The use of retro-reflective marker sets coupled with extensive knowledge of normal body motion allows an investigator to determine and define motion of body segments with a high degree of accuracy. It has been shown that a full inverse dynamics approach is necessary to accurately calculate moments about joint centers (Winter 2005). Most studies have been performed using male rather than female subjects, or at least a majority of male subjects. Men and women differ anatomically, especially in the lower limbs. In general, women have a larger quadriceps angle (Q-angle) than men. This change in the mechanical axis of the lower limb, coupled with foot shape, could lead to a difference in the response to in-shoe interventions. It has also been documented that “female feet and legs are not simply scaled-down versions of male feet but rather differ in a number of shape characteristics, particularly the arch, the lateral side of the foot, the first toe, and the ball of the foot” (Wunderlich and Cavanagh 2001). With these concepts in mind, thesis objectives were set.

Thesis Objectives

The objectives of this thesis were threefold. The first objective was to determine if variable midsole density shoes could alter the foot center of pressure and pressure distribution patterns of healthy male and female subjects during gait. The second objective of this thesis was to determine if the knee adduction moment changes when wearing production model full lateral stiffened and experimental shoes with a stiffened medial heel and a changing location of a pocket of lateral stiffness in healthy subjects. The third objective of the thesis was to determine if a novel user-controlled footwear technology could alter the amount of rear-foot motion in healthy subjects.

REFERENCES

References

Ahlback, S. (1968). "Osteoarthrosis of the knee. A radiographic investigation." Acta Radiol Diagn (Stockh): Suppl 277:7-72.

Crenshaw, S. J., F. E. Pollo, et al. (2000). "Effects of lateral-wedged insoles on kinetics at the knee." Clin Orthop Relat Res(375): 185-92.

Davis, M. A. (1988). "Epidemiology of osteoarthritis." Clin Geriatr Med **4**(2): 241-55.

Erhart, J. C., A. Mundermann, et al. (2008). "A variable-stiffness shoe lowers the knee adduction moment in subjects with symptoms of medial compartment knee osteoarthritis." Journal of Biomechanics **41**: 2720-2725.

Fisher, D. S., C. O. Dyrby, et al. (2007). "In healthy subjects without knee osteoarthritis, the peak knee adduction moment influences the acute effect of shoe interventions designed to reduce medial compartment knee load." J Orthop Res **25**(4): 540-6.

Kakihana, W., M. Akai, et al. (2005). "Effects of laterally wedged insoles on knee and subtalar joint moments." Arch Phys Med Rehabil **86**(7): 1465-71.

Kakihana, W., M. Akai, et al. (2004). "Changes of joint moments in the gait of normal subjects wearing laterally wedged insoles." Am J Phys Med Rehabil **83**(4): 273-8.

Kakihana, W., S. Torii, et al. (2005). "Effect of a lateral wedge on joint moments during gait in subjects with recurrent ankle sprain." Am J Phys Med Rehabil **84**(11): 858-64.

Kellgren, J. H. and J. S. Lawrence (1957). "Radiological assessment of osteo-arthrosis." Ann Rheum Dis **16**(4): 494-502.

Kerrigan, D. C., J. L. Lelas, et al. (2002). "Effectiveness of a lateral-wedge insole on knee varus torque in patients with knee osteoarthritis." Arch Phys Med Rehabil **83**(7): 889-93.

Mow, V. C. and R. Huiskes (2005). Basic Orthopaedic Biomechanics and Mechano-Biology. Philadelphia, Lippincott Williams & Wilkins.

Mundermann, A., B. M. Nigg, et al. (2003). "Foot orthotics affect lower extremity kinematics and kinetics during running." Clin Biomech (Bristol, Avon) **18**(3): 254-62.

Nigg, B. M. (2001). "The role of impact forces and foot pronation: a new paradigm." Clin J Sport Med **11**(1): 2-9.

Nigg, B. M., M. A. Nurse, et al. (1999). "Shoe inserts and orthotics for sport and physical activities." Med Sci Sports Exerc **31**(7 Suppl): S421-8.

Nigg, B. M., P. Stergiou, et al. (2003). "Effect of shoe inserts on kinematics, center of pressure, and leg joint moments during running." Med Sci Sports Exerc **35**(2): 314-9.

Schulthies, S. and D. O. Draper (1995). "A Modified Low-Dye Taping Technique to Support the Medial Longitudinal Arch and Reduce Excessive Pronation." Journal of Athletic Training **30**(3): 3.

Stacoff, A., C. Reinschmidt, et al. (2000). "Effects of foot orthoses on skeletal motion during running." Clin Biomech (Bristol, Avon) **15**(1): 54-64.

Ueda, S., C. O. Dyrby, et al. (2003). Adduction Moment, Radiographic Disease Severity, and Pain in Osteoarthritis of the Knee. 2003 Summer Bioengineering Conference. Key Biscayne, Florida.

Winter, D. A. (2005). Biomechanics and Motor Control of Human Movement. Hoboken, John Wiley & Sons, Inc.

Wunderlich, R. E. and P. R. Cavanagh (2001). "Gender differences in adult foot shape: implications for shoe design." Med Sci Sports Exerc **33**(4): 605-11.

Yasuda, K. and T. Sasaki (1987). "The mechanics of treatment of the osteoarthritic knee with a wedged insole." Clin Orthop Relat Res(215): 162-72.

CHAPTER 2 – CENTER OF PRESSURE AND PRESSURE DISTRIBUTION PROFILES OF SUBJECTS WEARING VARIABLE MIDSOLE DENSITY FOOTWEAR

Introduction

The study of the use of in-shoe interventions such as orthotics or wedges to elicit a positive biomechanical response (e.g. gait correction) has its roots in basic studies starting in the late 20th century. Sasaki and Yasuda studied orthotics in the 1980's through the use of wedges to elicit a change in the gait of patients with problems in their lower limbs (Yasuda & Sasaki, 1987). The novel idea that a non-invasive alternative to surgery, a custom fit insert, could alleviate or mitigate joint pain and disease has become a routine method of treatment for many lower limb ailments. The static studies performed by Yasuda and Sasaki led to a number of questions related to the efficacy of this kind of cost effective intervention. With the advent of the digital age and better measurement equipment, researchers have taken on the task of thoroughly evaluating the performance of footwear interventions in people with and without lower limb problems such as osteoarthritis, excessive joint motion, and general pain.

It has been shown that the changes in the center of pressure can be related to changes in joint moments (Fuller, 1999; Kakihana, Akai et al., 2005; Xu, Akai, Kakurai, Yokota, & Kaneko, 1999). It has been suggested that these changes in joint moments could alleviate some lower limb problems (Crenshaw, Pollo, & Calton, 2000; Kerrigan et al., 2002; Yasuda & Sasaki, 1987). The center of pressure (COP) is defined as the location at which the resultant of the ground reaction forces can be statically placed at any point in time (Winter, 2005). The foot COP curve is a track showing the time history of the COP during a step. Several different types of foot orthotics have been shown to change the COP using different measurement tools. Force plates are sometimes used to measure the center of pressure (Kakihana, Akai, Yamasaki, Takashima, &

Nakazawa, 2004; Xu et al., 1999). The drawback to force plates is that these researchers are limited in the number of concurrent steps that can be studied using force plates. For example, if a laboratory employs two force plates, they are limited to two center of pressure plots per trial. In order to record multiple COP plots, a different device must be used. One such set of devices that can measure the COP are plantar pressure measurement systems.

In a 1992 paper by Rose, et. al., an FScan Pressure System was used to measure the effects of external heel wedges and their effects on plantar pressures and the center of pressure (Rose, Feiwell, & Cracchiolo, 1992). Eleven subjects (6 men, 5 women; age range 25-45 years) were tested in five conditions – no heel wedge, quarter-inch lateral heel wedge, quarter-inch medial heel wedge, half-inch lateral heel wedge, and a half-inch medial heel wedge. The authors found that the quarter-inch heel wedge did not significantly change the pressure distribution, while the half-inch lateral wedge decreased pressures under the third, fourth and fifth metatarsal heads, while increasing the pressure underneath the first and second metatarsal heads. In addition, the half-inch medial wedge significantly decreased the pressure under the first and second metatarsals but did not significantly increase the pressure under the third, fourth, and fifth metatarsals. The COP curves were shifted laterally when using the quarter- and half-inch medial heel wedge, while the shift was medial during the use of the two lateral wedge designs. The half-inch varieties of each wedge shifted the COP more than the quarter-inch wedge. The largest shifts were found in the midfoot and metatarsal regions, with little to no COP change in the heel area.

Xu, et. al. describe changes in the COP when using Thomas and reverse Thomas heel modifications in addition to a rocker bar that was placed in three different locations (Xu et al., 1999). A Thomas heel is an external medial heel wedge, and a reverse Thomas heel is an external lateral heel wedge. Twenty subjects (10 male, 10 female) participated in this study. It was found that when wearing a shoe with the Thomas heel, the COP was shifted towards the lateral border of the shoe when compared to the standard heel and the reverse Thomas heel shifted the COP towards the medial border of the shoe as compared to the standard heel. The COP lines were measured with a force plate and changes in the COP were made by finding the area between the COP line and the center line of the foot.

Shoe orthotics can also be placed in between the foot and the shoe – not just on the outside of the shoe. A 2003 Nigg article discussed the effect that different in-shoe orthotics had on the COP as compared to a neutral condition using a PEDAR plantar measurement system to measure the COP (Nigg et al., 2003). The researchers compared a neutral shoe condition to four different inserts – a medial forefoot wedge, lateral forefoot wedge, full length medial wedge, and a full length lateral wedge. Each posting was 4.5mm at its maximum height. The authors noted that the only consistent and statistical change in the COP occurred with the full lateral wedge. The shift of the COP was towards the lateral border with a full lateral wedge – the opposite effect of an externally applied lateral wedge. A separate group of researchers also found changes in the COP towards the side of posting.

A 2004 paper by Van Gheluwe and Danaberg also used a plantar pressure measurement system to measure changes in COP when using seven different medial and lateral heel and forefoot wedges (Van Gheluwe & Dananberg, 2004). Twenty-three subjects were tested using the Footscan measurement system to obtain COP and plantar pressure distribution data. The forefoot inserts were 3 degrees valgus, 3 degrees varus, and 6 degrees varus. The heel inserts were 4 degrees valgus, 4 degrees varus and 8 degrees varus. Valgus wedges are the same as lateral wedges, while varus wedges are analogous to medial wedges. These inserts were all compared to a neutral condition. It was noted that the varus (medial) wedge caused a medial shift in the area that it was designed to affect (forefoot or heel), while the valgus (lateral) wedge caused a lateral shift the same area. It was noted that the COP did not change in the region opposite where the wedge was located. This was also true for changes in pressure distribution. That is, the forefoot wedge conditions did not change the heel pressure distribution and the heel wedge conditions did not change the forefoot pressure distributions.

One drawback of using an internal or external foot orthotic is the potential for user discomfort. A research study noted that some patients would remove and discontinue the use of a wedge because of this discomfort, even knowing their pain may return (Kerrigan et al., 2002). This potential disadvantage of orthotics has led researchers to explore other options to change the lower body joint moments. One such alternative to a wedge is a variable stiffness midsole. To date, little is known about the effects on the COP when changing patterns and densities of midsole materials and if it has the same effect on COP as traditional orthotics.

For this study, the Parotec System, an in-shoe pressure measurement device, was used to collect plantar pressure data over a given time period. From this plantar pressure data, COP plots could be created. In order for the Parotec to effectively create the center of pressure plots, it needed to be accurate and its measures repeatable. A 2000 study by Chesnin et. al. took on the task of validating the Parotec in-shoe pressure measurement system by comparing the COP generated by the Parotec to the COP from an AMTI force plate. The study indicated that the Parotec COP data were highly correlated with the COP data generated by the force plate (Chesnin, Selby-Silverstein, & Besser, 2000). This result allowed for the use of the Parotec System to draw accurate conclusions about possible changes in the COP. Therefore, this section of the thesis will discuss the methods associated with an attempt to change the center of pressure by changing the midsole density characteristics of a production model shoe.

The various midsole configurations used in the current study were designed by Wolverine World Wide, Inc. for the purpose of altering the foot center of pressure lines and pressure profiles. One objective of their pattern designs was to try and keep the COP along the centerline of the shoe. In order to test these designs in production-type shoes, an in-shoe plantar pressure measurement system was used because of its ability to capture multiple steps as well as for its ease of tracking the COP line for comparison purposes.

Materials and Methods

Subjects

Six subjects (3 men and 3 women) were recruited from a local running club. The participants had no prior history of injury or surgery to the lower body and ran a minimum of 10 miles per week. The average age was 54.0 years for the men and 29.7 years for the women. The average height and weight for the men were 172.0 cm and 68.4 kg respectively, while the women's average height and weight were 161.7 cm and 55.3 kg respectively.

Table 2.1 – Subject Demographics

For interpretation of the references to color in this and all other figures, the reader is referred to the electronic version of this thesis

Subject Demographics		
Subject Code	Height (m)	Weight (kg)
M1	1.68	61.4
M2	1.73	62.5
M3	1.75	81.4
F1	1.63	56.8
F2	1.65	59.1
F3	1.57	50.0

Plantar Pressure Measurement System

The pressure profile and center of pressure data were collected using the Parotec System® plantar pressure measuring device (Paromed, Neubeurn, Germany; Figure 2.1). In this study, the pressure profile was determined as the average pressure of each sensor during each individual step. The Parotec insoles contain 24 silicon-filled bladders spaced across the plantar surface with each bladder containing a piezoresistive sensor. Data were collected at 120 Hz using a belt-mounted controller and recorded on a PCMCIA memory card. Following each test sequence the data were transferred to a personal computer and analyzed with Parotec system software version 4.02.

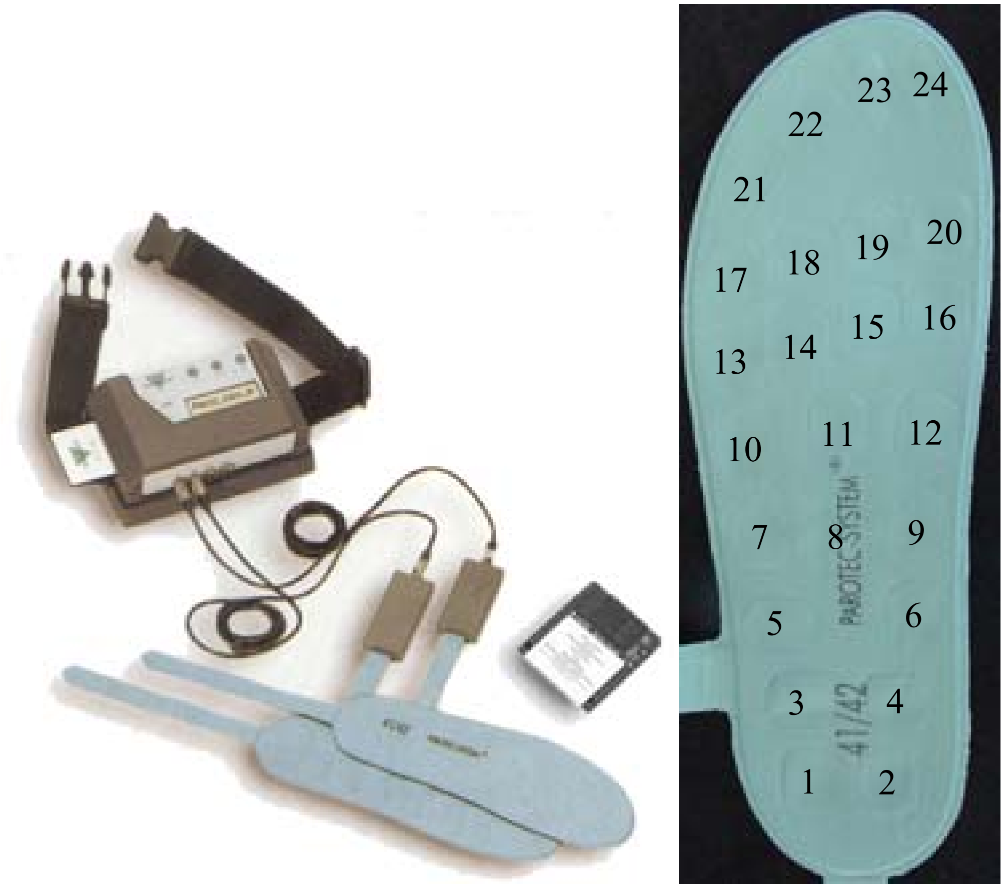

Figure 2.1 – The Parotec System and a sample insole

Footwear

The shoes were specially designed for these tests, but they were production-quality footwear based on the Merrell Full Pursuit trail running shoe (Figure 2.2). Six pairs of US men's size 9 shoes and six pairs of US women's size 8 shoes were used in the study. Each pair of shoes had a different midsole configuration (i.e. the stiffness of the midsole varied at different locations across the plantar surface of the shoe). Each midsole had varying densities of ethylene vinyl acetate (EVA). The Asker C scale was used to determine the hardness of the EVA material in each midsole region. The control shoe had a uniform EVA density across the entire midsole with an Asker C value of 53 (Figure 2.3). Larger Asker C values indicate stiffer materials.

Figure 2.2 – Picture of the experimental shoe based on the Merrell Full Pursuit model

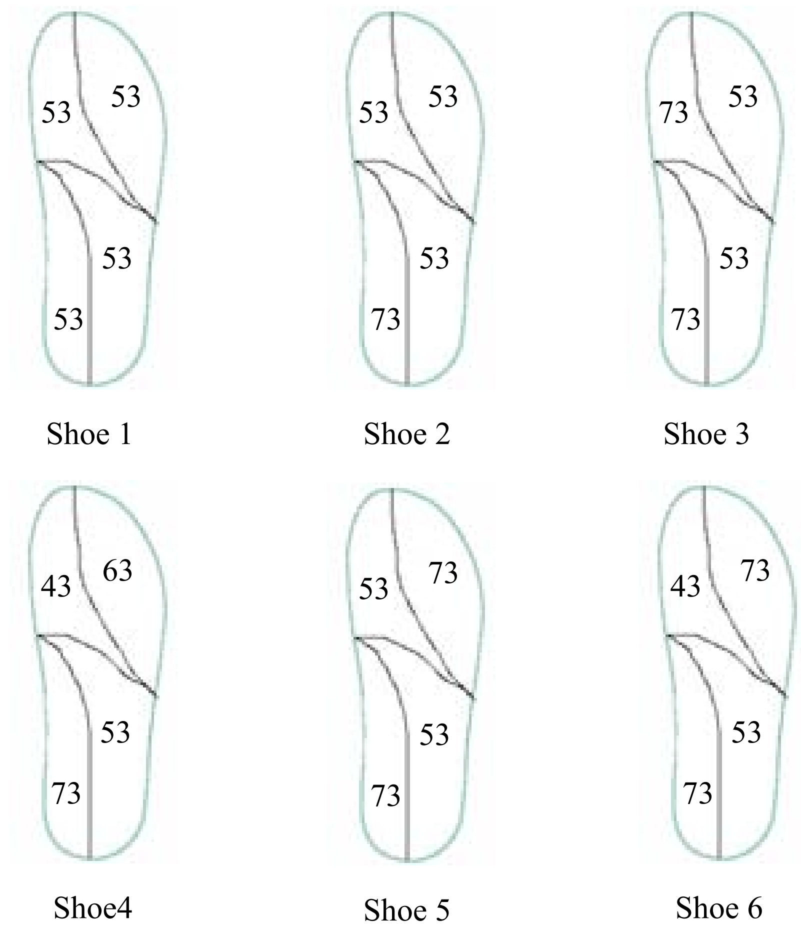

Figure 2.3 – Top view of the location and Asker C values for the experimental shoes. Right shoe configurations are shown – left shoe configurations mirror their counterparts.

Experimental Procedure

Prior to all tests, the factory insole was removed from the shoe. Sensor insoles matching the size of the shoes were inserted into each pair of test shoes. The factory insoles were removed in order to try and maximize the potential stiffening characteristics of each shoe by having the subject's foot as close to the midsole as possible. The Parotec insoles were then connected to the controller by the use of lead wires. These wires were held to the subject's ankles with Velcro straps so that the small data boxes on the insoles were not subjected to excessive movement and subsequently damaged. The insoles were zeroed as the subject raised their feet off the ground. Data were recorded during three trials of running over a distance of approximately ten foot strikes for both the left foot and the right foot. The subject was told to run at a comfortable, self-selected pace. Velocity was not recorded, as a comfortable pace for one subject may not have been comfortable for another and the goal of the study was to find out what happens at a comfortable running pace. The running surface was a tiled floor. Data collection was started and stopped by remote control. Data were collected after constant gait velocity was reached and prior to deceleration during each trial.

Data Analysis

The following parameters were measured with the Parotec Software: peak pressure in each sensor, the distribution of pressures, and the trace of the center of pressure. The peak pressure was the maximum pressure generated at each sensor of the Parotec insole during a trial. The pressure distribution allowed for a visual evaluation of high and low pressure regions across the plantar surface for shoes with different midsole density patterns.

When viewing Parotec data, a green box indicates a higher pressure in the second shoe compared to the first shoe (e.g. Shoe 1 vs Shoe 2 green box means a higher pressure in Shoe 2 compared to Shoe 1 in that particular sensor). A red COP line indicates the control shoe, while the blue COP line indicates the comparison shoe. The dominant foot, as informed by the subject, was analyzed in the study. Due to the way the pressure analysis software was set up, comparisons could only be made between the same number steps across different trials. For example, the center of pressure line from the control shoe step 1 could only be compared to step 1 of the other shoes. Figure 2.4 shows a typical step of comparison Parotec data. The steps that are presented in Figures 2.5 through 2.9 were picked because they best represented the trends from each subject. Results are presented as comparisons between a test shoe and the control shoe.

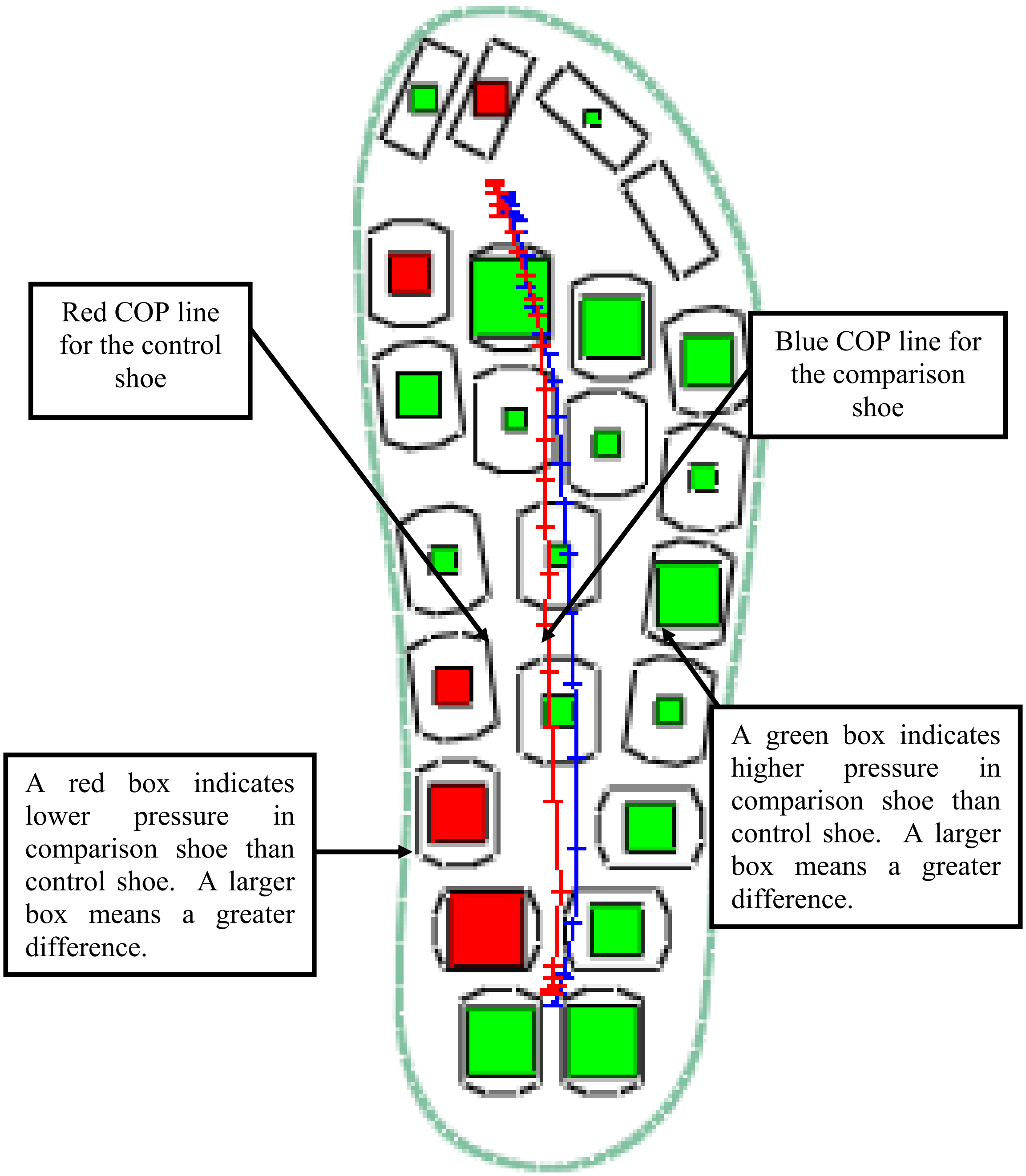

Figure 2.4 – Definitions of terms and visualizations for reading Parotec data

Results

Shoe 1 vs. Shoe 2 (Figure 2.5)

No significant differences were observed between the COP lines for any subject. It was noticed that all three female subjects had higher maximum pressures on the lateral border of the mid-foot and slightly lower pressures on the medial border in Shoe 2 as compared to Shoe 1 in a majority of step comparisons. This does not necessarily correlate to a COP change because the pressure values compared are maximum pressure values during a step and are independent of time. There was also a decrease in pressure at the distal phalange of the first metatarsal for all six subjects.

Shoe 1 vs. Shoe 3 (Figure 2.6)

Four subjects (F1, F2, F3, and M1) exhibited a lateral shift in the COP lines for a majority of the steps in Shoe 3 as compared to the control shoe (Shoe 1). These shifts occur in the midfoot region between the heel and metatarsals. There were no consistent areas of changes in plantar pressure between Shoe 3 and the control shoe for the subjects tested.

Shoe 1 vs. Shoe 4 (Figure 2.7)

None of the subjects exhibited a consistent change in the COP between the test shoe (Shoe 4) and the control shoe (Shoe 1). It was noticed that there was an increase in maximum pressure at the base and a decrease in maximum pressure at the head of the 1^{st} metatarsal in a majority of the steps of each trial for five subjects (three women, two men). It is also noted that the toe-off of the COP occurs earlier in the foot in shoe 4 as compared to the control shoe for all steps of all six subjects. This phenomenon is not noticed in any other shoe comparison.

Shoe 1 vs. Shoe 5 (Figure 2.8)

Three subjects (F1, F2, and F3) exhibited a consistent shift in COP to the lateral border of the shoe in Shoe 5 as compared to Shoe 1. Subject M1 had several trials of a lateral shift in COP, but it was not a change that was seen in a majority of the steps analyzed. Four subjects (F1, F2, F3, and M1) had a region of higher maximum pressure along the lateral border of the middle half of the foot in Shoe 5 as compared to Shoe 1.

Shoe 1 vs. Shoe 6 (Figure 2.9)

There was no consistent change in COP from Shoe 6 as compared to Shoe 1 for any of the six subjects. Four subjects (F1, F2, F3, and M3) had lower pressures in the tip of the 1st metatarsal in a majority of steps in each trial in Shoe 6 as compared to Shoe 1.

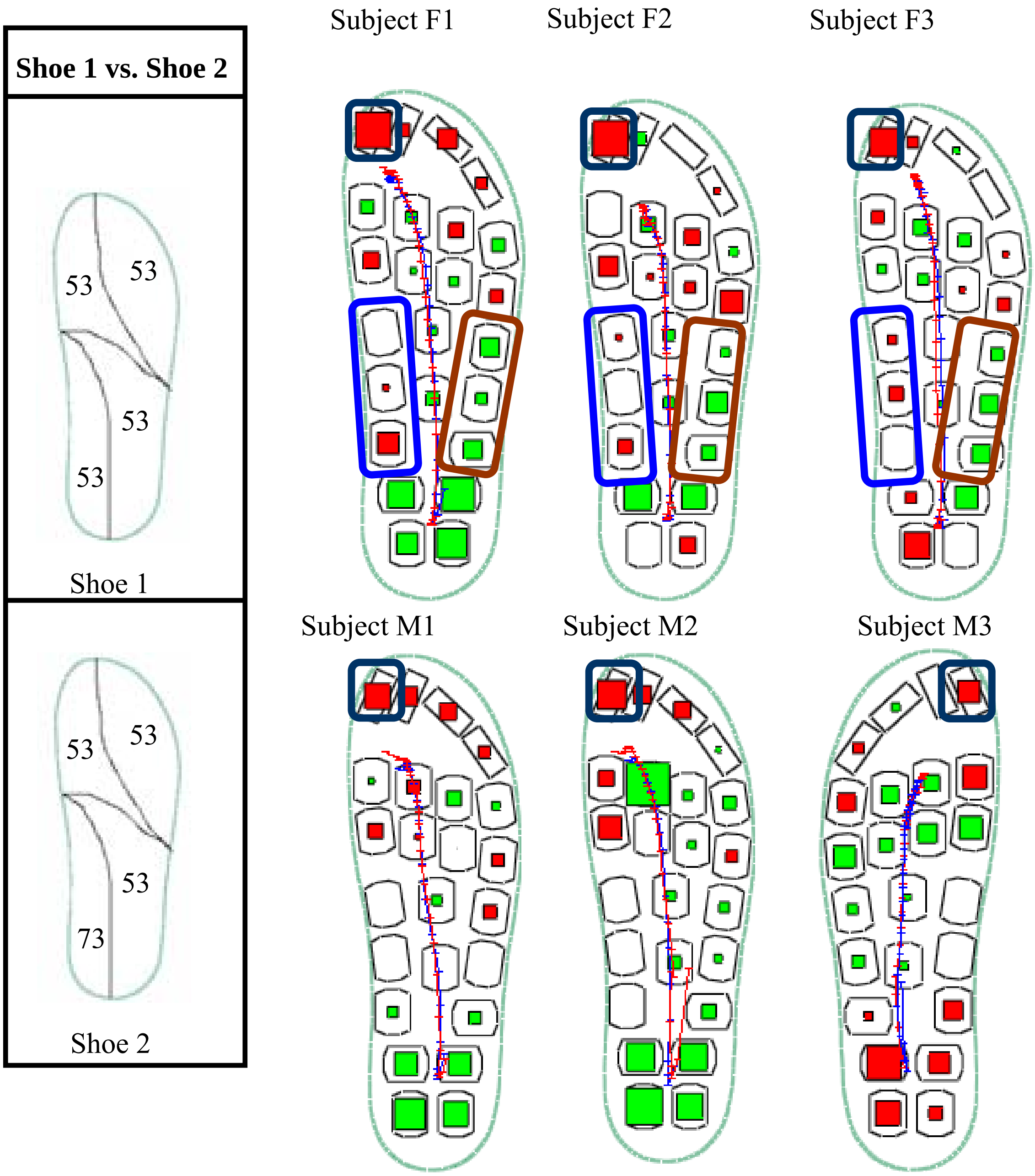

Figure 2.5—Comparison of Control Shoe (Shoe 1) and Experimental Shoe 2

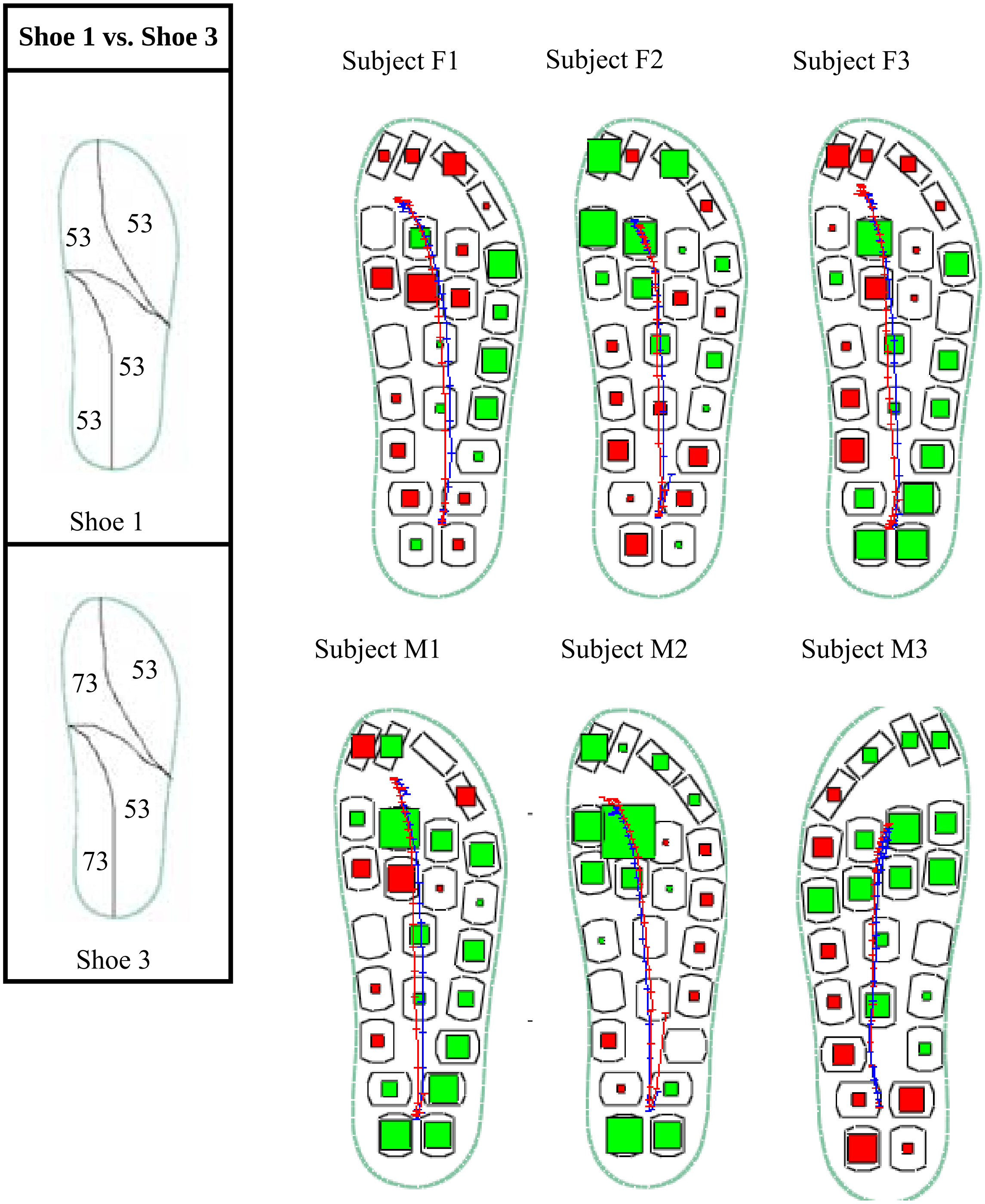

Figure 2.6—Comparison of Control Shoe (Shoe 1) and Experimental Shoe 3

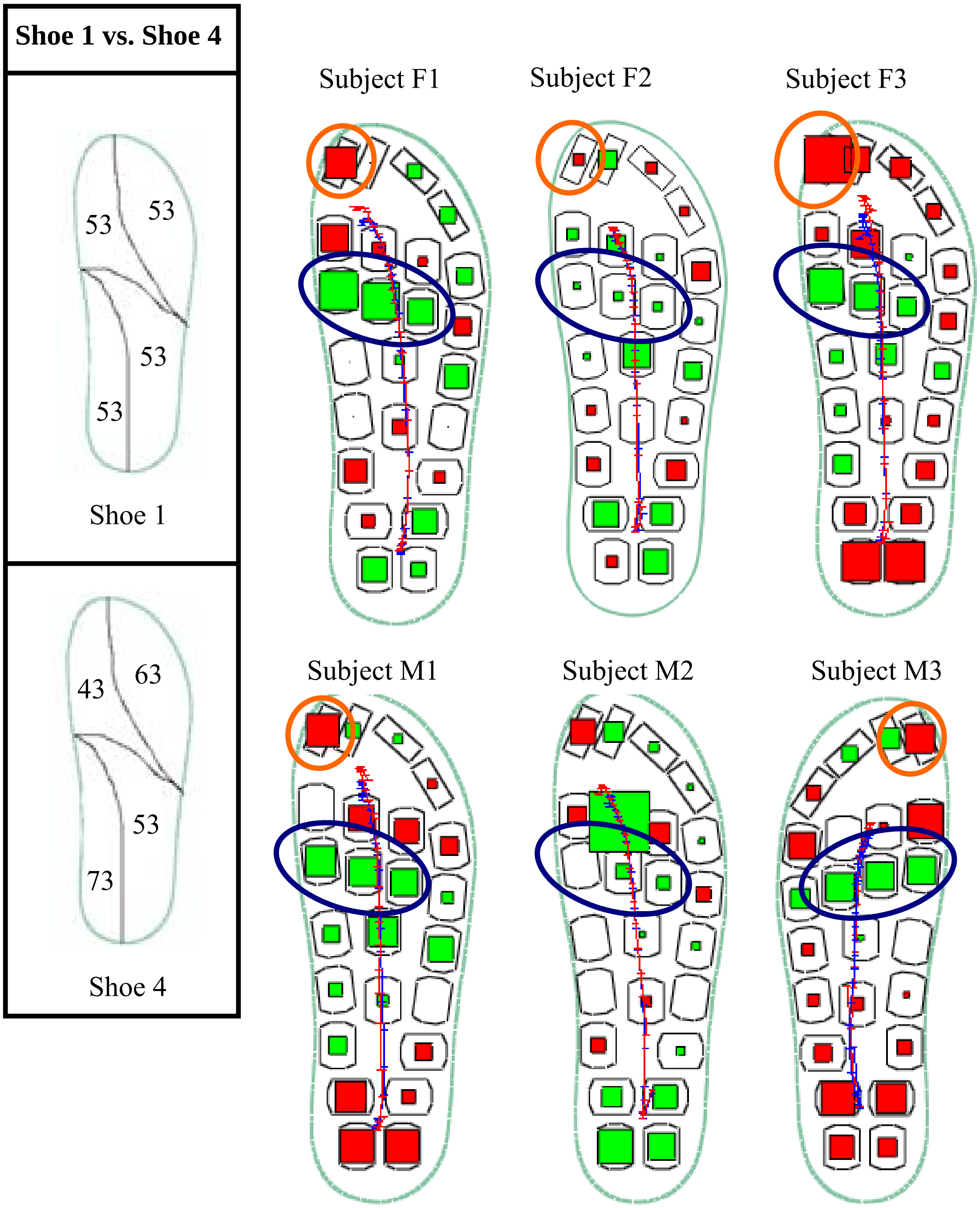

Figure 2.7—Comparison of Control Shoe (Shoe 1) and Experimental Shoe 4

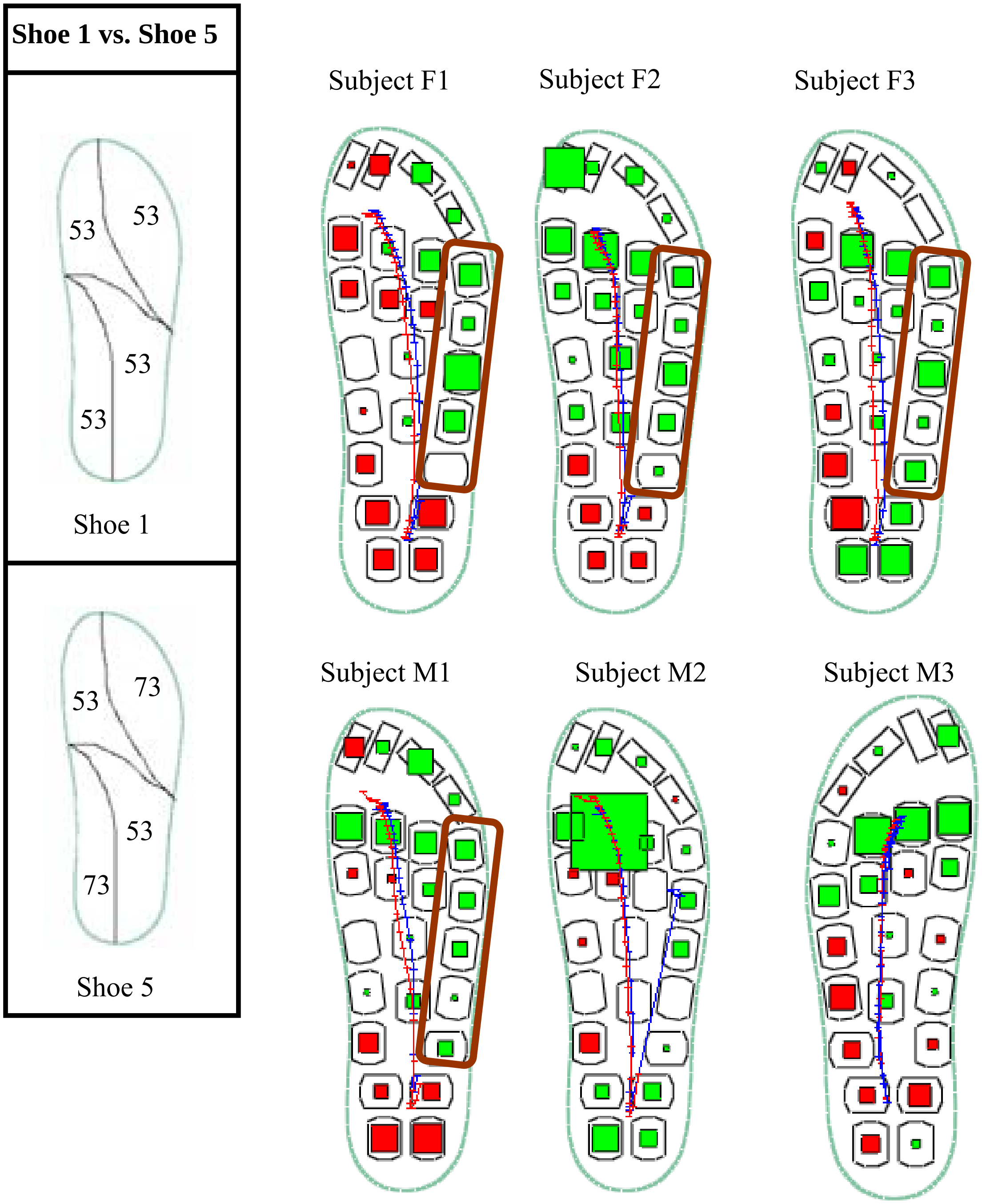

Figure 2.8—Comparison of Control Shoe (Shoe 1) and Experimental Shoe 5

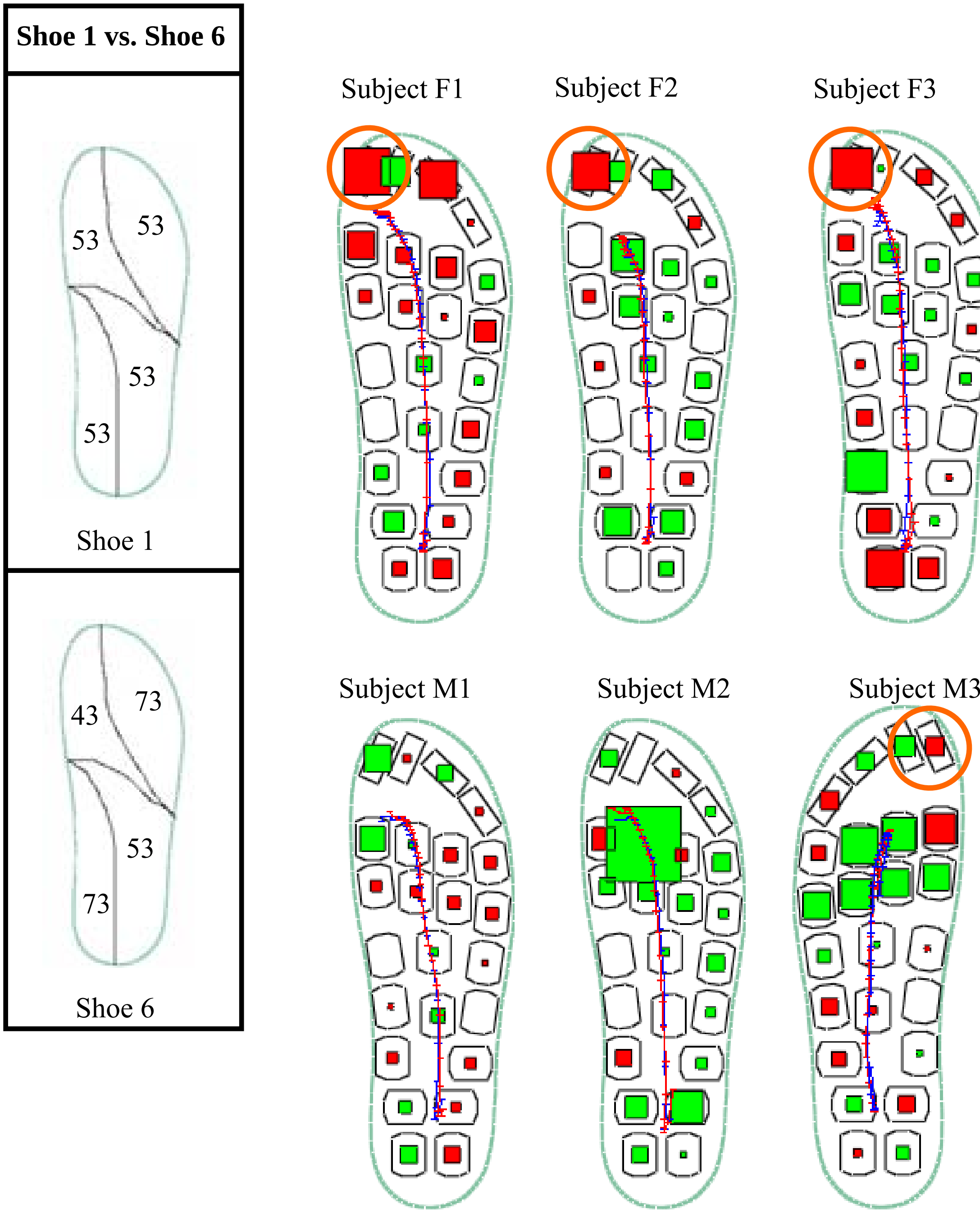

Figure 2.9—Comparison of Control Shoe (Shoe 1) and Experimental Shoe 6

Discussion

The current study focused on changes in the foot pressure distribution and the center of pressure between a neutral midsole shoe condition and several shoes with unique midsole density characteristics. It was hypothesized that the shoes would behave like an internal wedge and shift the COP toward the wedged components as documented in previous literature (Kakihana, Akai et al., 2005; Nigg et al., 2003; Van Gheluwe & Dananberg, 2004). However, the two variable midsole designs that exhibited a shift in the COP had a common area of increased medial heel stiffness causing a lateral shift in the center of pressure (Shoes 3 and 5). This result is similar to the literature regarding external heel wedges (Rose et al., 1992; Xu et al., 1999). It was noticed that changes in the COP occurred in the midfoot area and not at the heel or forefoot regions of the foot. This is important to note because Shoes 3 and 5 have exactly the opposite forefoot composition – Shoe 3 had a stiff medial forefoot and Shoe 5 had a stiff lateral component. In addition, the shoe with only medial heel stiffening did not create changes in the center of pressure location. These differences suggest that changes in midsole density may not affect the center of pressure in the forefoot region, but it is required to have different stiffness values in the forefoot region to elicit a response.

While there have been several studies that have incorporated the use of variable midsole density shoes (Erhart, Mundermann, Elspas, Giori, & Andriacchi, 2008; Fisher, Dyrby, Mundermann, Morag, & Andriacchi, 2007), this study was one of the first to evaluate such a wide distribution of different midsole EVA densities and their effects on the center of pressure. It was also a unique study in that it used production-model shoes and not just modified footwear. The rather unique distributions of high and low stiffness regions were supplied by Wolverine World Wide, Incorporated personnel, with no particular reason the designs shown. A full lateral stiffened shoe was not provided for this study because it was not considered to be a shoe model that could ever be sold. A full lateral stiffened shoe could possibly increase ankle pronation which was considered to go against running shoe manufacturing protocol according to Wolverine World Wide, Inc.

It should be noted that while differences in pressure and center of pressure lines were recorded, they were not necessary large in magnitude. This result coincides with previous literature that quantified the amount of change in the COP (Kakihana, Torii et al., 2005; Nigg et al., 2003; Rose et al., 1992). This may be a positive trait, however, as large changes in pressure distribution or medial and lateral COP tracks may lead to foot instability and possible injury (Fuller, 1999). This is a very important aspect that needs to be kept in mind when evaluating shoes for potential commercial use. One interesting finding from this study was that even in the shoes where shifts in the center of pressure were observed, the movement did not necessarily manifest itself in every step. This result is similar to the 2003 Nigg et. al. study which documented changes in the center of pressure not occurring in every step (Nigg et al., 2003). In addition, the two midsole configurations that shifted the COP (Shoes 3 and 5) only affected the COP in the midfoot region and not at heel strike or toe-off. This is important to consider if the biomechanical change desired manifests itself in these two regions.

These data could be useful to improve current orthotic prescription. If a patient is not comfortable with the footwear modification, they are less likely to continue to use it. In this study, an alternative to an orthotic wedge was introduced as a way to make the footwear intervention more comfortable while being able to control the pressure distribution and center of pressure. Further development and refinement of the locations and stiffness values of the midsole density pattern may prove to be a useful tool when orthotic wedges are not appropriate.

REFERENCES

References

Chesnin, K. J., Selby-Silverstein, L., & Besser, M. P. (2000). Comparison of an in-shoe pressure measurement device to a force plate: concurrent validity of center of pressure measurements. *Gait and Posture, 12*, 6.

Crenshaw, S. J., Pollo, F. E., & Calton, E. F. (2000). Effects of lateral-wedged insoles on kinetics at the knee. *Clin Orthop Relat Res*(375), 185-192.

Erhart, J. C., Mundermann, A., Elspas, B., Giori, N. J., & Andriacchi, T. P. (2008). A variable-stiffness shoe lowers the knee adduction moment in subjects with symptoms of medial compartment knee osteoarthritis. *Journal of Biomechanics, 41*, 2720-2725.

Fisher, D. S., Dyrby, C. O., Mundermann, A., Morag, E., & Andriacchi, T. P. (2007). In healthy subjects without knee osteoarthritis, the peak knee adduction moment influences the acute effect of shoe interventions designed to reduce medial compartment knee load. *J Orthop Res, 25*(4), 540-546.

Fuller, E. A. (1999). Center of pressure and its theoretical relationship to foot pathology. *J Am Podiatr Med Assoc, 89*(6), 278-291.

Kakihana, W., Akai, M., Nakazawa, K., Takashima, T., Naito, K., & Torii, S. (2005). Effects of laterally wedged insoles on knee and subtalar joint moments. *Arch Phys Med Rehabil, 86*(7), 1465-1471.

Kakihana, W., Akai, M., Yamasaki, N., Takashima, T., & Nakazawa, K. (2004). Changes of joint moments in the gait of normal subjects wearing laterally wedged insoles. *Am J Phys Med Rehabil, 83*(4), 273-278.

Kakihana, W., Torii, S., Akai, M., Nakazawa, K., Fukano, M., & Naito, K. (2005). Effect of a lateral wedge on joint moments during gait in subjects with recurrent ankle sprain. *Am J Phys Med Rehabil, 84*(11), 858-864.

Kerrigan, D. C., Lelas, J. L., Goggins, J., Merriman, G. J., Kaplan, R. J., & Felson, D. T. (2002). Effectiveness of a lateral-wedge insole on knee varus torque in patients with knee osteoarthritis. *Arch Phys Med Rehabil, 83*(7), 889-893.

Nigg, B. M., Stergiou, P., Cole, G., Stefanyshyn, D., Mundermann, A., & Humble, N. (2003). Effect of shoe inserts on kinematics, center of pressure, and leg joint moments during running. *Med Sci Sports Exerc, 35*(2), 314-319.

Rose, N. E., Feiwell, L. A., & Cracchiolo, A., 3rd. (1992). A method for measuring foot pressures using a high resolution, computerized insole sensor: the effect of heel wedges on plantar pressure distribution and center of force. *Foot Ankle, 13*(5), 263-270.

Van Gheluwe, B., & Dananberg, H. J. (2004). Changes in plantar foot pressure with in-shoe varus or valgus wedging. *J Am Podiatr Med Assoc, 94*(1), 1-11.

Winter, D. A. (2005). *Biomechanics and Motor Control of Human Movement* (3rd ed.). Hoboken: John Wiley & Sons, Inc.

Xu, H., Akai, M., Kakurai, S., Yokota, K., & Kaneko, H. (1999). Effect of shoe modifications on center of pressure and in-shoe plantar pressures. *Am J Phys Med Rehabil, 78*(6), 516-524.

Yasuda, K., & Sasaki, T. (1987). The mechanics of treatment of the osteoarthritic knee with a wedged insole. *Clin Orthop Relat Res*(215), 162-172.

CHAPTER 3 – DOES THE KNEE ADDUCTION MOMENT CHANGE WHEN WEARING LATERALLY STIFFENED PRODUCTION MODEL SHOES?

Introduction

Osteoarthritis is the breakdown of articular cartilage in a joint (Mow & Huiskes, 2005) and occurs in the knee joint of approximately 10% of all people age 55 and older (Davis, 1988). People with osteoarthritis of the knee are 10 times more likely to have the degenerative disease in the medial compartment as compared to the lateral compartment (Ahlback, 1968). In addition, women are more likely than men to develop osteoarthritis in the knee joint (Felson et al., 1997). An increase in the knee adduction moment can accentuate, accelerate, and even induce medial compartment knee osteoarthritis (Fisher, Dyrby, Mundermann, Morag, & Andriacchi, 2007). The knee adduction moment has also been linked to being responsible for transmitting 60% to 80% of the total load that occurs in the knee (Crenshaw, Pollo, & Calton, 2000). There are several invasive and non-invasive methods that have been found to decrease knee adduction moments in people with and without medial compartment knee osteoarthritis.

One surgical method that has been shown to decrease the knee adduction moment in people with medial compartment osteoarthritis is a high tibial osteotomy. Prodromos et. al. found that the knee joint adduction moment decreased when a wedge of bone was taken out of the tibia, thereby redistributing the forces in the knee joint (Prodromos, Andriacchi, & Galante, 1985). Non-invasive techniques have also been shown to be effective at reducing the adduction moment in symptomatic osteoarthritis patients. Kerrigan et. al. found that 5 and 10 degree wedges were effective at reducing the adduction moment (Kerrigan et al., 2002), while Kakihana et. al. found that 6 degree wedges also significantly reduced the adduction moment in patients with knee joint osteoarthritis (Kakihana, Akai et al., 2005). Kuroyanagi et. al. added subtalar strapping to a 6 degree lateral wedge to also significantly decrease the knee adduction moment

(Kuroyanagi et al., 2007). Lateral wedges have also been shown effective at reducing the adduction moment in non-symptomatic people. Crenshaw et. al., Kakihana et. al., and Fisher et. al. all found that lateral wedged insoles decrease the adduction moment in healthy subjects (Crenshaw et al., 2000; Fisher et al., 2007; Kakihana, Akai, Yamasaki, Takashima, & Nakazawa, 2004). In addition, Fisher et. al. also proposed a new, non-invasive method for decreasing the adduction moment at the knee joint by the use of a dual-density midsole. They found that by increasing the stiffness of the lateral half of an outsole/midsole combination by 20% and 50% more than the medial half, the knee adduction moment was significantly decreased at a rate similar to a 4 degree lateral wedge (Fisher et al., 2007). One drawback to this study was that the lateral stiffened shoes were prototype shoes that were not based on a conventional shoe build.

With this knowledge, this thesis chapter set out to accomplish four objectives. The first objective of this study was to develop a biomechanical model to determine the knee joint adduction moment. The second objective was to determine if a full, lateral stiffened midsole in a production shoe would decrease knee joint adduction moments. The third objective of the study was to determine if shoes with a stiff medial heel component and a changing location of a pocket of lateral stiffness could decrease the knee adduction moment. The fourth objective of the study was to determine if the response to the change in midsole stiffening was different between male and female subjects.

Biomechanical Model

Because it is difficult and expensive to surgically implant force transducers in the joints of subjects, different techniques must be used to measure the desired effect. In order to determine the knee joint adduction moment during walking gait, a biomechanical model was developed. Two methods for modeling joint moments are the floor reaction force vector (FRFV) method and the inverse dynamics solution in a segmented body model. Both model types require the use of some kind of system that can give the position of joint centers and the relative location of the ground reaction force, but the segmental model requires more information to compute joint moments.

The floor reaction force vector method is one way to calculate moment data. It calculates the moment by finding the product of the ground reaction force and the perpendicular distance from the joint center (d) in the different planes of motion. An example of how this method can be used to calculate the knee adduction moment is shown in Figure 3.1. The force components in the frontal plane (F) are multiplied by the perpendicular distance from the knee joint center (d) to obtain the adduction moment.

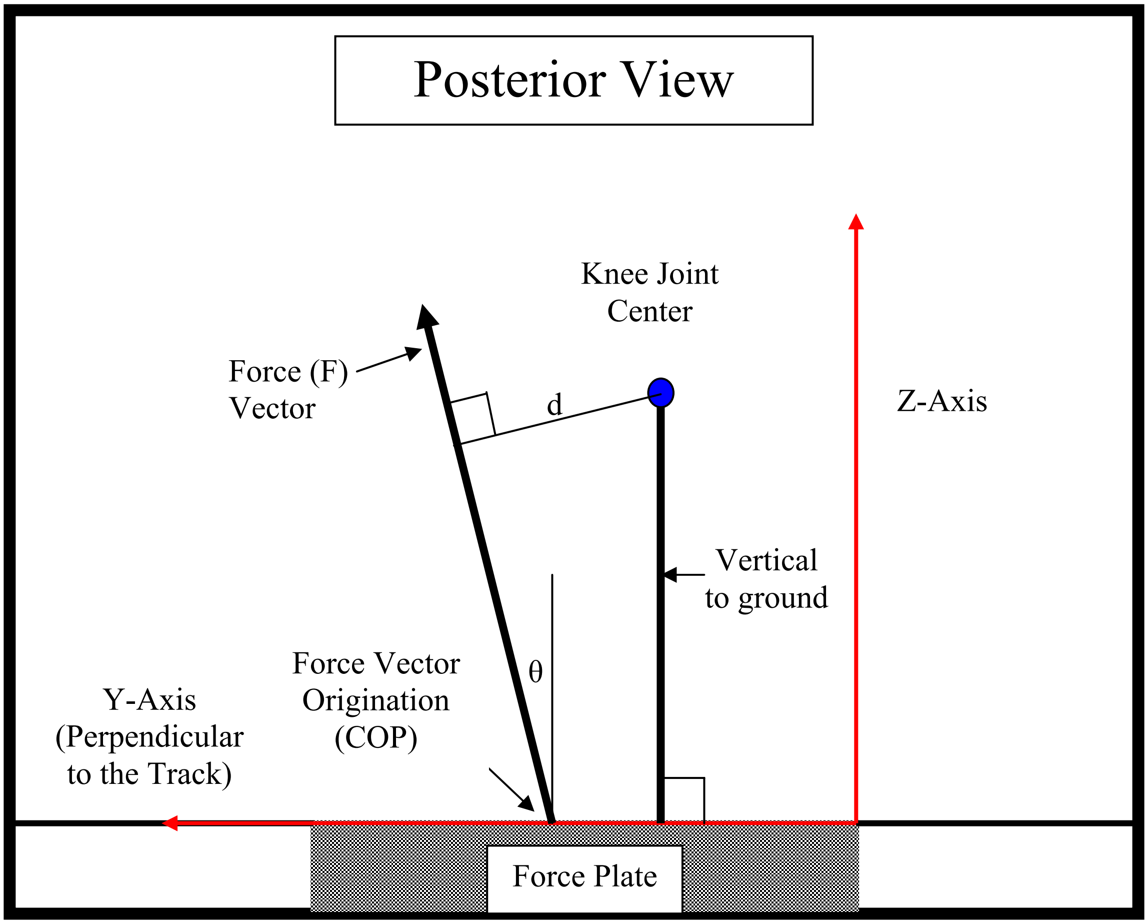

Figure 3.1 – Diagram of the calculation of the knee adduction moment using the FRFV method

There are significant drawbacks to this method, however. Winter outlined these problems in the third edition of Biomechanics and Motor Control of Human Movement (Winter, 2005). The first drawback to the method is that the moment values do not account for the acceleration of the segments below the joint in question. For example, using the FRFV method to measure moments at the knee do not take into account the mass and acceleration of the foot and shank segments. According to Wells, the error is negligible at the ankle, small but significant at the knee, and quite significant at the hip (Wells, 1981). A second problem is that the method only shows the cause of the moment and not what the body is actually doing. The example Winter gives is with respect to the ankle joint. When the ankle is performing a plantarflexion moment, the ground reaction force is forced forward. If the ankle muscles were not firing, the FRFV would stay under the ankle joint. With this knowledge, the FRFV was not chosen as the method to measure the knee adduction moment.

The second type of model used to compute joint moments in the body is the segmental model. Segmental models are characterized by breaking down the human anatomy into simplified segments. The first level of a segmental model only takes into account that each body segment acts on its own with respect to the ground reaction force and is known as a massless model. The second level of a segmental model includes the effect of the weight of each segment. This is known as a quasi-static model. The top level of a segmental model includes everything from the massless and quasi-static models and then adds the effect of the accelerated moments of inertia from each segment and is called a full dynamic model. The different segmental model types can be seen in Figures 3.2 through 3.5.

Figure 3.2 -- Anatomical
Model

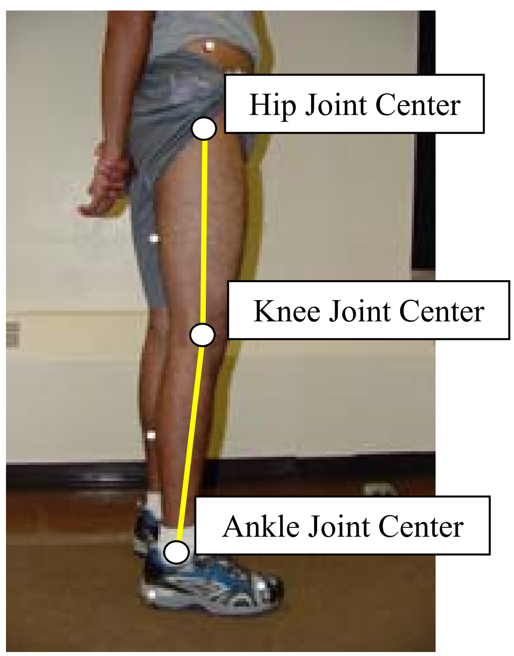

Figure 3.3 --Massless
Segmental Model

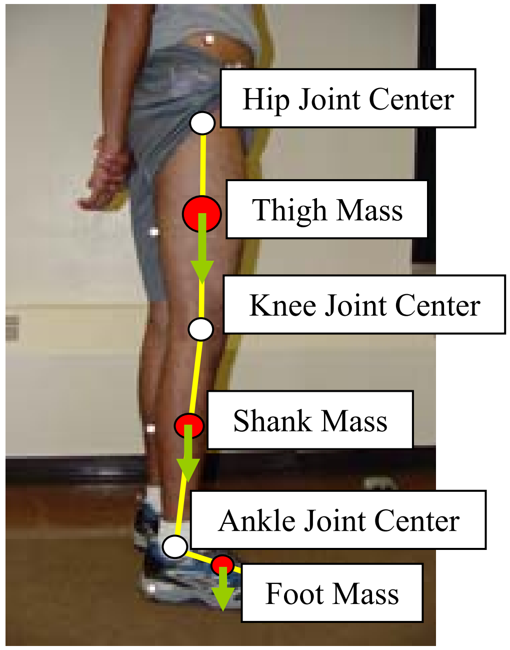

Figure 3.4 --Quasi-Static Segmental Model

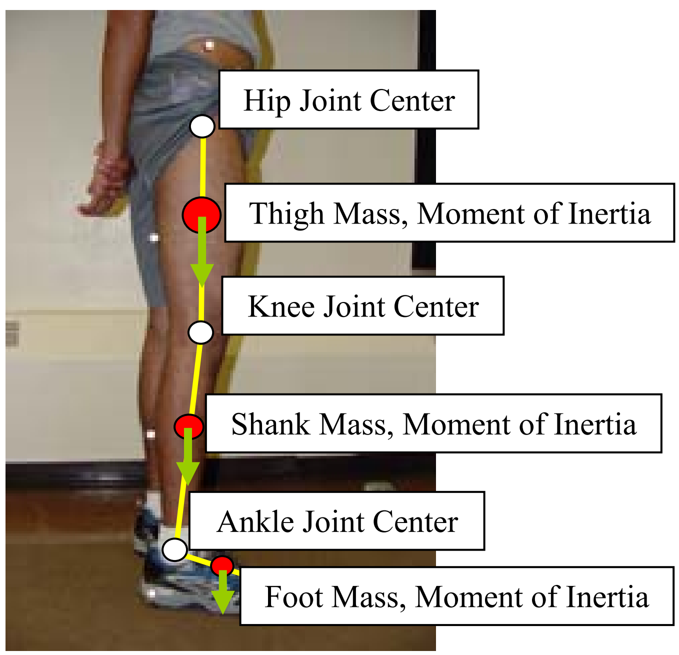

Figure 3.5 --Full Dynamic Model

In the current studies, anthropometric data from Dempster (1955) was used to determine the location of the mass centers for the various body segments and for each segment weight for use in the dynamic model. Dempster performed experiments on cadavers to establish locations and segment weights as a function of total body mass. His data is still used in most inverse dynamic biomechanical models. Sample calculations comparing the FRFV, the massless segmental, the quasi-static segmental, and the full dynamic model can be found following the marker set description.

Model Terms and Sample Calculations

The following section details the terms and equations used to determine the knee adduction moment using the FRFV method and the three segmental models. All four models needed the medial/lateral and vertical components of the reaction force from the force plate in addition to the medial/lateral origin of the force vector, also known as the center of pressure (COP_y). Also, the four methods all needed the location of the knee joint center, while three segmental methods also needed the ankle joint center location. These values, in addition to the mass of the foot and shank segments and the spatial location of these masses, were known quantities either from measurement or definition. The mass and location of the foot and shank segments were calculated based on work by Dempster (1955), the force and center of pressure data were measured by the force plate, and the knee and ankle joint centers were located using the motion capture system.

FRFV Method

Using trigonometry, the perpendicular distance from the knee joint center to the projection of the force vector in the medial/lateral and vertical plane (distance d) was calculated for the FRFV method. This value was not required for the segmental models. As can be seen in Figure 3.6, the resultant knee adduction moment is different for the FRFV method compared to the Full Dynamic Segmental model. This is due to the fact that the FRFV model does not use segments and does not take into account for the inertial properties of the foot and shank segments.

FRFV Method – Terms

K_{add} – Knee Adduction Moment

$F_{y\text{-}z}$ – Projection of force vector in the Y-Z plane (medial/lateral and vertical force)

F_y – Force component in the Y – direction (medial/lateral)

F_z – Force component in the Z – direction (vertical)

d – Perpendicular distance from knee joint center to $F_{y\text{-}z}$

KJC_y – Y component of the location of the knee joint center

KJC_z – Z component of the location of the knee joint center

COP_y – Y component of the center of pressure

FRFV Method – Calculations

$$K_{add} = d * F_{y\text{-}z} \text{ or}$$
$$K_{add} = KJC_z * F_y + (COP_y - KJC_y) * F_z$$

Massless Segmental Model

To obtain the knee adduction moment, calculations had to be made to obtain the reaction forces and moments at the ankle. These reaction forces and moments were then used to determine the knee adduction moment. This is a statically determinant model, and the calculation of the knee adduction moment does not require knowledge of any value before or after the frame of calculation.

Massless Segmental Model – Terms

K_{add} – Knee Adduction Moment

F_y – Force component in the Y – direction (medial/lateral)

F_z – Force component in the Z – direction (vertical)

AJC_y – Y component of the location of the ankle joint center

AJC_z – Z component of the location of the ankle joint center

KJC_y – Y component of the location of the knee joint center

KJC_z – Z component of the location of the knee joint center

COP_y – Y component of the center of pressure

ARF_y – Y component of the ankle reaction force

ARF_z – Z component of the ankle reaction force

A_{abd} – Ankle abduction moment

KRF_y – Y component of the knee reaction force

KRF_z – Z component of the knee reaction force

Massless Segmental Model – Ankle Force and Moment Calculations

$$\sum F_{AJC} = 0$$
$$F_y + ARF_y = 0$$
$$ARF_y = -F_y$$
$$F_z + ARF_z = 0$$
$$ARF_z = -F_z$$
$$\sum M_{AJC} = 0$$
$$A_{abd} + AJC_z * F_y + (AJC_y - COP_y) * F_z = 0$$
$$A_{abd} = -AJC_z * F_y - (AJC_y - COP_y) * F_z$$

Massless Segmental Model – Knee Force and Moment Calculations

$$\sum F_{KJC} = 0$$
$$ARF_y + KRF_y = 0$$
$$KRF_y = -ARF_y$$
$$ARF_z + KRF_z = 0$$
$$KRF_z = -ARF_z$$
$$\sum M_{KJC} = 0$$
$$A_{abd} + (KJC_z - AJC_z) * ARF_y + (KJC_y - AJC_y) * ARF_z = 0$$
$$K_{add} = -(KJC_z - AJC_z) * ARF_y + (KJC_y - AJC_y) * ARF_z$$

Quasi-Static Segmental Model

The addition of segment masses and their locations as defined by Dempster (1955) is what differentiates the quasi-static segmental model. This model still does not taken into account acceleration of the limbs, but it does account for how the mass of each segment with respect to gravity acts on the system.

Quasi-Static Segmental Model -- Terms

COP_y – Y Component of the Center of Pressure

F_y – Force component in the Y-direction

F_z – Force component in the Z-direction

g – Gravitational Acceleration

AJC_y – Y Component of the Ankle Joint Center

AJC_z – Z Component of the Ankle Joint Center

$COM_{f,y}$—Y Component of the Foot Center of Mass

$COM_{f,z}$—Z Component of the Foot Center of Mass

M_f—Mass of the Foot Segment

KJC_y – Y Component of the Location of the Knee Joint Center

KJC_z – Z Component of the Location of the Knee Joint Center

$COM_{s,y}$—Y Component of the Shank Center of Mass

$COM_{s,z}$—Z Component of the Shank Center of Mass

M_s—Mass of the Shank Segment

ARF_y – Y Component of the Ankle Reaction Force

ARF_z – Z Component of the Ankle Reaction Force

A_{abd} – Ankle Abduction Moment

KRF_y – Y Component of the Knee Reaction Force

KRF_z – Z Component of the Knee Reaction Force

K_{add} – Knee Adduction Moment

Quasi-Static Segmental Model – Ankle Force and Moment Calculations

$$\sum F_{AJC} = 0$$

$$F_y + ARF_y = 0$$

$$ARF_y = -F_y$$

$$F_z + M_f * g + ARF_z = 0$$

$$ARF_z = -F_z - M_f * g$$

$$\sum M_{AJC} = 0$$

$$A_{abd} + (AJC_y - COP_y) * F_z + AJC_z * F_y$$
$$+ (AJC_y - COM_{f,y}) * (M_f * g) = 0$$

$$A_{abd} = -(AJC_y - COP_y) * F_z - AJC_z * F_y$$
$$- (AJC_y - COM_{f,y}) * (M_f * g)$$

Quasi-Static Segmental Model – Knee Force and Moment Calculations

$$\sum F_{KJC} = 0$$
$$ARF_y + KRF_y = 0$$
$$KRF_y = -ARF_y$$
$$ARF_z + KRF_z + M_s * g = 0$$
$$KRF_z = -ARF_z - M_s * g$$
$$\sum M_{KJC} = 0$$
$$K_{add} - A_{abd} + (KJC_z - AJC_z) * ARF_y + (KJC_y - AJC_y) * ARF_z$$
$$+ (KJC_y - COM_{s,y}) * (M_s * g) = 0$$
$$K_{add} = A_{abd} - (KJC_z - AJC_z) * ARF_y - (KJC_y - AJC_y) * ARF_z$$
$$- (KJC_y - COM_{s,y}) * (M_s * g)$$

Full Dynamic Segmental Model

This model is the most accurate because it takes into account everything that the massless and quasi-static models do, but it adds the effects of linear and angular acceleration of the foot and shank segments to the system. This is the only model that requires knowledge of segment motion before and after the frame being calculated in order to compute the adduction moment. This is because the model takes a running average of the acceleration between the frames before and after the frame in question.

Full Dynamic Segmental Model – Terms

COP_y – Y Component of the Center of Pressure
F_y – Force component in the Y-direction
F_z – Force component in the Z-direction
g – Gravitational Acceleration
AJC_y – Y Component of the Ankle Joint Center

AJC_z – Z Component of the Ankle Joint Center

$COM_{f,y}$ —Y Component of the Foot Center of Mass

$COM_{f,z}$ —Z Component of the Foot Center of Mass

M_f —Mass of the Foot Segment

$LA_{f,y}$ – Linear Acceleration of the foot segment in the Y - Direction

$LA_{f,z}$ – Linear Acceleration of the foot segment in the Z - Direction

I_f— Foot Segment Moment of Inertia

$\alpha_{f,x}$—Angular Acceleration of the Foot about the X-Axis

KJC_y – Y Component of the Location of the Knee Joint Center

KJC_z – Z Component of the Location of the Knee Joint Center

$COM_{s,y}$—Y Component of the Shank Center of Mass

$COM_{s,z}$—Z Component of the Shank Center of Mass

M_s—Mass of the Shank Segment

$LA_{s,y}$ – Linear Acceleration of the foot segment in the Y - Direction

$LA_{s,z}$ – Linear Acceleration of the foot segment in the Z - Direction

I_f—Shank Segment Moment of Inertia

$\alpha_{s,x}$—Angular Acceleration of the Shank about the X-Axis

ARF_y – Y Component of the Ankle Reaction Force

ARF_z – Z Component of the Ankle Reaction Force

A_{abd} – Ankle Abduction Moment

KRF_y – Y Component of the Knee Reaction Force

KRF_z – Z Component of the Knee Reaction Force

K_{add} – Knee Adduction Moment

Full Dynamic Segmental Model – Ankle Force and Moment Calculations

$$\sum F_{AJC} = M_f * LA_f$$

$$F_y + ARF_y = M_f * LA_{f,y}$$

$$ARFy = -Fy + Mf * LAf, y$$

$$F_z - M_f * g + ARF_z = M_f * LA_{f,z}$$

$$ARF_z = M_f * LA_{f,z} - F_z - M_f * g$$

$$\sum M_{COMf} = I_f * \alpha_{f,x}$$

$$A_{abd} + (COM_{f,y} - COP_y) * F_z + COM_{f,z} * F_y$$
$$+ (AJC_y - COM_{f,y}) * ARF_z + (AJC_z - COM_{f,z}) * ARF_y = I_f * \alpha_{f,x}$$

$$A_{abd} = I_f * \alpha_{f,x} - (COM_{f,y} - COP_y) * F_z - COM_{f,z} * F_y -$$
$$(AJC_y - COM_{f,y}) * ARF_z - (AJC_z - COM_{f,z}) * ARF_y$$

Full Dynamic Segmental Model – Knee Force and Moment Calculations

$$\sum F_{KJC} = M_s * LA_s$$

$$ARF_y + KRF_y = M_s * LA_{s,y}$$

$$KRF_y = M_s * LA_{s,y} - ARF_y$$

$$ARF_z + KRF_z + M_s * g = M_s * LA_{s,z}$$

$$KRF_z = M_s * LA_{s,z} - ARF_z - M_s * g$$

$$\sum M_{COM_s} = I_s * \alpha_{s,x}$$

$$K_{add} - A_{abd} + (COM_{s,z} - AJC_z) * ARF_y + (COM_{s,y} - AJC_y) * ARF_z +$$
$$(KJC_z - COM_{s,z}) * KRF_y + (KJC_y - COM_{s,y}) * KRF_z = I_s * \alpha_{s,x}$$

$$K_{add} = I_s * \alpha_{s,x} + A_{abd} - (COM_{s,z} - AJC_z) * ARF_y$$
$$- (COM_{s,y} - AJC_y) * ARF_z - (KJC_z - COM_{s,z}) * KRF_y$$
$$- (KJC_y - COM_{s,y}) * KRF_z$$

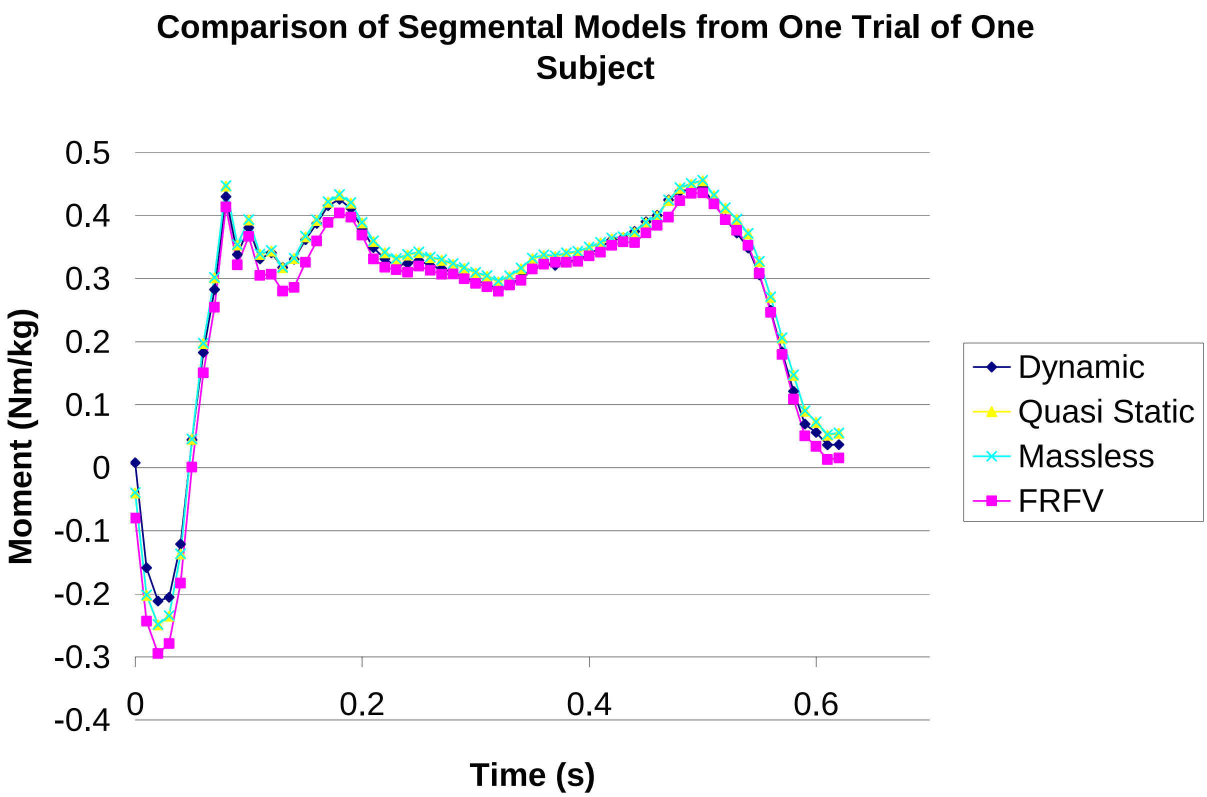

Figure 3.6 – Comparison of segmental models from one trial of one subject

In order to calculate the knee adduction moment from the dynamic segmental model, a lower body marker had to be developed to estimate joint centers.

Marker Set

Ten markers were placed on body landmarks for static measurements and 8 retro-reflective markers were used for the dynamic measurements. Table 3.1 lists the markers and whether they are used for static only or static and dynamic models. The marker set chosen here was similar to the set used by Fisher et. al. and Mundermann et. al. to determine lower body joint segments for use in an inverse dynamics model (Figure 3.6) (Fisher et al., 2007; Mundermann, Dyrby, Hurwitz, Sharma, & Andriacchi, 2004).

Table 3.1 –Marker Locations and Names for Static and Dynamic Trials

Marker Name	Abbreviation	Static	Dynamic
Right Superior Iliac Spine	RSIS	X	X
Right Greater Trochanter	RGTR	X	X
Right Posterior Thigh	RPOT	X	X
Right Lateral Knee Joint	RLKJ	X	X
Right Medial Knee Joint	RMKJ	X	
Right Posterior Calf	RPOC	X	X
Right Lateral Malleolus	RLMA	X	X
Right Medial Malleolus	RMMA	X	
Right Lateral Aspect of the Calcaneus	RLAC	X	X
Right 5th Metatarsal Head	R5MH	X	X

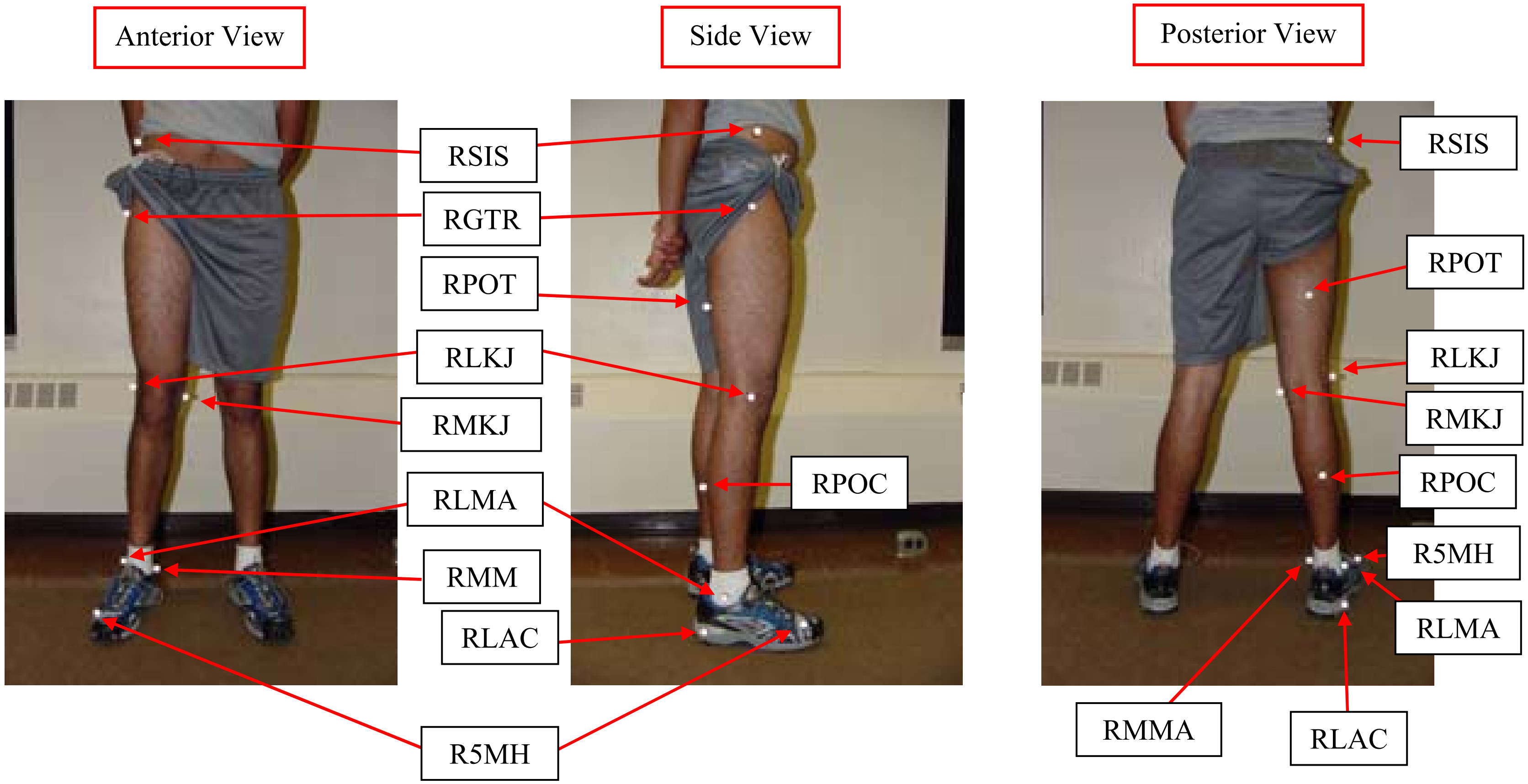

Figure 3.7 – Anterior, Lateral, and Posterior Views
of the Anatomical Model with Marker Set

Physical Markers

This section describes the marker set used to generate segments for the inverse dynamics model.

Figure 3.7 illustrates the anatomical skeletal landmarks that the marker set uses for reference.

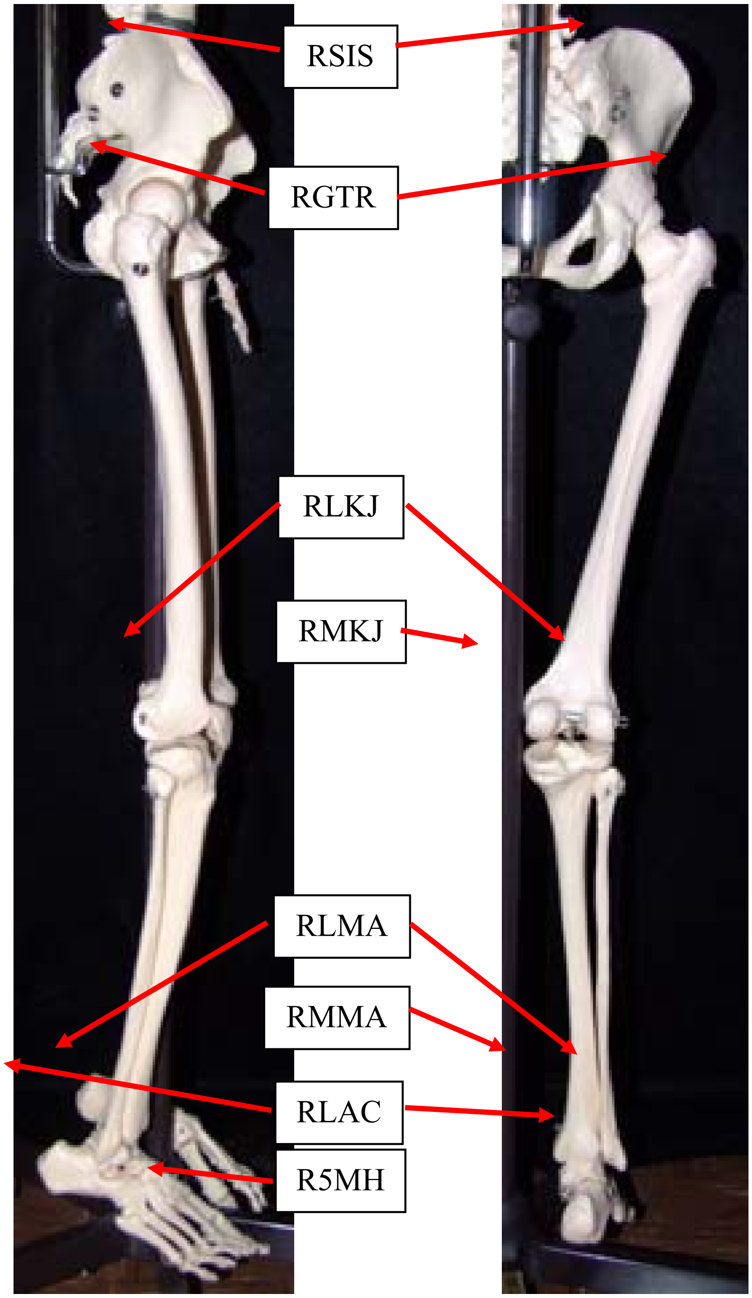

Figure 3.8 – Anatomical skeletal landmark references for the marker set

Superior Iliac Spine (RSIS) – This anatomical location is located at the top of the pelvic iliac crest. This bony landmark is found by palpation after finding the anterior superior iliac spine on the pelvis. From this landmark, the superior iliac spine is found by moving up the pelvic girdle in a posterior fashion on the border of the iliac crest until the top is reached. The marker attached to this landmark was not used in calculations, but was used as a check for correct direction of motion.

Greater Trochanter (RGTR) – In the anatomical position, the greater trochanter is the protrusion on the femur that is lateral to the femoral head. To locate the landmark, the subject would internally and externally rotate their leg with their foot off the ground while the investigator placed their hand on the hip and felt for a bony prominence. The marker was then attached to this location.

Lateral and Medial Knee Joint Line (RLKJ, RMKJ) – To find the lateral knee joint line, the subject sat in a chair and oriented themselves such that their thighs would be parallel to the floor and the knee joint flexed at a 90 degree angle. A small mark was placed where the lateral aspect of the knee rotation line appeared to be. To confirm if the mark was on the correct location, the subject extended and flexed their leg about their knee joint without moving the thigh. If the marker moved in an arc during this visual inspection, it was not at the knee joint line. The marker was then adjusted until it only rotated and did not translate when the leg was flexed and extended. This method was repeated for the medial aspect of the knee. These two markers defined the rotation line of the knee. The midpoint between these two markers was important as it was identified as the knee joint center.

Posterior Thigh (RPOT) – This location was not an anatomical landmark, but the marker that was placed there allowed for a better visual understanding of how the gait cycle was progressing and the direction of movement. The marker position was located by finding the midpoint between the greater trochanter marker and the lateral knee joint line marker while the subject was standing with their feet together. When the midpoint was found, an imaginary line was traced around to the posterior side of the thigh. The marker was then placed at that position.

Medial Malleolus (RMMA) – The medial malleolus was round by palpating the inner portion of the ankle joint. This landmark was used to help determine the width of the ankle joint. This marker was not used during dynamic testing because it became occluded from the cameras during the swing phase of the opposite leg.

Lateral Malleolus (RLMA) – The lateral malleolus was located in the same manner as the medial malleolus. It is the bony landmark that protruded the furthest away from the ankle on the lateral inferior border. This mark was used in conjunction with the medial malleolus to determine the location of the center of the ankle joint during the static trial. The ankle joint center was the midpoint between the medial and lateral malleoli. The ankle joint center was calculated from the lateral malleolus marker during dynamic trials.

Posterior Calf (RPOC) – The posterior calf marker was placed in the same manner that the posterior thigh marker was placed. The midpoint between the lateral knee joint line and lateral malleolus markers was determined and a marker was placed on the posterior portion of the lower leg. Again, this marker was only used to visualize the leg and was not used in subsequent calculations.

Lateral Aspect of the Calcaneus (RLAC) – This marker was applied directly to the footwear. The marker was applied to the lateral heel of the shoe, as the calcaneus is typically covered by a shoe. This marker was placed lateral to the approximate location of the center of the calcaneus when visualized from the lateral side of the body. This marker placement helped define the foot segment in subsequent analyses.

5th Metatarsal Head (R5MH) – This marker was applied to the outside of the shoe because metatarsal heads were covered by the footwear. This landmark was found by palpating the 5th metatarsal until the distal portion of the digit was found. This marker also helped define the foot segment by being the reference marker for the 2nd metatarsal head.

Virtual Markers

These next marker descriptions were virtual markers. This means that the actual position of the marker was relative to locations of physical markers and had to be referenced to a physical marker.

Hip Joint Center – In the current study, the hip joint was idealized as being located horizontally and collinear with the marker placed on the greater trochanter. This marker was then offset by a value that was determined by estimating the distance from the greater trochanter to the acetabulum by using a ruler.

Knee Joint Center – The knee joint center was also a virtual marker. This marker was idealized as being horizontal and collinear with the lateral knee joint line. It was offset by half of the length between the lateral and medial knee joint line markers. The amount of offset was determined by measuring the distance between the lateral and medial knee joint line markers during the static trial and was verified using an anthropometer

Ankle Joint Center – The ankle joint center was also a virtual marker. This marker was estimated to be horizontal and collinear with the lateral malleolus marker. As with the knee joint center, this offset dimension was determined by measuring the distance between the lateral and medial malleolus markers during the static trial and was verified using an anthropometer.

2nd Metatarsal Head – The position of the second metatarsal head was estimated by using the position data from the fifth metatarsal head and the ankle joint center. The anterior/posterior and vertical components of the fifth metatarsal head were used, while the medial/lateral value of the ankle joint center was used to estimate this marker.

Materials and Methods

A Vicon Motion Analysis System (Vicon Inc., Oxford, UK) was used to capture positional data at 100Hz from a skin mounted marker set. Reference videos were captured at 50Hz using a Basler 602f digital video camera. Force data were collected at 1000Hz using an Advanced Mechanical Technology Incorporated AMTI force platform Model OR6-7-1000 (Advanced Mechanical Technology Incorporated, Watertown, MA). All data were recorded and time-synchronized to a personal computer through the Vicon Nexus program. Force plate data were first sent through an AMTI SGA6-4 Signal Conditioner/ Amplifier, to the A2D converter board, to the Vicon MX Control Unit, through the Vicon MX Ultranet unit. The force platform collected six channels of data: forces F_x, F_y, & F_z, and moments M_x, M_y, & M_z. The three motion cameras fed directly into the MX Ultranet unit and into the computer. The motion cameras each had a resolution of 0.3 Megapixels. Each camera recorded a two-dimensional grayscale image of the retro-reflective markers which were placed on the body. Calibration of the system allowed for recreation of the three-dimensional marker motion from these two-dimensional grayscale images. Because the lab has only one force plate embedded in the raised track, markers were only placed on the right side of the body. The right leg was also self-identified as the dominant leg for each subject.

Test Subject Descriptions

Eight healthy subjects (4 male, 4 female) with no history of lower body surgery or other recent lower body problems and the needed shoe sizes (men's size 9 and women's size 8) were recruited for this study. The height and mass of each subject can be found in Table 3.2

Table 3.2 – Subject Demographics

Subject Demographics		
Subject Code	Height (m)	Weight (kg)
Subject F1	1.65	83.9
Subject F2	1.70	54.9
Subject F3	1.65	61.2
Subject F4	1.65	65.8
Subject M1	1.78	86.2
Subject M2	1.83	59.0
Subject M1	1.78	72.3
Subject M2	1.88	68.0

Each subject was tested in seven pairs of shoes designed by Merrell (Wolverine World Wide, Rockford, MI) specifically for this battery of tests. The shoe design was based off the Merrell

Full Pursuit model trail running shoe. The stiffness values of the shoes were measured using an Asker C Durometer scale to measure the stiffness of the ethylene-vinyl acetate (EVA) midsole material. The control shoe had a density of 53 on the Asker C durometer scale across the entire midsole. The lateral stiffened shoe was divided into right and left halves geometrically. The medial half of the midsole was a C 43 and the lateral half was a C 73 (Figure 3.9). The other five prototype production quality shoes were called T-Form shoes. Each T-Form shoe had a stiff medial component that extended from the heel to the medial arch of C 73 durometer. The difference between these shoes was the changing location of a pocket of lateral stiffness at C 73 stiffness. T-Form Shoe 1 had the stiff lateral pocket in the posterior part of the lateral heel. The pocket of stiffness moved anterior with each subsequent shoe, ending with T-Form Shoe 5 having the pocket in the most anterior position of any shoe (Figure 3.10).

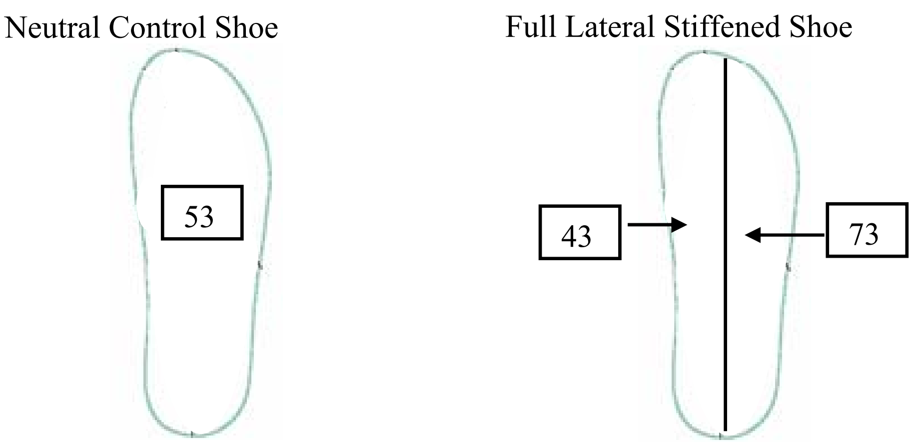

Figure 3.9 – Photo of Merrell Full Pursuit shoe style for neutral control shoe and full lateral stiffened shoe (top) and the location and Asker C Stiffness values for the midsole configurations (bottom)

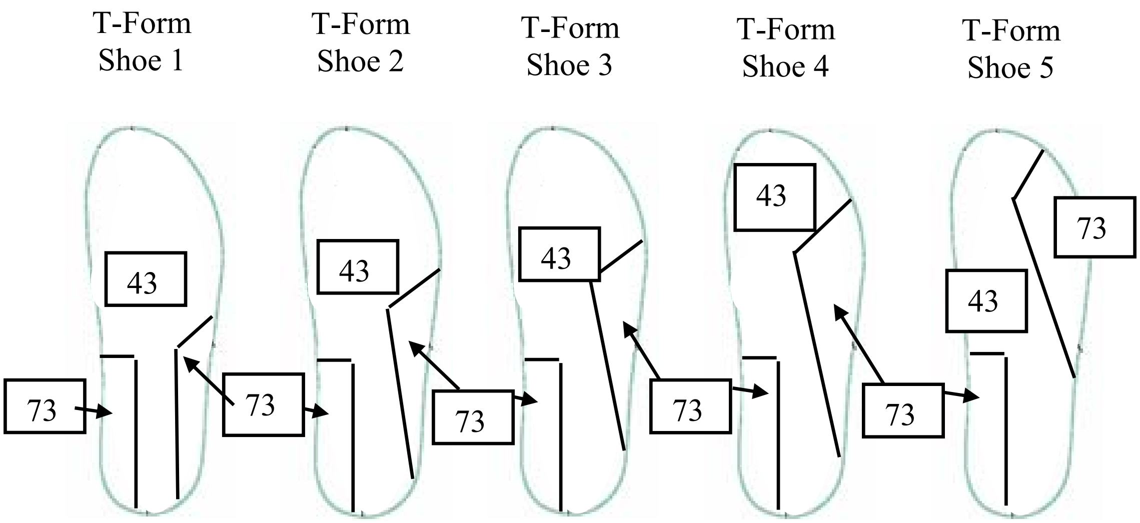

Figure 3.10 – Photo of the Merrell Full Pursuit shoe style for the five T-Form shoes (top) and the location and Asker C Stiffness values for the midsole configurations (bottom)

Testing Procedures

Prior to any walking trials being performed, the scope of the study was explained to the test subject. Informed consent was obtained from each subject. The next step was to apply retro-reflective markers to the skin using 3M double-sided tape reinforced with athletic training paper tape. After application of the markers, the subject was asked to stand straight with their feet shoulder width apart and parallel to each other facing down the length of the track for a static trial. This trial was performed to obtain widths of the knee and ankle joints. The subject was then allowed to practice walking down the track at a self-selected pace so that they could hit the force plate with their right foot. The subject was told not to look down at the force plate during testing to ensure that they did not shorten or lengthen their natural stride to hit the plate. Each subject performed at least three good walking trials in each shoe model (Figure 3.11).

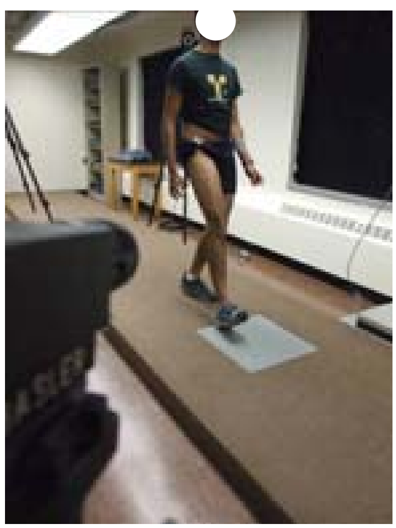

Figure 3.11 – Subject walking in a T-Form model shoe across the force plate

Data Analysis

After data collection was complete, each trial was processed through the Vicon Nexus program. The three-dimensional positional marker data were combined with the force plate data and stored in a .c3d file. The .c3d file was then opened in the Vicon BodyBuilder program. The marker trajectories were then labeled and the dynamic model that was written by the author was applied to the data. The knee adduction moment data could then be exported with units of Newton-millimeters from the BodyBuilder program as a .txt file. These values were then converted to Newton-meters and normalized by dividing this value by the mass of the subject. The units of the normalized data were Newton-meters per kilogram body mass. The data were then plotted (Figure 3.12) and the maximum peak knee adduction moments were recorded for each trial.

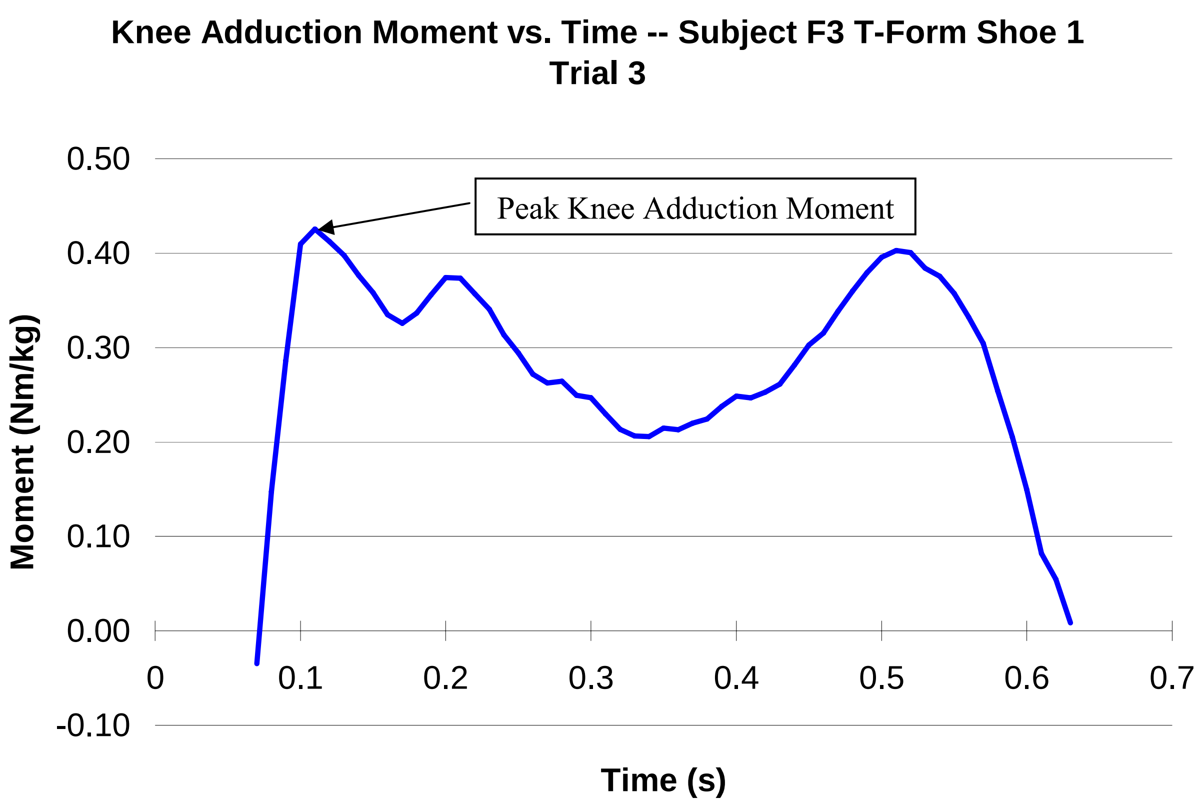

Figure 3.12 – A typical knee adduction moment vs. time plot

Results

As can be seen in Table 3.3, the range of average knee adduction moments was from 0.17 Nm/kg in the Neutral Shoe for Subject M3 to 0.81 Nm/kg in Subject M1 for T-Form Shoe 3. Because there were no statistically significant differences (two-way ANOVA, α =.05, all p>.05) due to the large standard deviation between subjects, trends were said to be changes in the knee adduction moment greater than or equal to 0.05 Nm/kg. These differences are similar to differences found in comparable literature on knee adduction moment changes (Crenshaw et al., 2000; Fisher et al., 2007; Kakihana, Torii et al., 2005; Kerrigan et al., 2002).

Table 3.3 – Average and Standard Deviation of the Knee Adduction Moment (Nm/kg) for Each Subject

	Subject F1		Subject F2		Subject F3		Subject F4	
Footwear Condition	Average	S.D.	Average	S.D.	Average	S.D.	Average	S.D.
Neutral	0.29	0.01	0.35	0.06	0.45	0.03	0.36	0.01
Lateral Stiff	0.31	0.01	0.46	0.04	0.47	0.06	0.38	0.01
T-Form 1	0.35	0.01	0.38	0.03	0.48	0.04	0.40	0.06
T-Form 2	0.32	0.01	0.35	0.02	0.45	0.04	0.44	0.03
T-Form 3	0.32	0.01	0.29	0.03	0.44	0.04	0.48	0.04
T-Form 4	0.32	0.04	0.38	0.06	0.44	0.03	0.39	0.03
T-Form 5	0.30	0.03	0.25	0.09	0.46	0.03	0.44	0.02

	Subject M1		Subject M2		Subject M3		Subject M4	
Footwear Condition	Average	S.D.	Average	S.D.	Average	S.D.	Average	S.D.
Neutral	0.75	0.04	0.37	0.08	0.17	0.03	0.38	0.07
Lateral Stiff	0.57	0.08	0.28	0.00	0.24	0.02	0.31	0.03
T-Form 1	0.73	0.03	0.27	0.08	0.25	0.01	0.37	0.05
T-Form 2	0.76	0.05	0.21	0.07	0.20	0.02	0.39	0.03
T-Form 3	0.81	0.06	0.22	0.06	0.24	0.02	0.35	0.03
T-Form 4	0.75	0.07	0.28	0.01	0.29	0.01	0.35	0.03
T-Form 5	0.80	0.02	0.25	0.11	0.27	0.03	0.35	0.02

Neutral (Control) vs. Lateral Stiffened Shoe

Three of the eight subjects (F1, F3, and F4) had differences less than 0.05 Nm/kg between the neutral and lateral stiffened shoes. In addition, two subjects (F2 and M3) had increases in the adduction moment greater than 0.05 Nm/kg from the neutral shoe to the lateral stiffened shoe. The remaining three subjects (M1, M2, and M4) had decreases in the adduction moment greater than 0.05 Nm/kg.

Neutral (Control) vs. T-Form Shoe 1

Five of the eight subjects (F2, F3, F4, M1, and M4) had less than a 0.05 Nm/kg difference between the control and T-Form Shoe 1. Two subjects (F1 and M3) had an increase in the moment from the neutral shoe to T-Form Shoe 1, and one subject (M2) had a decrease in the knee adduction moment.

Neutral (Control) vs. T-Form Shoe 2

Six of eight subjects (F1, F2, F3, M1, M2, and M4) had a knee adduction moment difference of less than 0.05 Nm/kg between the neutral and T-Form Shoe 2. Subject F4 had an increase in the moment greater than 0.05 Nm/kg from the neutral to T-Form Shoe 2, while Subject M3 had a decrease in knee adduction moment between the neutral and T-Form Shoe 2.

Neutral (Control) vs. T-Form Shoe 3

Four of eight subjects (F1, F3, M1, and M4) did not have a change of greater than 0.05 Nm/kg between the two shoes. Two subjects (F4 and M3) had increases in the adduction moment from the neutral shoe to T-Form Shoe 3 while two subjects (F2 and M2) had a decrease in the adduction moment.

Neutral (Control) vs. T-Form Shoe 4

Six of the eight subjects (F1, F2, F3, F4, M1, and M4) had changes of less than 0.05 Nm/kg between the neutral and T-Form Shoe 4. Subject M2 had a decrease in the adduction moment greater than 0.05 Nm/kg between the neutral shoe and T-Form Shoe 4, while Subject M3 had an increase in the adduction moment.

Neutral (Control) vs. T-Form Shoe 5

Three subjects (F1, F3, and M4) had changes in the adduction moment less than 0.05 Nm/kg between the neutral shoe and T-Form Shoe 5. In addition, Subjects F4, M1, and M3 had an increase in the adduction moment from the neutral shoe to T-Form Shoe 5. Two subjects (F2 and M2) showed a decrease in the adduction moment between the neutral shoe and T-Form Shoe 5.

Average Overall Knee Adduction Moment

As can be seen from Table 3.4, there was almost no difference in the overall average of the knee adduction moment between any of the footwear conditions. The overall variation in values was 0.02 Nm/kg.

Table 3.4 –Average Overall Knee Adduction Moment

	Knee Joint Adduction Moment (Nm/kg) Average (± Standard Deviation)
Neutral	0.39 (± 0.17)
Lateral Stiff	0.38 (± 0.11)
T-Form 1	0.40 (± 0.15)
T-Form 2	0.39 (± 0.18)
T-Form 3	0.39 (± 0.19)
T-Form 4	0.40 (± 0.15)
T-Form 5	0.39 (± 0.18)

Gendered Average Knee Adduction Moment

It can be seen from Table 3.5 that there was an increase of 0.05 Nm/kg in the average female adduction moment from the neutral shoe to the lateral stiff shoe, but a decrease in the male average knee adduction moment of 0.07 Nm/kg. There were no changes greater or equal to 0.05 Nm/kg between the neutral and any of the T-Form style shoes.

Table 3.5 – Gendered Average of the Knee Adduction Moment

	Female Knee Joint Adduction Moment (Nm/kg) Average (± Standard Deviation)
Neutral	0.36 (± 0.07)
Lateral Stiff	0.41 (± 0.08)
T-Form 1	0.40 (± 0.06)
T-Form 2	0.39 (± 0.06)
T-Form 3	0.38 (± 0.09)
T-Form 4	0.38 (± 0.05)
T-Form 5	0.36 (± 0.10)

	Male Knee Joint Adduction Moment (Nm/kg) Average (± Standard Deviation)
Neutral	0.42 (± 0.18)
Lateral Stiff	0.35 (± 0.12)
T-Form 1	0.41 (± 0.19)
T-Form 2	0.39 (± 0.23)
T-Form 3	0.41 (± 0.24)
T-Form 4	0.42 (± 0.20)
T-Form 5	0.42 (± 0.23)

Discussion

The first purpose of this chapter was to develop a dynamic biomechanical model to determine the knee joint adduction moment. This was accomplished with a full dynamic segmental model that accounted for the weight, orientation, and moment of inertia of each lower limb segment. The adduction moment calculation was made with knowledge of the joint center locations, segment orientation, the motion of the limbs, and the ground reaction force. This model would be improved with the addition of markers to each body segment. This would allow for more accurate representation of each segment and allow for additional joints to be represented. Specifically, additional markers on the foot segment would help to better identify the three main planes of subtalar motion to improve the foot kinematics. Also, additional markers in the shank and leg segments could help to extend the model to measure the kinematics and kinetics of the hip joint.

The second and third purposes of the study were to determine the effects of change in midsole density patterns in production model shoes on the knee adduction moment. It was hypothesized that the full lateral stiffened shoes would decrease the knee adduction moment as compared to the neutral shoe condition in a manner similar to the changes documented previously by others (Fisher et al., 2007). In addition, it was unclear whether the T-Form model shoes would significantly change the knee adduction moment because of the shifting lateral stiffened regions and the stiffened medial heel component. It was found that while some subject specific responses to different shoe conditions were found, overall the knee adduction moment was not significantly less in either the full lateral stiffened shoe or any T-Form shoe model, as compared to the neutral control condition. This result was in contrast with the study done by Fisher et. al. study which found differences between a neutral control shoe and a lateral stiffened experimental shoe (Fisher et al., 2007). The effects of the lateral stiffened shoe may have been mitigated by an outsole configuration in the model used in this study versus standing directly on the midsole in the 2007 Fisher et. al. study. In addition, when changes in the knee adduction moment were grouped by gender, there was an increase in the moment in the lateral stiffened shoe as compared to the neutral shoe for female subjects of 0.05 Nm/kg, but an average decrease of 0.07 Nm/kg between the neutral shoe and lateral stiffened shoe for male subjects. These results were not expected, as gender-specific differences in the knee adduction moment in similar conditions were not noted in any prior studies (Kerrigan, Riley, Nieto, & Della Croce, 2000) and the fact that subjects from both genders were used in the studies documenting decreases in adduction moments using lateral wedges and prototype lateral stiffened shoes (Crenshaw et al., 2000; Fisher et al., 2007; Kakihana et al., 2004; Kerrigan et al., 2002).

It is possible that lack of difference in the knee adduction moment between the neutral shoe and any of the T-Form shoes could be attributed to the stiffened medial heel for each design. It has been shown that a medial wedge can effectively increase the adduction moment, decreasing the lateral compartment knee load and mitigating pain in people with lateral compartment knee osteoarthritis (Gross & Hillstrom, 2008). It is possible that stiffening the medial heel of the T-Form shoes helped cancel out the effect of the various laterally stiffened portions of the shoes.

Even though no overall change was found between the neutral and lateral stiffened production shoe condition in subjects without medial compartment knee osteoarthritis, the concept of changing midsole stiffness to elicit a biomechanical response could still have utility. Variable density midsole shoes are sometimes used to prevent or limit the amount of pronation in the form of motion control footwear. If proper density limits and locations could be determined, it could lead to more comfortable footwear interventions to biomechanical problems. It has been said that one reason for a subject to not continuing to wear an orthotic is because of the discomfort of the intervention method (Kerrigan et al., 2002). If variable density midsole shoes were to be explored further, it may lead to more comfortable orthotic intervention methods.

REFERENCES

References

Ahlback, S. (1968). Osteoarthrosis of the knee. A radiographic investigation. *Acta Radiol Diagn (Stockh)*, Suppl 277:277-272.

Crenshaw, S. J., Pollo, F. E., & Calton, E. F. (2000). Effects of lateral-wedged insoles on kinetics at the knee. *Clin Orthop Relat Res*(375), 185-192.

Davis, M. A. (1988). Epidemiology of osteoarthritis. *Clin Geriatr Med, 4*(2), 241-255.

Felson, D. T., Zhang, Y., Hannan, M. T., Naimark, A., Weissman, B., Aliabadi, P., et al. (1997). Risk factors for incident radiographic knee osteoarthritis in the elderly: the Framingham Study. *Arthritis Rheum, 40*(4), 728-733.

Fisher, D. S., Dyrby, C. O., Mundermann, A., Morag, E., & Andriacchi, T. P. (2007). In healthy subjects without knee osteoarthritis, the peak knee adduction moment influences the acute effect of shoe interventions designed to reduce medial compartment knee load. *J Orthop Res, 25*(4), 540-546.

Gross, K. D., & Hillstrom, H. J. (2008). Noninvasive Devices Targeting the Mechanics of Osteoarthritis. *Rheumatic Disease Clinics of North America, 34*, 755-776.

Kakihana, W., Akai, M., Nakazawa, K., Takashima, T., Naito, K., & Torii, S. (2005). Effects of laterally wedged insoles on knee and subtalar joint moments. *Arch Phys Med Rehabil, 86*(7), 1465-1471.

Kakihana, W., Akai, M., Yamasaki, N., Takashima, T., & Nakazawa, K. (2004). Changes of joint moments in the gait of normal subjects wearing laterally wedged insoles. *Am J Phys Med Rehabil, 83*(4), 273-278.

Kakihana, W., Torii, S., Akai, M., Nakazawa, K., Fukano, M., & Naito, K. (2005). Effect of a lateral wedge on joint moments during gait in subjects with recurrent ankle sprain. *Am J Phys Med Rehabil, 84*(11), 858-864.

Kerrigan, D. C., Lelas, J. L., Goggins, J., Merriman, G. J., Kaplan, R. J., & Felson, D. T. (2002). Effectiveness of a lateral-wedge insole on knee varus torque in patients with knee osteoarthritis. *Arch Phys Med Rehabil, 83*(7), 889-893.

Kerrigan, D. C., Riley, P. O., Nieto, T. J., & Della Croce, U. (2000). Knee joint torques: a comparison between women and men during barefoot walking. *Arch Phys Med Rehabil, 81*(9), 1162-1165.

Kuroyanagi, Y., Nagura, T., Matsumoto, H., Otani, T., Suda, Y., Nakamura, T., et al. (2007). The lateral wedged insole with subtalar strapping significantly reduces dynamic knee load in the medial compartment gait analysis on patients with medial knee osteoarthritis. *Osteoarthritis Cartilage, 15*(8), 932-936.

Mow, V. C., & Huiskes, R. (2005). *Basic Orthopaedic Biomechanics and Mechano-Biology* (3rd ed.). Philadelphia: Lippincott Williams & Wilkins.

Mundermann, A., Dyrby, C. O., Hurwitz, D. E., Sharma, L., & Andriacchi, T. P. (2004). Potential strategies to reduce medial compartment loading in patients with knee osteoarthritis of varying severity: reduced walking speed. *Arthritis Rheum, 50*(4), 1172-1178.

Prodromos, C. C., Andriacchi, T. P., & Galante, J. O. (1985). A relationship between gait and clinical changes following high tibial osteotomy. *J Bone Joint Surg Am, 67*(8), 1188-1194.

Wells, R. P. (1981). The projection of the ground reaction force as a predictor of internal joint moments. *Bull Prosthet Res, 10-35*, 15-19.

Winter, D. A. (2005). *Biomechanics and Motor Control of Human Movement* (3rd ed.). Hoboken: John Wiley & Sons, Inc.

CHAPTER 4—EVALUATION OF A NOVEL FOOTWEAR DESIGN AND ITS EFFECTS ON REAR-FOOT MOTION AND MECHANICAL STIFFNESS COMPARISON TO COMMERCIAL MOTION CONTROL SHOES

Introduction

Excessive motion of the foot during gait has been linked to several problems in the lower body. Specifically, excessive pronation and supination have been suggested to be a possible cause of patellofemoral pain syndrome (Duffey, Martin, Cannon, Craven, & Messier, 2000; Tiberio, 1987), Achilles tendon issues (Clement & Taunton, 1981; McCrory et al., 1999; Smart, Taunton, & Clement, 1980), plantar fasciitis (Martin et al., 2001), and shin splints (Viitasalo & Kvist, 1983). In the literature, the terms pronation and supination are often used interchangeably with eversion and inversion, respectively. It is often unclear whether authors are using these terms to describe triplanar or single plane rotations of the foot or heel. In this study, pronation and supination refer to rotations about the anteroposterior axis of the rear-foot, as has been the case in previous studies (Perry & Lafortune, 1995; Stacoff, Kalin, & Stussi, 1991). During gait, the initial motion of pronation and supination takes place in the heel or calcaneus region of the foot. Supination of the foot is shown in Figure 4.1a and pronation of the foot is shown in Figure 4.1b.

Figure 4.1—Anterior view of supination (a) and pronation (b)

Orthotic interventions and footwear alterations have been used as methods to modify the amount of pronation or supination. Stacoff et. al., in a review of orthotic insert studies, reported that orthotics had positive effects (i.e. less pain, better motion control) at rates between 70% and 80% on injured runners (Stacoff et al., 2000). When attempting to modify pronation or supination of the foot, interventions in the posterior part of the shoe are frequently used. Medial stiffening or posting is a typical example of an orthotic design used to treat excessive pronation. Conversely, lateral stiffening or posting may be used to treat excessive supination. Current literature provides two suggestions for the efficacy of orthotics. First, the orthotic may change the anatomical orientation of the foot and ankle structure (Stacoff et al., 2000). Second, the orthotic may stimulate subcutaneous receptors in the foot and cause a change in the neural pathway, thereby altering the progression of the step (Feuerbach, Grabiner, Koh, & Weiker, 1994). In actuality, it may be a combination of these two theories.

Using knowledge of successful orthotic designs, the Bates division of Wolverine World Wide, Inc. (Rockford, MI) developed a novel insole technology designed to mitigate excessive pronation or supination. This design was called the Wave Disk Comfort Technology. The Wave Disk Comfort Technology, or WDCT, was designed to be a user-operated mechanism for people to improve comfort and correct excessive rear-foot motion (Figure 4.2). Top and bottom views of a ring can be found in Figures 4.3 and 4.4. The bottom of the ring contains the disk insertion directions (Figure 4.5). If a user desired to have a strictly anti-pronation setting, they would line up the P arrow on the disk with the arrow on the insole. The disks fit snugly onto a center post in the heel of the modified insole. The post was not designed to carry a load, as it was not in contact with the ground when the heel area was loaded. The post provided an attachment area to ensure the stability of the WDCT disk. This study represents the first biomechanical evaluation of this product.

Figure 4.2 – Posterior view of the modified insert with a Wave Disk (left) and the control insert (right)

Figure 4.3—Top view of a red Wave Disk

Figure 4.4—Bottom view of a blue Wave Disk

Figure 4.5—Bottom view of a right WDCT insole with Wave Disk placed in the anti-pronation setting

The disks work on a simple support principle. The peaks of the insole correspond with the valleys of the WDCT rings and vice versa. The 8 peaks on the WDCT ring are 5 different heights, decreasing in height around half the circumference (Figure 4.6 and Figure 4.7). The ring design allows a user to determine the orientation of the directionally labeled disk. For persons who would be considered excessive pronators, the disks would be aligned in the insole as shown in Figure 4.6. For a person that needs more heel support on the lateral side, the disks would be placed in the position as shown in Figure 4.7. The additional support is believed to bias an individual so that they favor an altered rear-foot position; and as a result, limit the amount of excessive rear-foot motion.

The other two extremes that the WDCT rings could be placed in were designated Firm (F), and Regular (R), and would place the tallest peak at the rear of the heel or the anterior portion of the heel, respectively. It is noted that these two positions represented a comfort setting rather than a biomechanically-active setting, and therefore were not tested for their rearfoot motion-limiting capabilities. It should be noted that it would also be possible for the WDCT rings to be placed in a manner such that the user would experience elements of anti-pronation and firm, anti-pronation and regular, anti-supination and firm, and anti-supination and regular. Biomechanical evaluations of these settings were not performed during this round of testing as the settings were not thought to provide maximum anti-pronation or anti-supination characteristics because of the offset orientation of the technology.

Figure 4.6—Posterior view of the red Wave Disks in the anti-pronation setting

Figure 4.7—Posterior view of the red Wave Disks in the anti-supination setting

The purpose of this study was to determine if the novel WDCT footwear technology could alter the amount of rear-foot pronation or supination during gait. It was hypothesized that the anti-pronation setting would reduce rear-foot pronation as measured in human subjects during walking gait. In addition, it was hypothesized that the amount of medial stiffness, as measured in the heel region of the insole, would exceed the stiffness in the lateral facet when the disc was placed in the anti-pronation setting. The anti-supination setting was thought to exhibit similar alterations in rear-foot motions and insole stiffness, but affecting the opposite side of the foot and insole heel region. The results of this study may influence future orthotic and insert design towards designs that are able to be changed by the end user for comfort and function, rather than having just one permanent setting.

Materials and Methods

Footwear and Wave Disk Comfort Technology

Two different pairs of Bates Stock Number B06-21 boots were used for these tests (Figure 4.8). Both pairs were men's size 8 boots with medium width characteristics and the same outer shell. The control pair of boots was unmodified, while the test pair of boots was modified in order to be able to house the Wave Disk Comfort Technology rings with a special insole that housed the rings. The modification was most noticeable in the heel region, as extra vertical room was made for allowable clearances between the foot and the boot while factoring in the extra height of the circular inserts.

Figure 4.8 – Bates B06-21 Boots

For this study, the disks were tested in their anti-pronation and anti-supination settings.

Subjects

Two male subjects without a history of foot or ankle surgery or other orthopaedic problems were tested in three experimental conditions – a control setting, an anti-supination setting, and an anti-pronation setting.

Kinematics and Kinetics

Ground reaction force data were collected at 1000 Hz using an AMTI OR 6-7 force plate (Advanced Mechanical Technology, Inc., Watertown, MA) embedded in a raised track in the Orthopaedic Biomechanics Gait Laboratory. Kinematic ankle data were collected using a three camera Vicon motion capture system (Vicon, OMB plc., Oxford, UK) at 100 Hz. In order to evaluate ankle motion, retro-reflective marker sets were attached posterior to the calcaneus

(Figure 4.9) and at the base of the third metatarsal on the dorsal (top) side of the foot (Figure 4.10). Each marker was 9 mm in diameter.

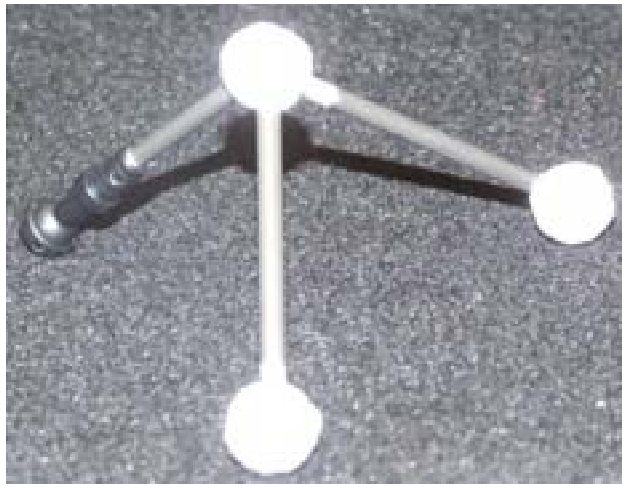

Figure 4.9—Marker set for the posterior calcaneus

Figure 4.10—Marker set for the dorsal forefoot

The attachment sites for the custom marker arrays were made by taping a flexible receiving piece to the foot (Figure 4.11). This type of attachment is not suitable for measurement of precise skeletal motion (Stacoff et al., 2000) because the arrays cannot be directly attached to the bone, but is suitable to measure the motions of the posterior foot during the gait cycle. The custom marker arrays were designed for ease of rear foot motion calculation. The Euler angle measurement was based on defining the axis of rear-foot rotation that was defined to be pronation and supination motions. The forward-placed marker set was important in discerning the spacial orientation of the foot during the testing as well as defining the direction of motion for visualization in the motion capture software.

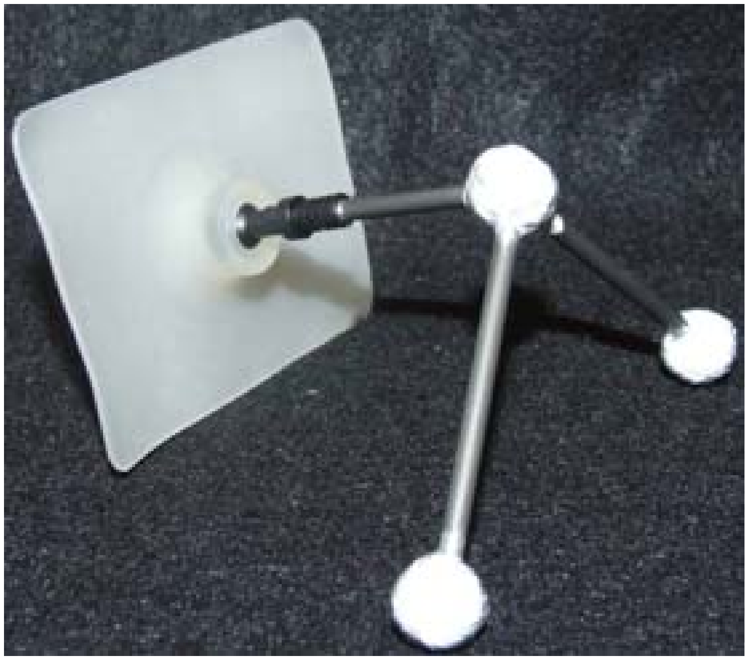

Figure 4.11—Picture of the posterior calcaneus marker set placed in the flexible receiving piece

Kinetic and Kinematic Procedure

Subjects had their right foot taped such that the cup portion of the flexible receiving piece was firmly in contact with both the skin posterior to the calcaneus and the base of the third metatarsal (Figure 4.12a). Figure 4.12b shows how the marker sets appear before placing the foot in the boot. Because of the size of the marker sets, the foot could not be placed inside of the boot with the marker sets already attached. The subject then placed the boot over the taped foot without the maker sets such that the insertion cups were visible through the holes that were cut in the shoe. The marker sets were then placed in their subsequent locations and were checked to ensure that the posts emanating from the foot did not contact the sides of the holes or the ground in the shoes during walking gait (Figure 4.12c).

Figure 4.12—From top left, clockwise—(a) Right foot taped with flexible receiving pieces exposed; (b) Right foot with marker sets attached; (c) Right foot with boot and marker sets attached

Prior to performing recorded trials, the subject was allowed to practice walking at a self-selected pace along the raised track in order to ensure that the force plate would capture their entire step without looking at the force plate. This was done to ensure that the subject did not alter their gait in order to hit the force plate with either a short or long stride which would produce data inconsistent with a normal walking gait pattern. Once the subject was comfortable with the walking protocol, the rear-foot marker set was aligned such that the axis of rear-foot motion was perpendicular to the plane of the marker set. This was done to easily measure the rotation angle between the ground and rear-foot. The kinetics and kinematics were then collected using the force plate and motion capture system. Each subject performed at least three walking trials in the control shoe, three in the test shoe with the disk in anti-pronation setting, and three in the disk in the anti-supination setting. The control shoe was an unmodified version of the Bates B06-21 boots. Analysis was performed using a custom program designed in the Vicon BodyBuilder software package to measure the angle of the heel with respect to the horizontal plane.

Changes in angular rotation were measured between different established events that occur during a typical gait cycle. The measurements were made at three time intervals – between maximum braking force and first peak vertical force, between first peak vertical force and mid-stance, and between braking force and mid-stance. The maximum braking force occurs in the anterior-posterior direction, while the first peak and mid-stance events are determined from the vertical force component of the ground reaction force (Figure 4.13).

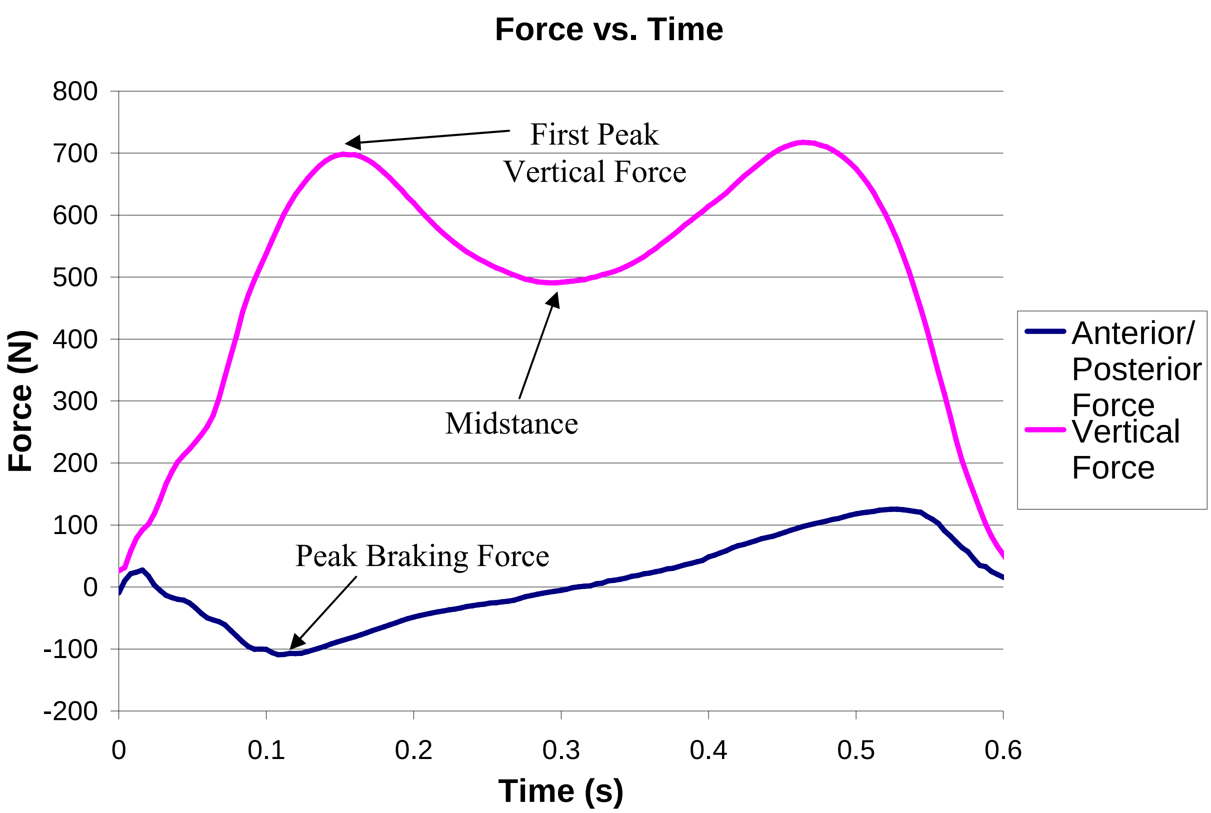

Figure 4.13 – Graphical Explanation of Standard Gait Events

Motions that occur after mid-stance were not considered because the majority of the force that is being applied through the foot after mid-stance does not contact the area where the WDCT is applied. The angles reported are the changes in the angle from the first event to the second event (i.e. change in angle from braking to first peak). A positive value means a pronation motion, while a negative value indicates a supination motion. Change in rear-foot angles were measured until mid-stance because Hintermann and Nigg (1998) have documented that the foot rotates from initial contact with the ground until the mid-stance phase of gait. Also, after mid-stance, the heel begins to rise off the ground, making the motion forward of the heel technology.

Mechanical Footwear Construction Testing Procedure

The impact of the WDCT on the physical properties of the insole was assessed via mechanical testing. The right insole was taken out of the boot and tested in a custom stiffness test using an Instron machine (Instron, Inc., Norwood, MA) and a rectangular indenter head measuring 19mm x 42mm. This indenter head had a surface area that was exactly half of the area used in a standard shoe impact test (ASTM F1976-06). The heel of the Wave Disk insole was divided into two areas (medial and lateral) centered about the hole in the WDCT ring. The two divisions are highlighted in the following figure (Figure 4.14).

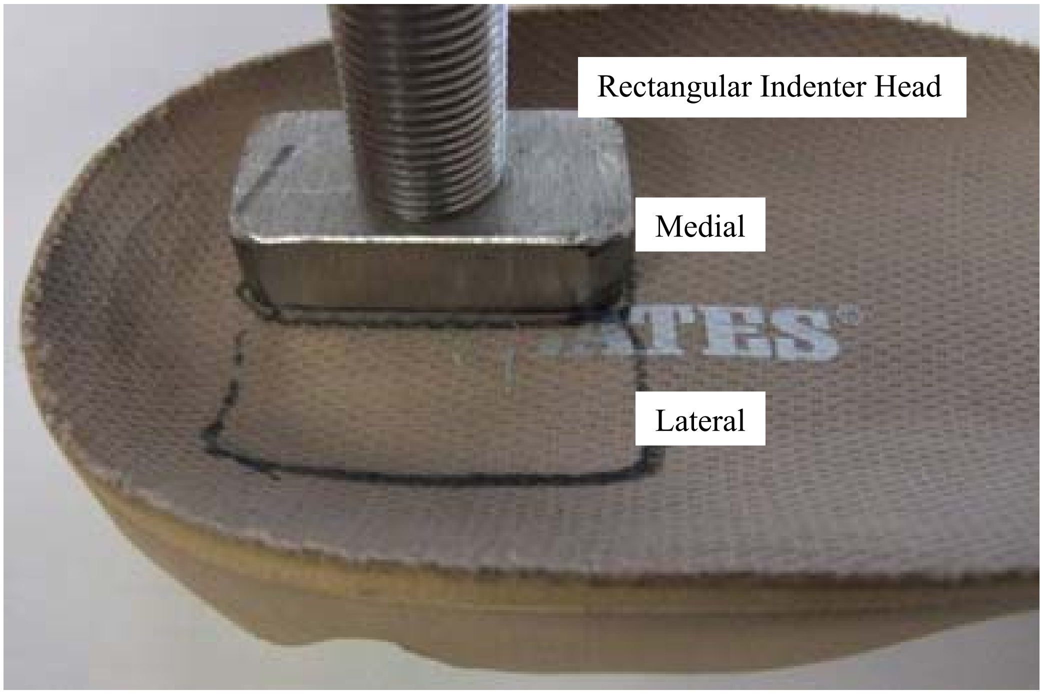

Figure 4.14 – Location of Instron stiffness testing using 19mm x 42mm rectangular indenter head

Each part of the heel was loaded to 623 N and the amount of deformation of the insole was measured. The stiffness was calculated by dividing the peak load by the peak deformation. These tests were performed using the WDCT ring in anti-pronation and anti-supination settings. For stiffness comparison purposes, the same stiffness test was performed on other shoes that were considered to be motion control shoes based on their marketing and design.

Kinematic Results

As can be seen in all tables, the amount of inversion or eversion occurring was generally small in magnitude. In Table 4.1, the amount of rotation from braking to the first peak vertical force was described. Subject 1 exhibited more eversion in both the Anti-Pronation and Anti-Supination setting when compared to the Control setting, but had less eversion in the Anti-Pronation setting as compared to the Anti-Supination setting. Subject 2 did not exhibit a significant difference in the average change in angle for any of the three test conditions.

Table 4.1 – Summary of angle change from braking to first peak

Subject 1 Shoe Condition	Braking to First Peak Change in Angle (deg.)	Average Change
Control Trial 1	0.85	-0.32
Control Trial 2	-2.48	
Control Trial 3	0.67	
Red Disk, Anti-Pronation Trial 1	2.22	1.09
Red Disk, Anti-Pronation Trial 2	0.00	
Red Disk, Anti-Pronation Trial 3	1.05	
Red Disk, Anti-Supination Trial 1	2.60	1.87
Red Disk, Anti-Supination Trial 2	0.44	
Red Disk, Anti-Supination Trial 3	2.56	

Subject 2 Shoe Condition	Braking to First Peak Change in Angle (deg.)	Average Change
Control Trial 1	-0.53	-0.23
Control Trial 2	0.60	
Control Trial 3	-0.75	
Red Disk, Anti-Pronation Trial 1	0.15	-0.16
Red Disk, Anti-Pronation Trial 2	-0.39	
Red Disk, Anti-Pronation Trial 3	-0.24	
Red Disk, Anti-Supination Trial 1	-0.33	-0.31
Red Disk, Anti-Supination Trial 2	-0.19	
Red Disk, Anti-Supination Trial 3	-0.41	

In the comparison of the angle change from the first peak to midstance phases of gait, Subject 1 had decreases in eversion in both the Anti-Pronation setting and the Anti-Supination setting when compared to the Control setting. Subject 2 exhibited a small decrease in eversion in the

Anti-Pronation setting compared to the Control setting and no significant change in the comparison between the Anti-Supination setting and the Control setting.

Table 4.2 – Summary of Angle Change from First Peak to Midstance

Subject 1 Shoe Condition	First Peak to Midstance Change in Angle (deg.)	Average Change
Control Trial 1	-0.25	1.37
Control Trial 2	2.84	
Control Trial 3	1.51	
Red Disk, Anti-Pronation Trial 1	0.27	0.75
Red Disk, Anti-Pronation Trial 2	0.77	
Red Disk, Anti-Pronation Trial 3	1.21	
Red Disk, Anti-Supination Trial 1	-3.86	-1.40
Red Disk, Anti-Supination Trial 2	-0.51	
Red Disk, Anti-Supination Trial 3	0.17	

Subject 2 Shoe Condition	First Peak to Midstance Change in Angle (deg.)	Average Change
Control Trial 1	0.57	1.24
Control Trial 2	1.93	
Control Trial 3	1.23	
Red Disk, Anti-Pronation Trial 1	2.26	0.70
Red Disk, Anti-Pronation Trial 2	1.07	
Red Disk, Anti-Pronation Trial 3	-1.23	
Red Disk, Anti-Supination Trial 1	0.41	1.33
Red Disk, Anti-Supination Trial 2	1.46	
Red Disk, Anti-Supination Trial 3	2.12	

Subject 1 had an increase in eversion when comparing the Anti-Pronation to the Control, and a decrease when comparing the Anti-Supination to the Control. Subject 2 showed a decrease in eversion from the Anti-Pronation setting as compared to the Control setting, and no change between the Anti-Supination setting and the Control.

Table 4.3 – Summary of Angle Change from Braking to Midstance

Subject 1 Shoe Condition	Braking to Midstance Change in Angle (deg.)	Average Change
Control Trial 1	0.60	1.05
Control Trial 2	0.36	
Control Trial 3	2.18	
Red Disk, Anti-Pronation Trial 1	2.49	1.84
Red Disk, Anti-Pronation Trial 2	0.77	
Red Disk, Anti-Pronation Trial 3	2.26	
Red Disk, Anti-Supination Trial 1	-1.26	0.47
Red Disk, Anti-Supination Trial 2	-0.07	
Red Disk, Anti-Supination Trial 3	2.73	

Subject 2 Shoe Condition	Braking to Midstance Change in Angle (deg.)	Average Change
Control Trial 1	0.04	1.02
Control Trial 2	2.53	
Control Trial 3	0.48	
Red Disk, Anti-Pronation Trial 1	2.41	0.54
Red Disk, Anti-Pronation Trial 2	0.68	
Red Disk, Anti-Pronation Trial 3	-1.47	
Red Disk, Anti-Supination Trial 1	0.08	1.02
Red Disk, Anti-Supination Trial 2	1.27	
Red Disk, Anti-Supination Trial 3	1.71	

Mechanical Testing Results

As can be seen from Table 4.4, the insole with the Wave Disk performed as intended, with the stiffness of the medial side in the anti-pronation setting being stiffer than the lateral side. The technology is also properly working in the anti-supination setting, with the lateral side being stiffer than the medial side.

Table 4.4 – Stiffness values for B06-21 Insole with Red Wave Disk

Description	Disk Setting	Heel Location	Input Force (N)	Displacement (mm)	Stiffness Values (N/mm)	% Difference
Right B 06-21 Insole, Red Wave Disk	Anti-Pronation	Medial	625.059	6.209	100.67	10.74%
Right B 06-21 Insole, Red Wave Disk	Anti-Pronation	Lateral	624.317	6.947	89.87	
Right B 06-21 Insole, Red Wave Disk	Anti-Supination	Medial	624.873	7.539	82.89	19.40%
Right B 06-21 Insole, Red Wave Disk	Anti-Supination	Lateral	625.337	6.081	102.83	

In order to understand how the stiffness of the anti-pronation setting values compared with production model shoes designed to prevent excessive pronation, the same Instron test was performed on three motion control shoes.

Table 4.5 – Stiffness Values for Select Motion Control Shoes

Shoe Description	Heel Location	Input Force (N)	Displacement (mm)	Stiffness Values (N/mm)	% Difference
Merrell Motion Control	Medial	623.791	8.017	77.81	13.90%
Merrell Motion Control	Lateral	624.207	9.317	67.00	
Saucony Grid Stabil 6	Medial	624.115	9.003	69.33	12.28%
Saucony Grid Stabil 6	Lateral	623.466	10.252	60.82	
Asics Gel Foundation	Medial	623.744	8.092	77.08	18.37%
Asics Gel Foundation	Lateral	623.791	9.914	62.92	

The results of comparing the lateral and medial sides of the three motion control shoes were similar, as a Merrell motion control shoe was 10.81 N/mm stiffer on the medial side as compared to the lateral side, the Saucony Grid Stabil 6 was 8.51 N/mm stiffer medial, and the Asics Gel Foundation VI was 14.16 N/mm stiffer medial.

Discussion

This study focused on how a novel footwear design affected pronation and supination during walking and how the design mechanically compared to current rear-foot motion control footwear. It was hypothesized that the footwear design would change the amount of rear-foot motion compared to a control setting. Also, it was hypothesized that the new footwear design would have similar medial and lateral stiffness characteristics as compared to commercially-available motion control shoes. Motion control shoes have been shown to be effective at reducing rear-foot motion (Cheung & Ng, 2007). It was found that the WDCT insole had similar stiffness characteristics as commercial motion control shoes, but results from subject testing did not indicate that the technology was effective at changing the amount of rear-foot motion during walking. Even though there was a medial and lateral heel stiffness difference similar to motion control shoes, both sides of the WDCT insole were stiffer than any motion control shoe.

Because the insole behaved as intended in the mechanical tests, it was thought that the change in subtalar motion during the biomechanical tests may be attributed to the construction of the boot. The boot upper, heel cup and medial mid-foot region of the boot were stiff, and did not allow much rotational movement when the boot was laced. This feature may have limited the effects of the WDCT in this particular style of boot. In this study, the change in angle was measured with respect to the horizontal. If the study was to be repeated, it is suggested that the angle of rear-foot motion should be measure with respect to the angle of the tibia instead of a fixed horizontal. This would provide a consistent reference plane with respect to the rear-foot motion and is similar to testing described in literature (Cheung & Ng, 2007; Stacoff et al., 2000).

Even though no difference was found in the rear-foot kinematics in this boot model, the WDCT still may be a viable idea. If the technology was implemented in a mid-top or low top shoe, the technology may be more effective because of the increase in subtalar mobility in footwear with shorter upper construction. However, there is generally more vertical heel room in a taller boot as compare to a low-top shoe, and without modifying the WDCT it could be difficult to successfully put the disc in a lower profile type of footwear. Also, to fully validate the technology, more subjects as well as subjects who have excessive pronation problems should be tested. Further testing of the WDCT may reveal a decrease in excessive rear-foot motion during the gait of certain individuals, possibly mitigating the risk of injury and discomfort.

REFERENCES

References

Cheung, R. T. H., & Ng, G. Y. F. (2007). Efficacy of motion control shoes for reducing excessive rearfoot motion in fatigued runners. *Physical Therapy in Sport, 8*, 6.

Clement, D. B., & Taunton, J. E. (1981). A guide to the prevention of running injuries. *Aust Fam Physician, 10*(3), 156-161, 163-154.

Duffey, M. J., Martin, D. F., Cannon, D. W., Craven, T., & Messier, S. P. (2000). Etiologic factors associated with anterior knee pain in distance runners. *Med Sci Sports Exerc, 32*(11), 1825-1832.

Feuerbach, J. W., Grabiner, M. D., Koh, T. J., & Weiker, G. G. (1994). Effect of an ankle orthosis and ankle ligament anesthesia on ankle joint proprioception. *Am J Sports Med, 22*(2), 223-229.

Martin, J. E., Hosch, J. C., Goforth, W. P., Murff, R. T., Lynch, D. M., & Odom, R. D. (2001). Mechanical treatment of plantar fasciitis. A prospective study. *J Am Podiatr Med Assoc, 91*(2), 55-62.

McCrory, J. L., Martin, D. F., Lowery, R. B., Cannon, D. W., Curl, W. W., Read, H. M., Jr., et al. (1999). Etiologic factors associated with Achilles tendinitis in runners. *Med Sci Sports Exerc, 31*(10), 1374-1381.

Perry, S. D., & Lafortune, M. A. (1995). Influences of inversion/eversion of the foot upon impact loading during locomotion. *Clin Biomech (Bristol, Avon), 10*(5), 253-257.

Smart, G. W., Taunton, J. E., & Clement, D. B. (1980). Achilles tendon disorders in runners--a review. *Med Sci Sports Exerc, 12*(4), 231-243.

Stacoff, A., Kalin, X., & Stussi, E. (1991). The effects of shoes on the torsion and rearfoot motion in running. *Med Sci Sports Exerc, 23*(4), 482-490.

Stacoff, A., Reinschmidt, C., Nigg, B. M., van den Bogert, A. J., Lundberg, A., Denoth, J., et al. (2000). Effects of foot orthoses on skeletal motion during running. *Clin Biomech (Bristol, Avon), 15*(1), 54-64.

Tiberio, D. (1987). The effect of excessive subtalar joint pronation on patellofemoral mechanics: a theoretical model. *J Orthop Sports Phys Ther, 9*(4), 160-165.

CHAPTER 5 – SUMMARY AND FUTURE DIRECTIONS OF STUDY

This thesis documented methods for measuring biomechanical changes due to modifications in footwear midsole characteristics. Shifts in the foot center of pressure related to changes in midsole stiffness and varying locations of increased midsole stiffness were measured using an insole plantar pressure measurement system. In addition, knee adduction moments and their response to full lateral stiffened shoes, as well as five other experimental shoe designs were measured by using a full dynamic biomechanical model. Also, a novel footwear technology designed to alter rear-foot motion was evaluated using a motion capture system.

In Chapter 2, an insole pressure measurement system was used to measure shifts in the center of pressure in response to variations in midsole stiffening characteristics. The two shoe conditions that elicited changes in the center of pressure were the full medial stiffened and the medial stiffened heel with a lateral stiffened forefoot. Both footwear conditions consistently shifted the center of pressure toward the lateral border of the shoe. It was noted that when the shift did occur, it happened in the midfoot region and not at the heel and toe-off areas. In addition, even when the center of pressure shift did occur for a majority of steps, it did not occur in each step. This result coincided with results documented in the literature (B. M. Nigg et al., 2003). The shift in the center of pressure was not large, as large shifts in the center of pressure may lead to ankle joint instability and possible injury (Fuller, 1999). The knowledge that changes in midsole density can change the center of pressure could be important to provide an alternative to uncomfortable orthotics. If a patient is not comfortable with an orthotic intervention, they are less likely to continue its use. If the same biomechanical end results from an orthotic can be achieved through a less invasive method, such as a variable stiffness midsole, patients may benefit by use of this more comfortable intervention.

In Chapter 3, a lower body biomechanical model was developed in order to measure knee adduction moments. It is important to be able to manipulate this moment, as it has been shown that decreasing the knee adduction moment can slow the onset or progression of medial compartment knee osteoarthritis. People with knee osteoarthritis are 10 times for likely to have osteoarthritis in the medial compartment compared to the lateral compartment (Ahlback, 1968). Current methods for decreasing the adduction moment include lateral wedges and invasive surgeries, such as the high tibial osteotomy. A study by Fisher et. al. documented that stiffening the lateral half of the midsole by 20% and 50%, as compared to the medial half, decreased the adduction moment in a fashion similar to a 4 degree lateral wedge (Fisher, Dyrby, Mundermann, Morag, & Andriacchi, 2007). This result was important, but their footwear was experimental and not a typical production quality shoe. The biomechanical model was used to evaluate the knee adduction moment in eight healthy subjects (four male, four female) while walking over a force plate in seven different shoe conditions with different midsole characteristics. The footwear conditions were a neutral control shoe with a constant density throughout, a full lateral stiffened shoe, and five T-Form shoes with a stiff medial heel component and a changing location of a pocket of lateral stiffness. All shoes were production quality. On average, no significant change was found between the neutral control shoe and any of the six test shoes. The overall variation in the average knee adduction moment for all subjects was 0.02 Nm/kg. One interesting finding was that the adduction moment decreased on average from the neutral to the lateral stiffened shoe in male subjects, but increased in female subjects. No differences were found between the T-Form model shoes and the neutral control shoe. It was also interesting that the neutral shoe generated a larger adduction moment in the male subjects than in the female subjects. This was not expected, as gender-specific differences have not been noted in previous literature. In fact, Kerrigan et. al. found no difference in the adduction moment between men and women walking barefoot (Kerrigan, Riley, Nieto, & Della Croce, 2000). Even though no overall change was found between the neutral control shoe and the other shoe conditions, the concept of variable density midsole stiffness shoes could still have utility. Refining the midsole design and stiffness characteristics could lead to effect subject specific biomechanical interventions to not only medial compartment knee osteoarthritis, but lateral compartment osteoarthritis as well.

In Chapter 4, a novel footwear technology was designed to alter rear-foot motion. The design was compared mechanically to current rear-foot motion control footwear. This technology was called the Wave Disk Comfort Technology (WDCT). It was documented that the WDCT insole had similar medial and lateral heel stiffness characteristics as commercial motion control shoes, but subject testing did not indicate that it was effective in changing the amount of rear-foot pronation in our subjects. Because the insole behaved as intended in mechanical testing, it was surmised that the lack of significant results in the subject testing could possibly be attributed to the commercial boot construction. The build of the boot may have been such that there were rear-foot motion limiting characteristics built into the shoe via the stiffness and rigidity of the heel cup and boot upper. Even though no significant differences were documented in rear-foot motion in the current study on the WDCT, it may still have utility when implemented in a low or mid top model boot. It may be more effective because there may be more subtalar mobility in those types of footwear. In fact, this design concept has been implemented in a number of footwear models by Wolverine World Wide, Inc. The device is also currently being re-designed to improve efficacy across a wider range of footwear designs. Based on the studies performed for this thesis, we have suggested that it would be appropriate to test more subjects, both male and female, and test subjects who might have excessive rear-foot motion to fully evaluate this footwear technology. To date, only subjects considered "normal" have been used in evaluations of such technologies.

This research was performed to develop biomechanical models and use them to begin to evaluate changes in the midsole characteristics of footwear that is designed to elicit changes in various gait patterns. The work often represented early studies in the Orthopaedic Biomechanics Laboratories Gait Lab at MSU. The studies described here suggest changes in midsole stiffness characteristics may be able to alter center of pressure and knee adduction moments in selected test subjects.

In addition to developing baseline experimental methods to compare more completely the effects of various footwear technologies in Wolverine World Wide, Inc. footwear versus its competitors, this thesis has allowed this laboratory to begin research in the area of "whole–body" biomechanics. In the process the Vicon Motion Capture system was purchased, the BodyBuilder software and BodyLanguage modeling was learned, an insole pressure measurement has been developed and used for gait evaluations, and future plans are to incorporate the measurement of muscle activity through electromyography (EMG) data into these evaluation technologies. Such information is of current interest in unstable shoe design to provide muscle toning (B. Nigg, Hintzen, & Ferber, 2006) and barefoot running shoes to help strengthen foot and lower body musculature (Lieberman et al., 2010).

REFERENCES

References

Ahlback, S. (1968). Osteoarthrosis of the knee. A radiographic investigation. *Acta Radiol Diagn (Stockh)*, Suppl 277:277-272.

Fisher, D. S., Dyrby, C. O., Mundermann, A., Morag, E., & Andriacchi, T. P. (2007). In healthy subjects without knee osteoarthritis, the peak knee adduction moment influences the acute effect of shoe interventions designed to reduce medial compartment knee load. *J Orthop Res, 25*(4), 540-546.

Fuller, E. A. (1999). Center of pressure and its theoretical relationship to foot pathology. *J Am Podiatr Med Assoc, 89*(6), 278-291.

Kerrigan, D. C., Riley, P. O., Nieto, T. J., & Della Croce, U. (2000). Knee joint torques: a comparison between women and men during barefoot walking. *Arch Phys Med Rehabil, 81*(9), 1162-1165.

Lieberman, D. E., Venkadesan, M., Werbel, W. A., Daoud, A. I., D'Andrea, S., Davis, I. S., et al. (2010). Foot strike patterns and collision forces in habitually barefoot versus shod runners. *Nature, 463*(7280), 531-535.

Nigg, B., Hintzen, S., & Ferber, R. (2006). Effect of an unstable shoe construction on lower extremity gait characteristics. *Clin Biomech (Bristol, Avon), 21*(1), 82-88.

Nigg, B. M., Stergiou, P., Cole, G., Stefanyshyn, D., Mundermann, A., & Humble, N. (2003). Effect of shoe inserts on kinematics, center of pressure, and leg joint moments during running. *Med Sci Sports Exerc, 35*(2), 314-319.

APPENDICES

APPENDIX A

DATA FROM CHAPTER 2

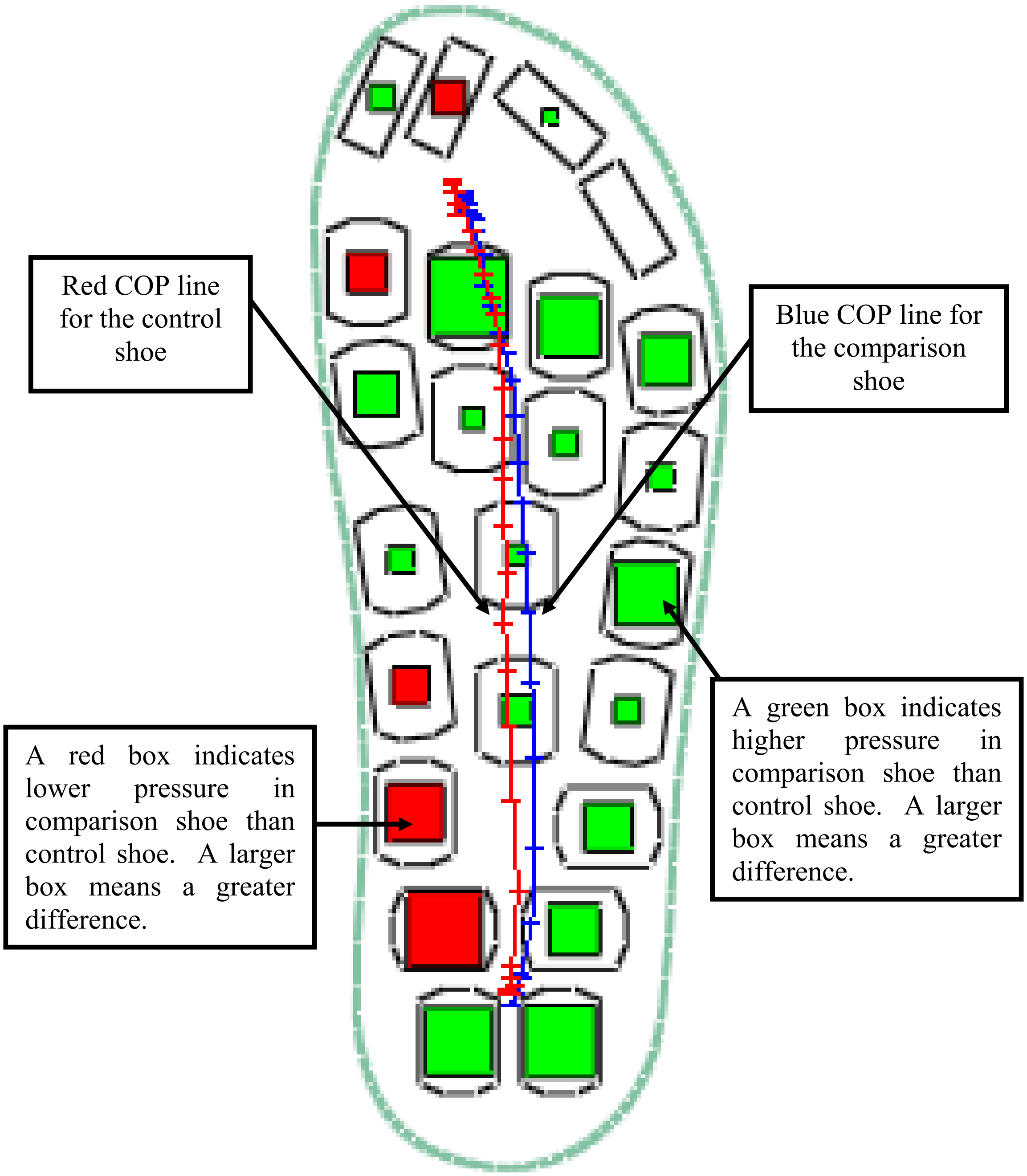

Figure A.1 – Definitions of terms and visualizations for reading Parotec data

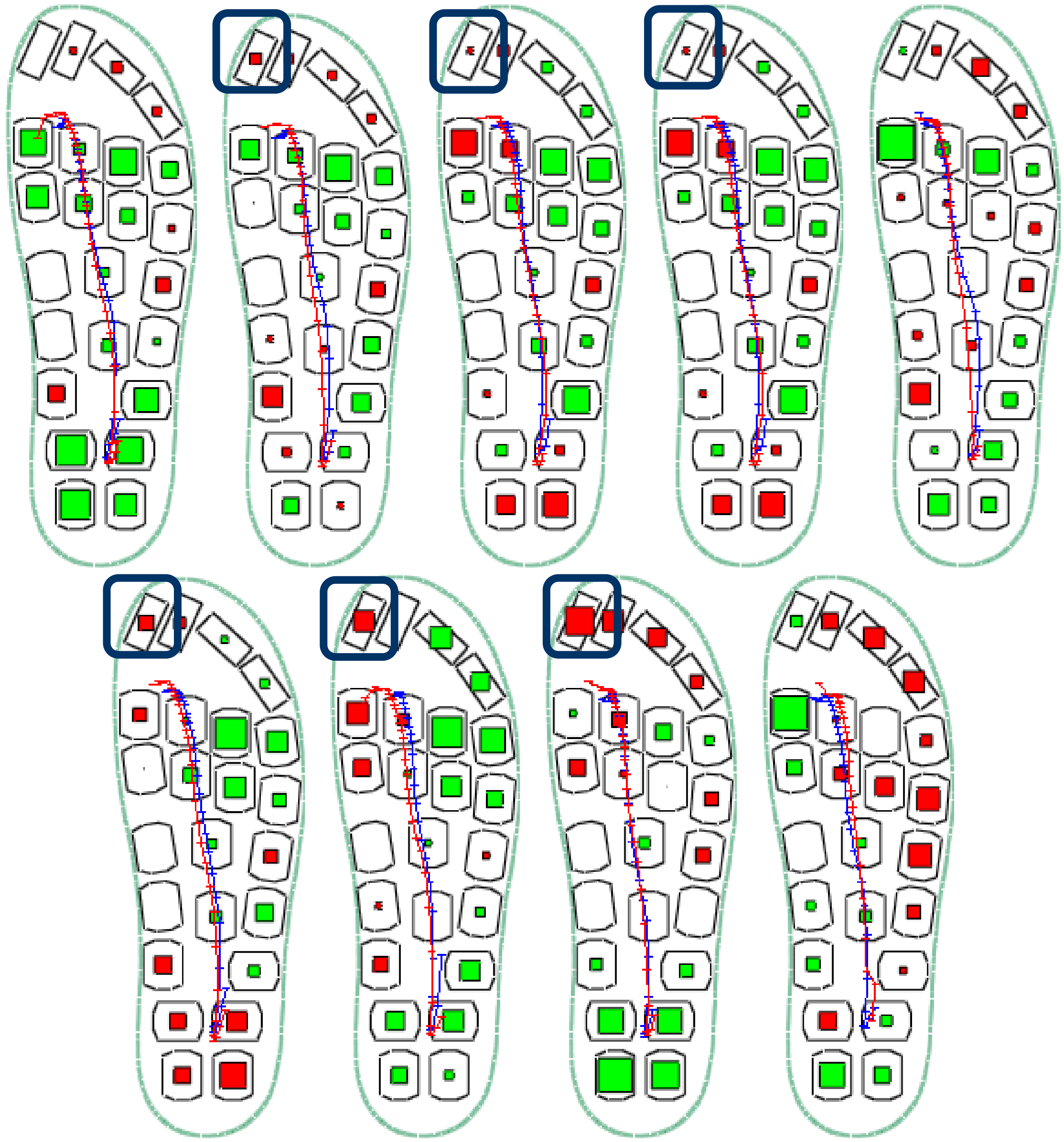

Figure A.2 – Subject M1 Data - Shoe 1 vs. Shoe 2

Figure A.3 – Subject M1 Data - Shoe 1 vs. Shoe 3

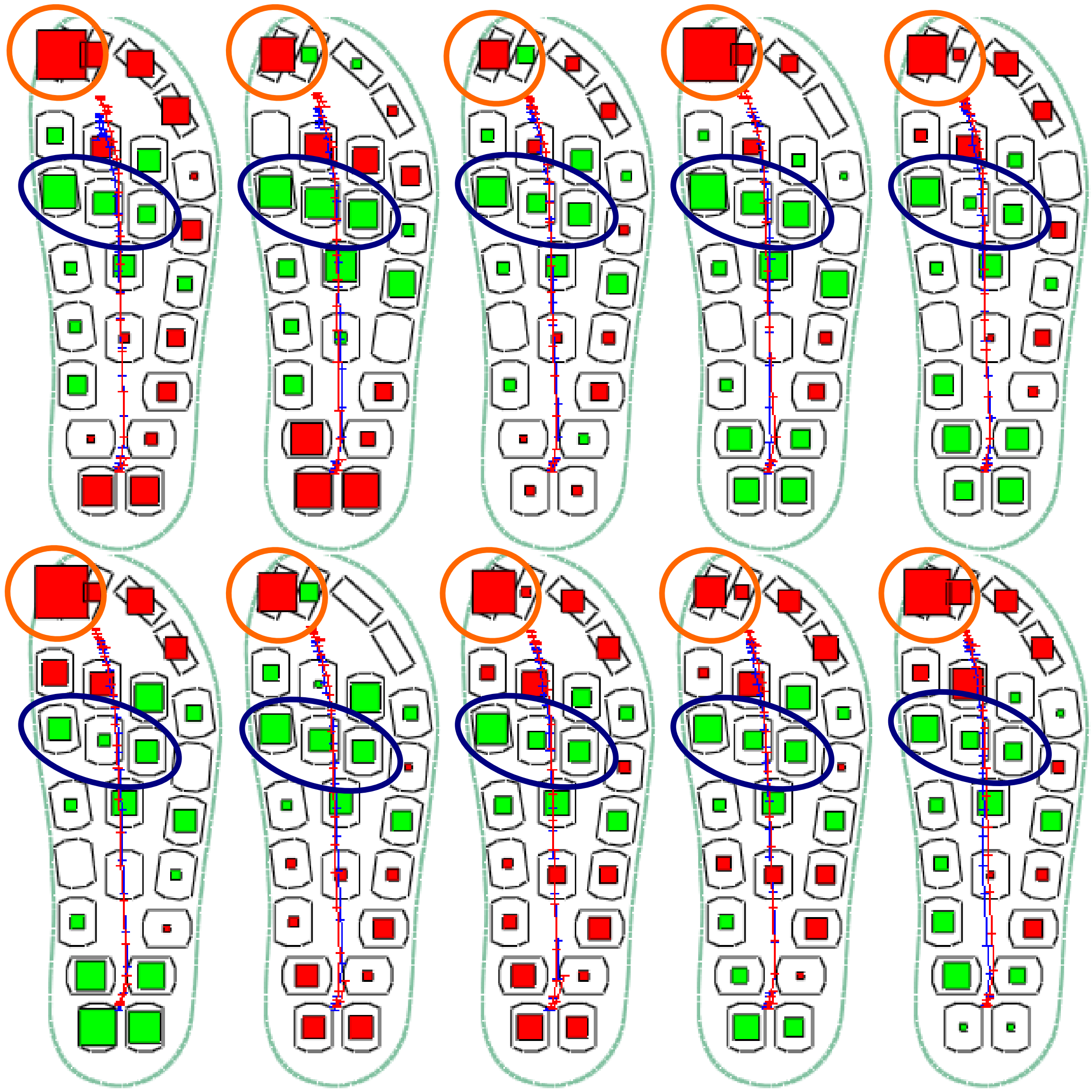

Figure A.4 – Subject M1 Data - Shoe 1 vs. Shoe 4

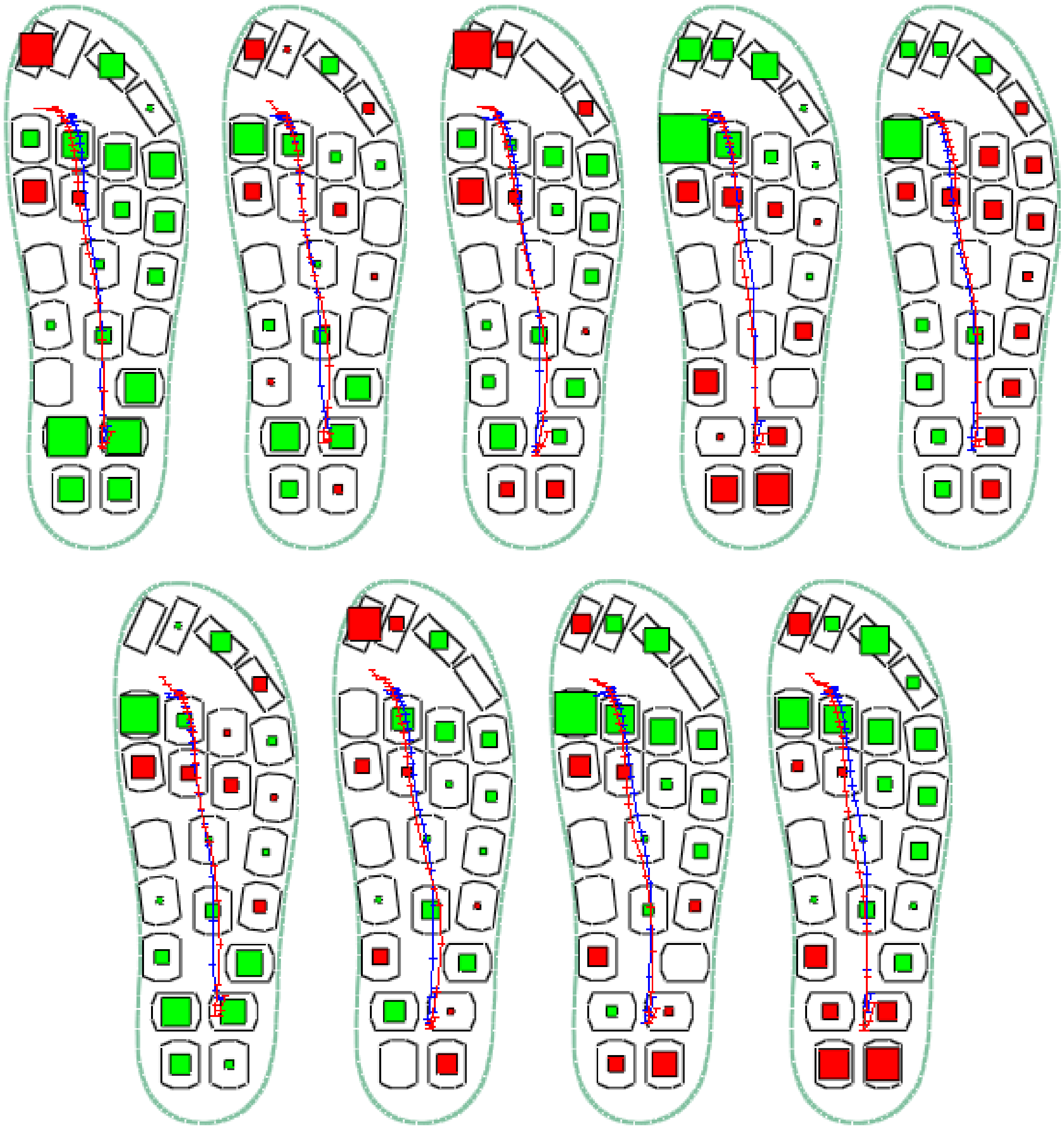

Figure A.5 – Subject M1 - Data Shoe 1 vs. Shoe 5

Figure A.6 – Subject M1 Data - Shoe 1 vs. Shoe 6

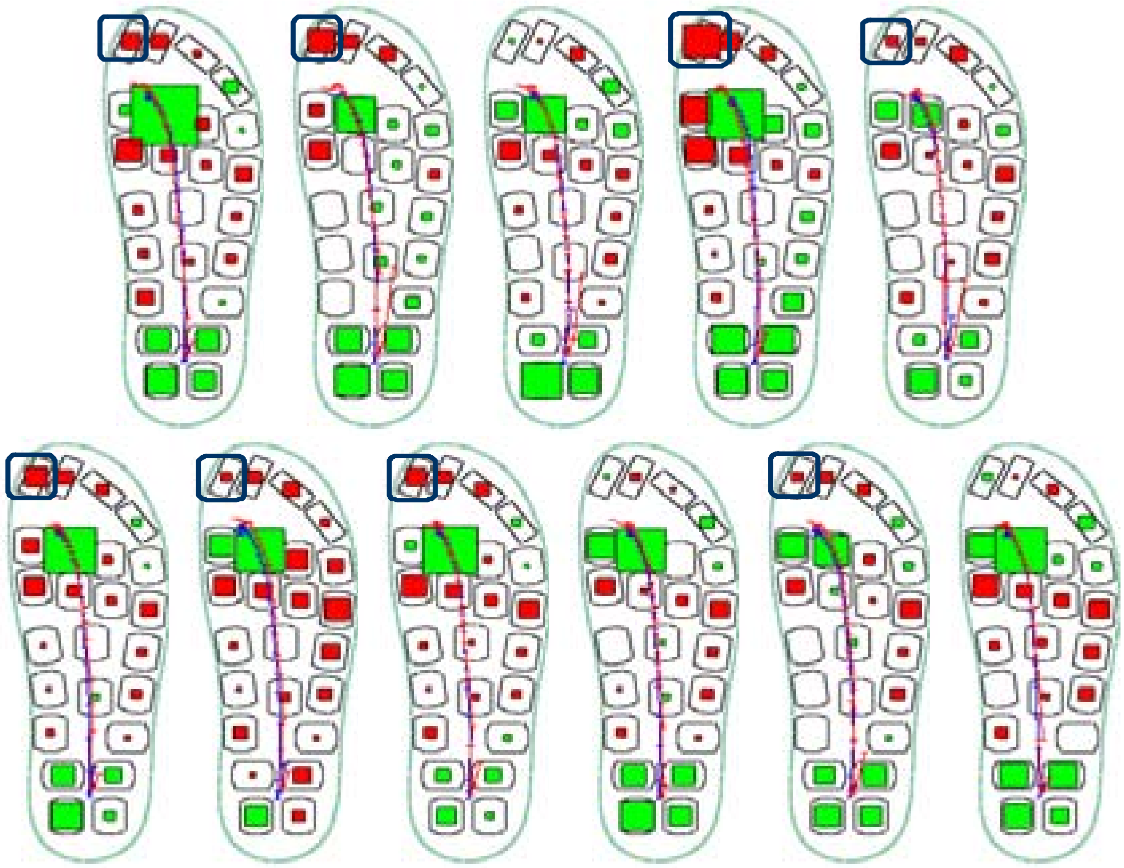

Figure A.7 – Subject M2 Data - Shoe 1 vs. Shoe 2

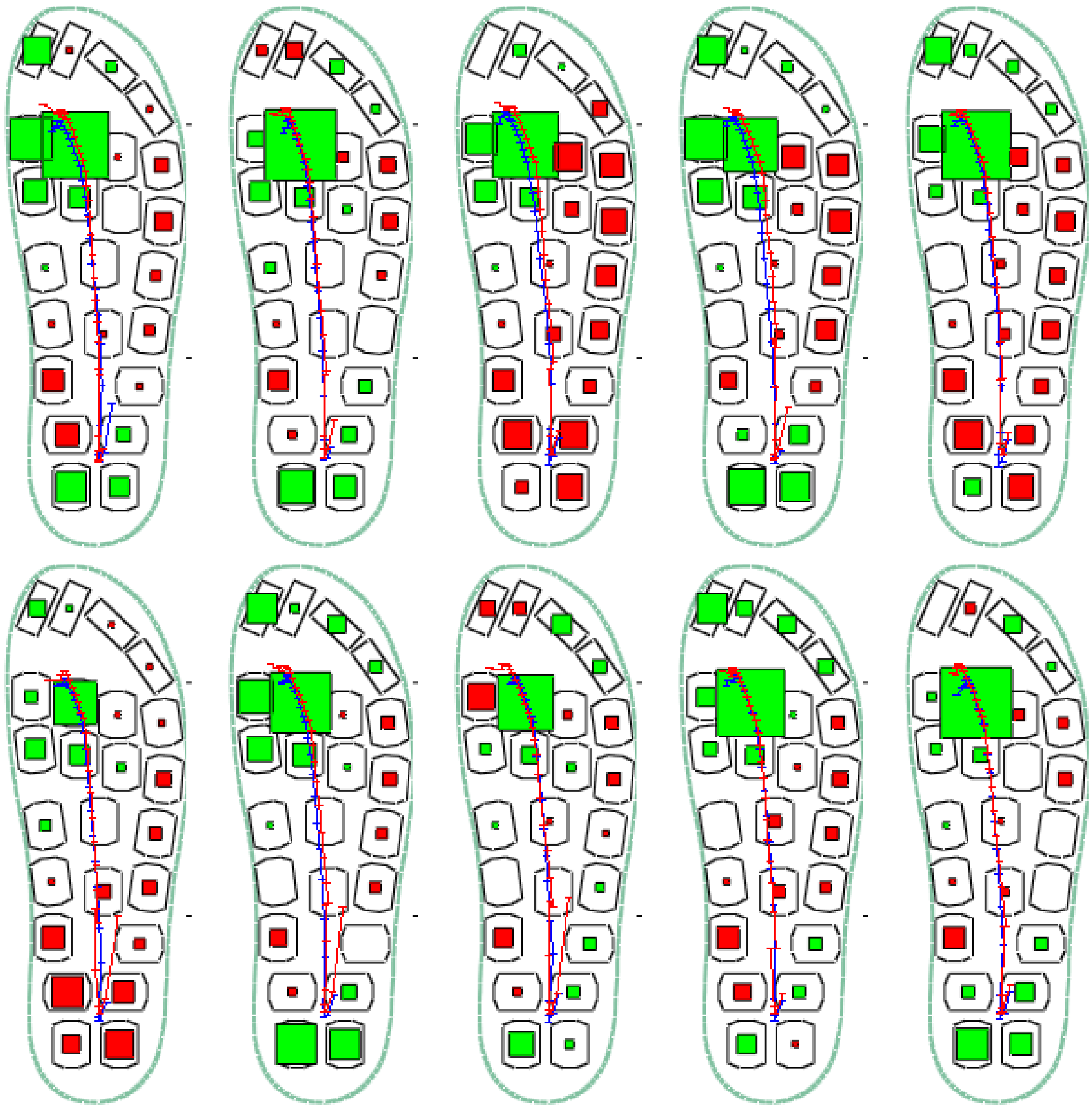

Figure A.8 – Subject M2 Data - Shoe 1 vs. Shoe 3

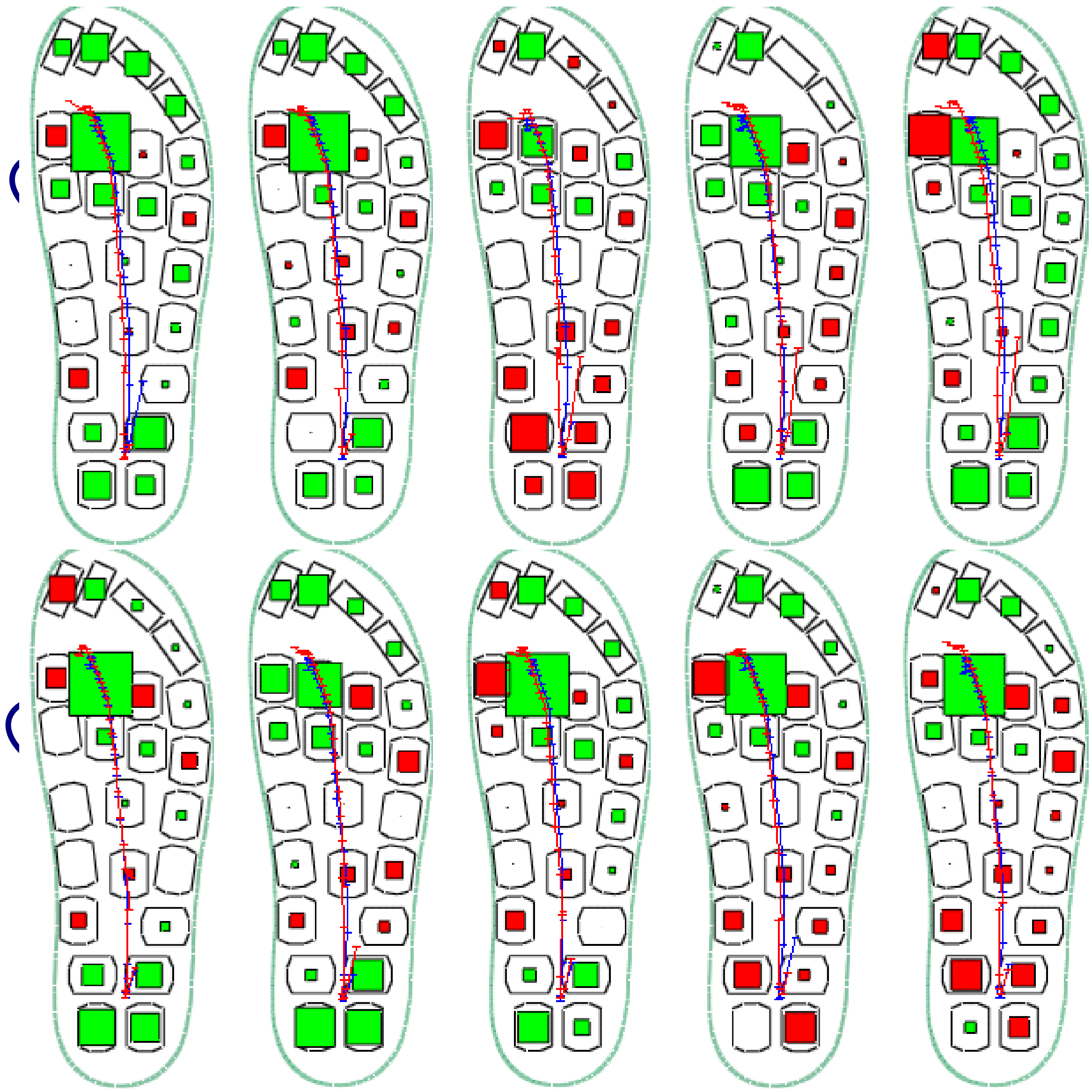

Figure A.9 – Subject M2 Data - Shoe 1 vs. Shoe 4

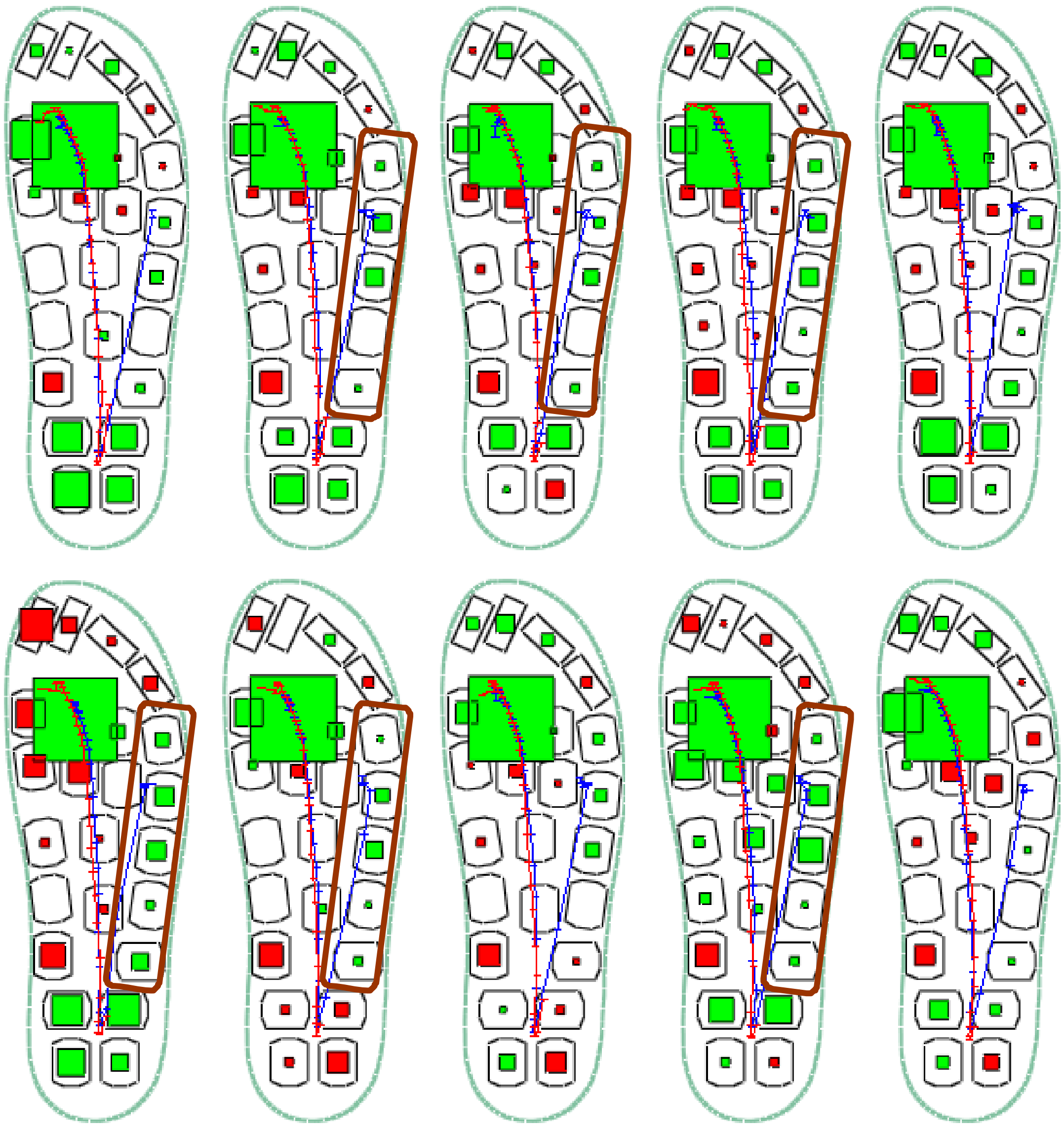

Figure A.10 – Subject M2 Data - Shoe 1 vs. Shoe 5

Figure A.11 – Subject M2 Data - Shoe 1 vs. Shoe 6

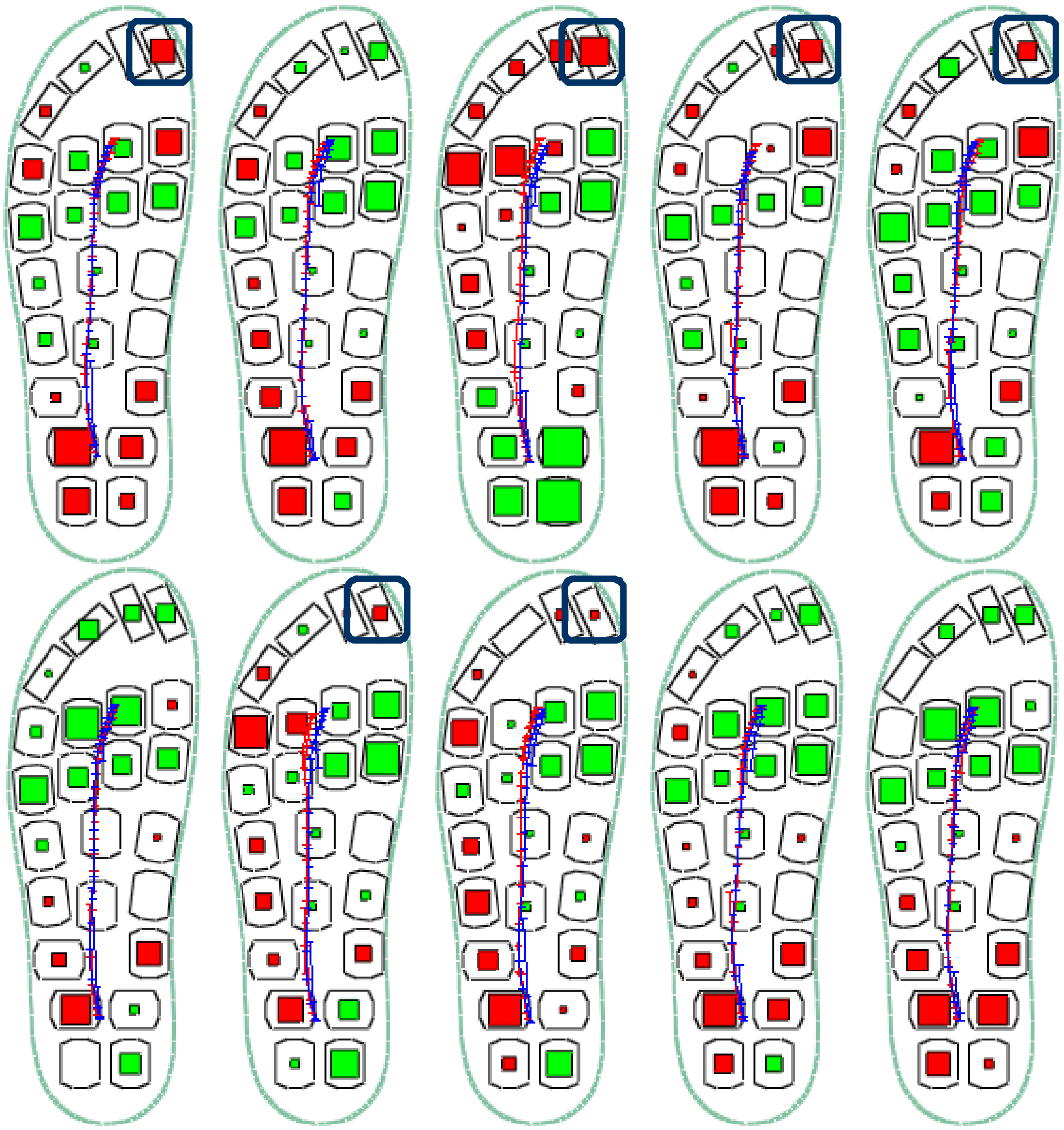

Figure A.12 – Subject M3 Data - Shoe 1 vs. Shoe 2

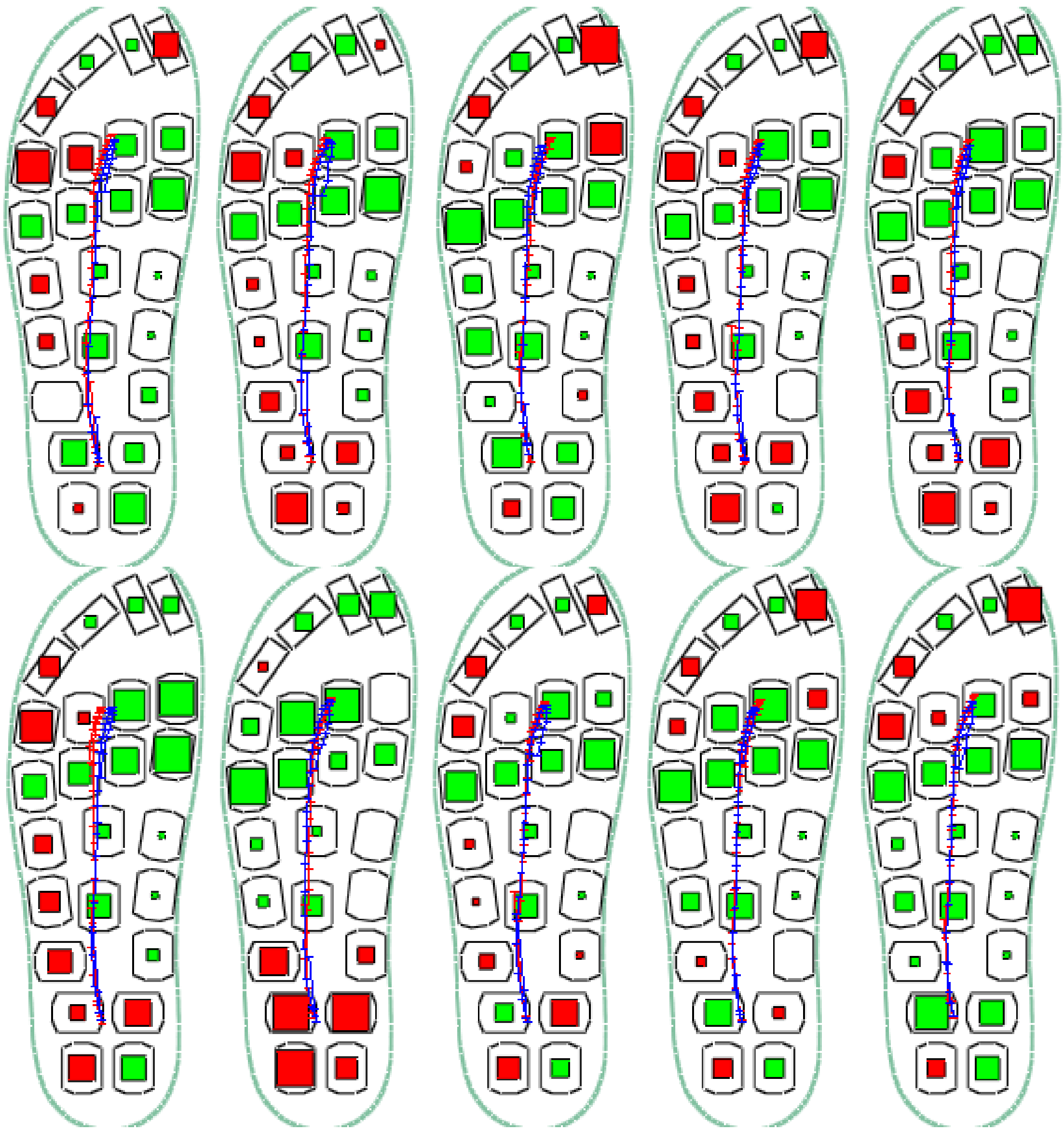

Figure A.13 – Subject M3 Data - Shoe 1 vs. Shoe 3

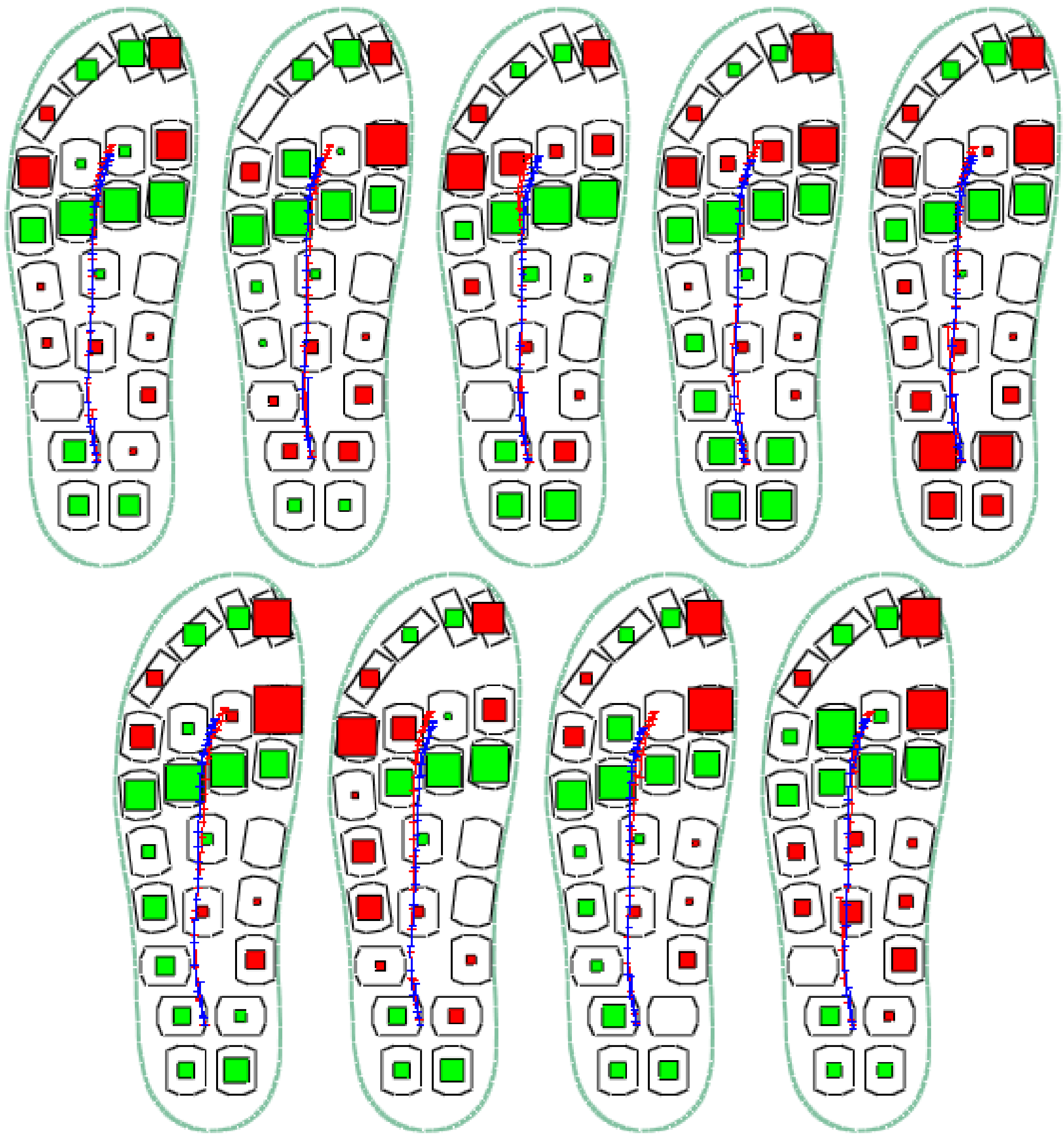

Figure A.14 – Subject M3 Data - Shoe 1 vs. Shoe 4

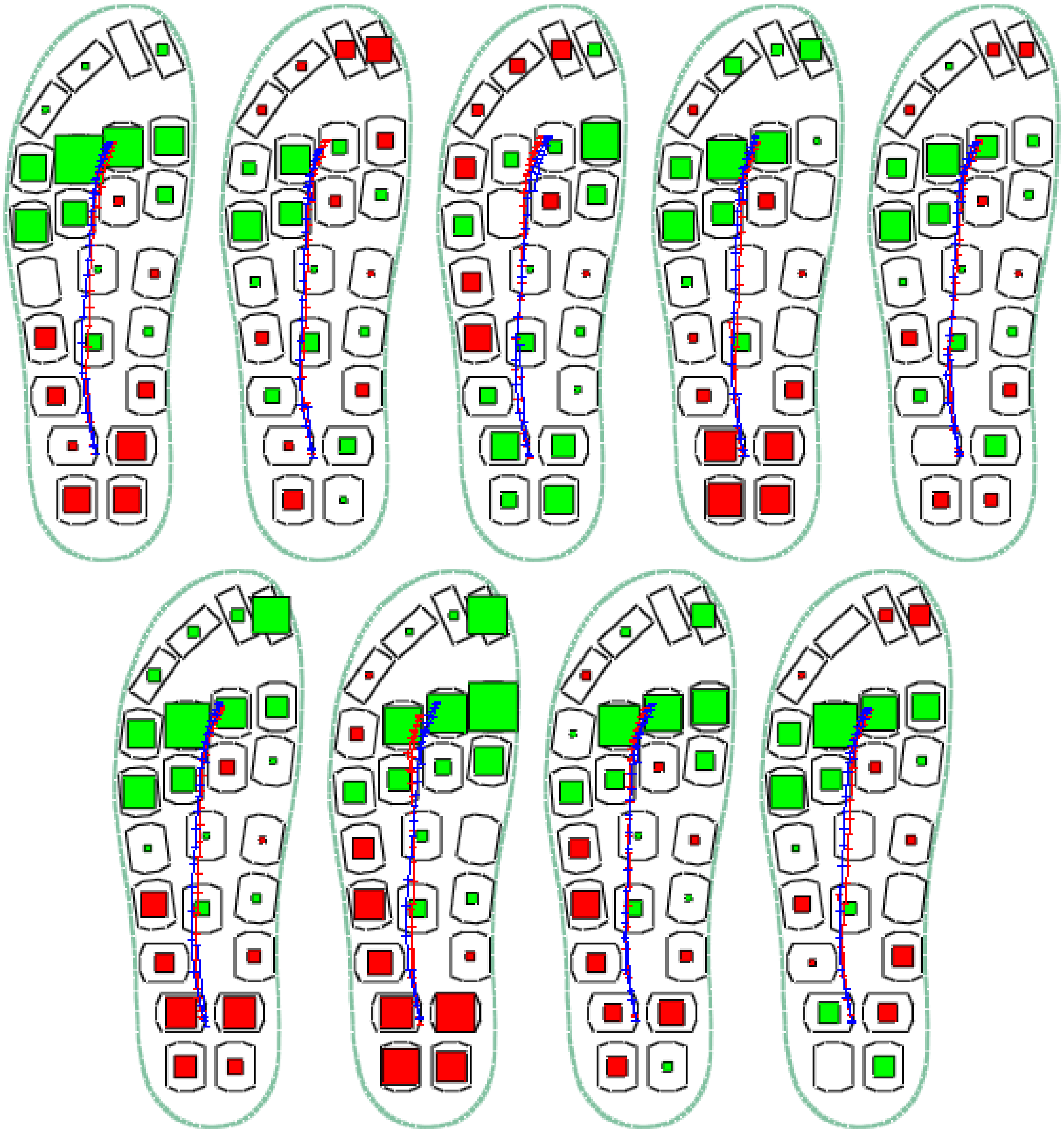

Figure A.15 – Subject M1 Data - Shoe 1 vs. Shoe 5

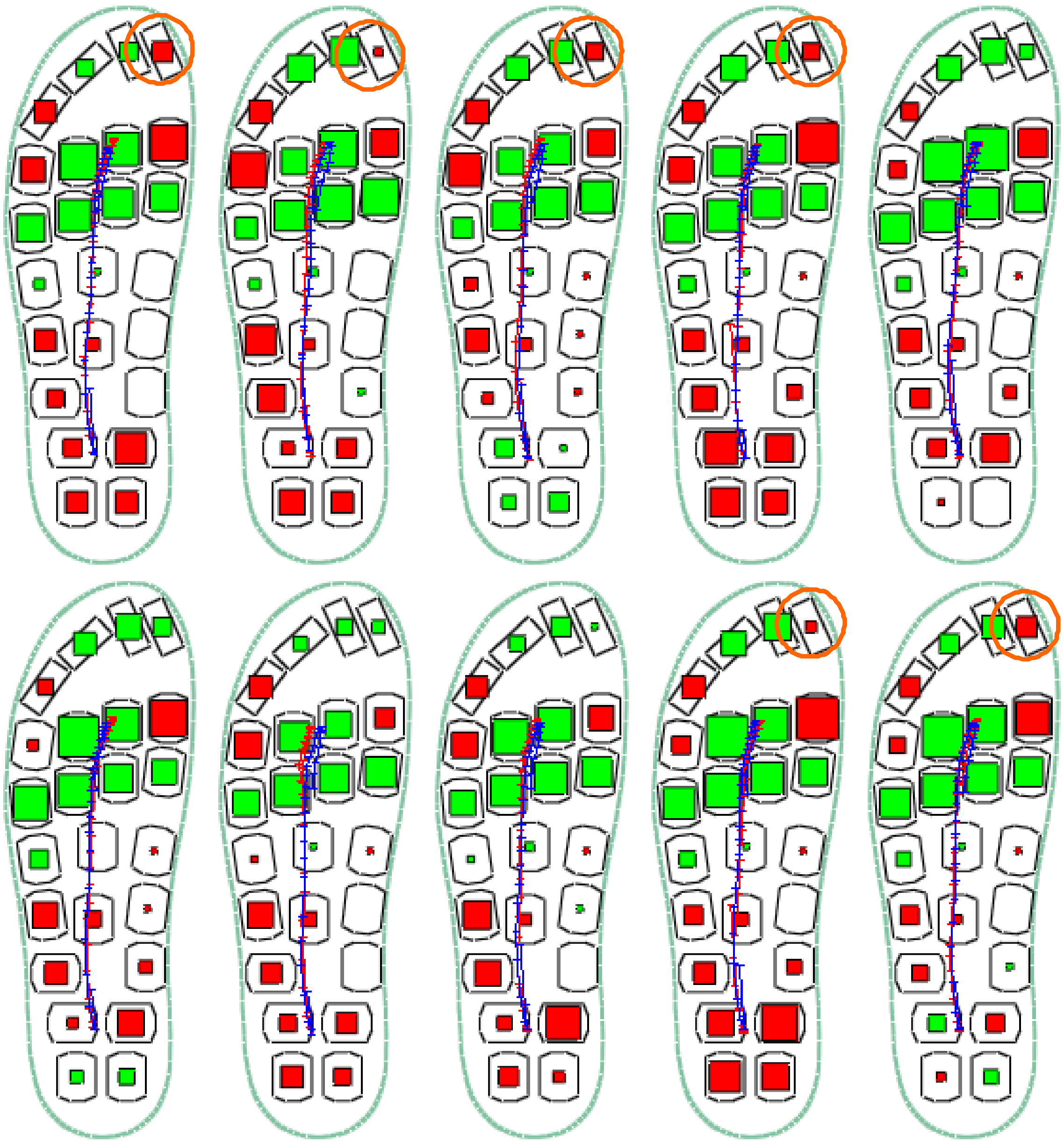

Figure A.16 – Subject M3 Data - Shoe 1 vs. Shoe 6

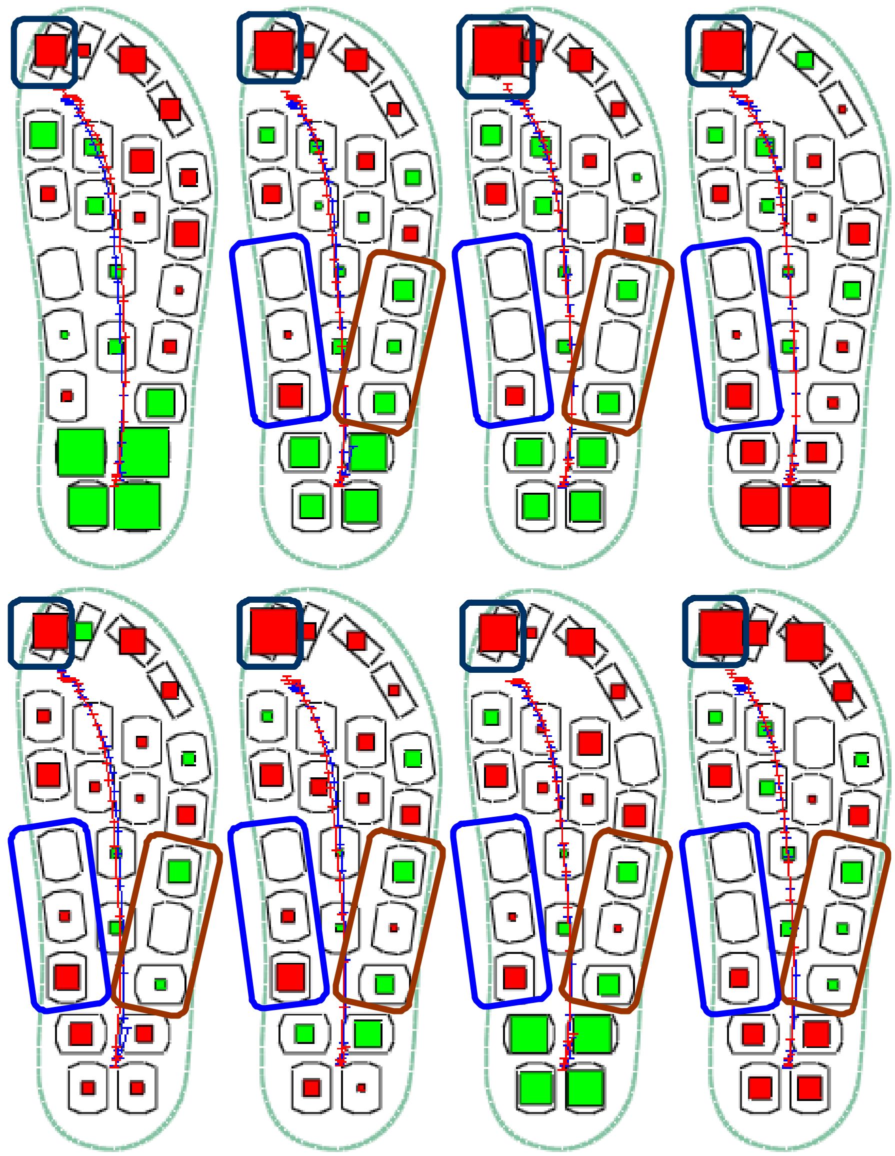

Figure A.17 – Subject F1 Data - Shoe 1 vs. Shoe 2

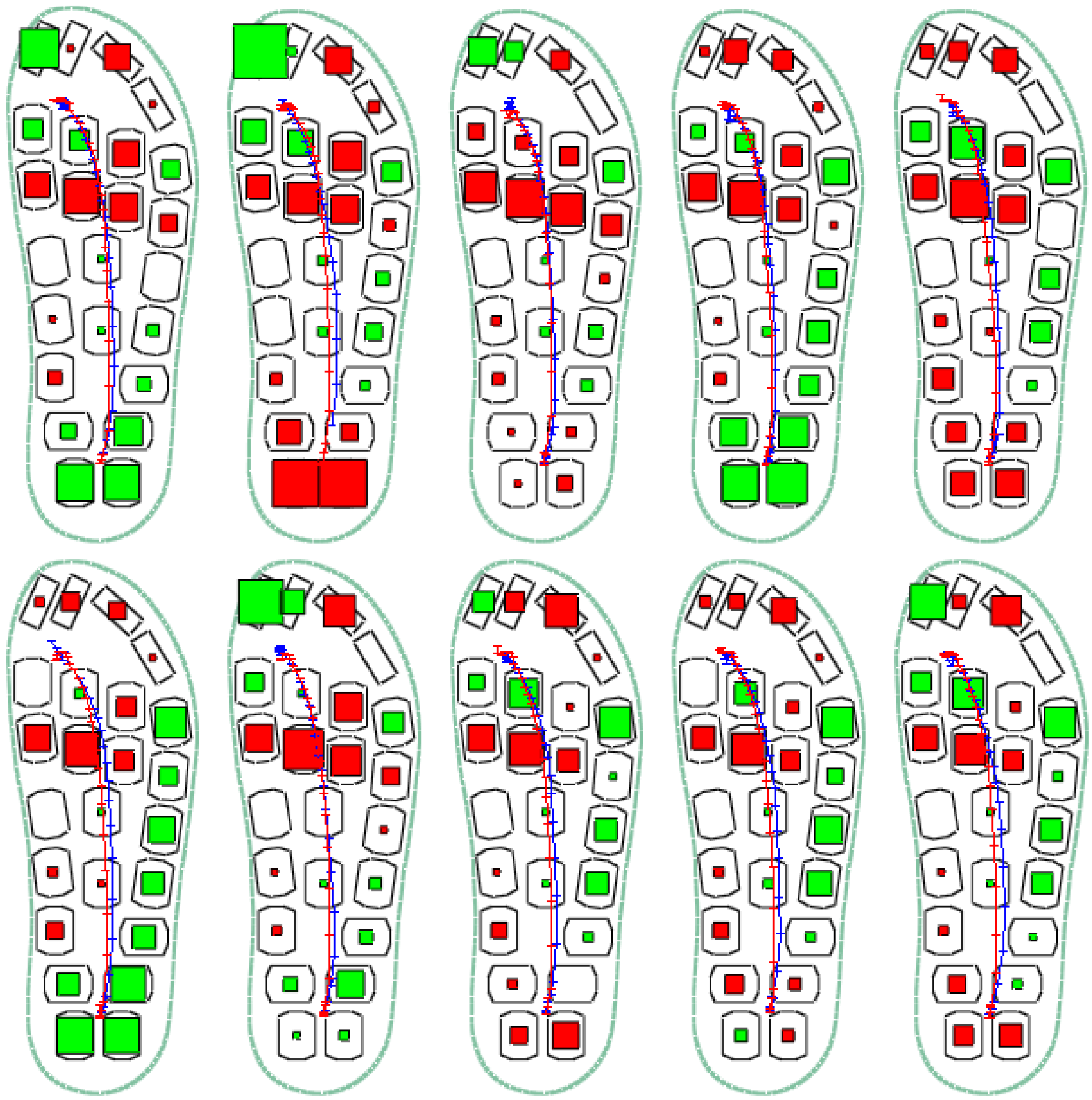

Figure A.18 – Subject F1 Data - Shoe 1 vs. Shoe 3

Figure A.19 – Subject F1 Data - Shoe 1 vs. Shoe 4

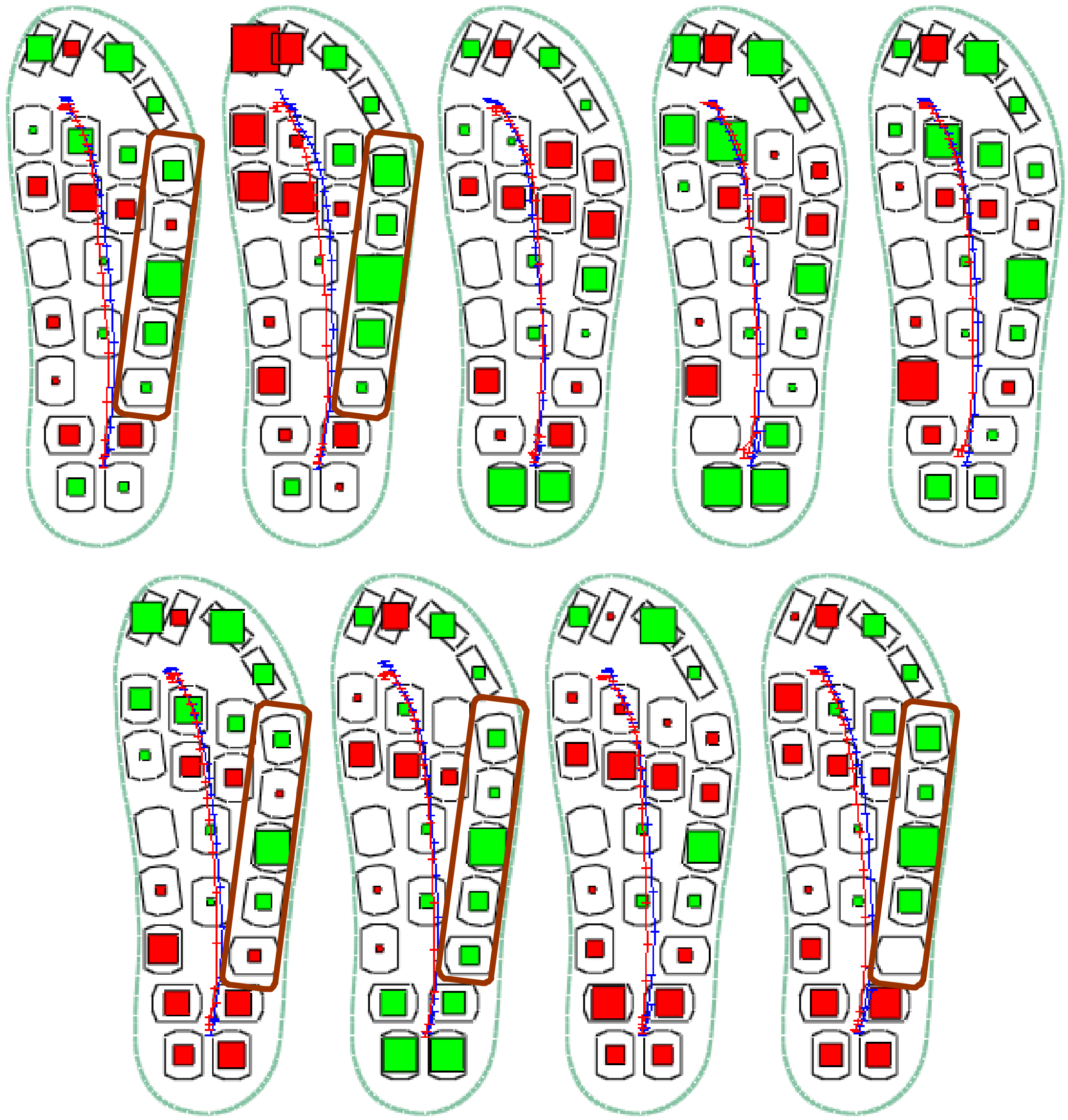

Figure A.20 – Subject F1 Data - Shoe 1 vs. Shoe 5

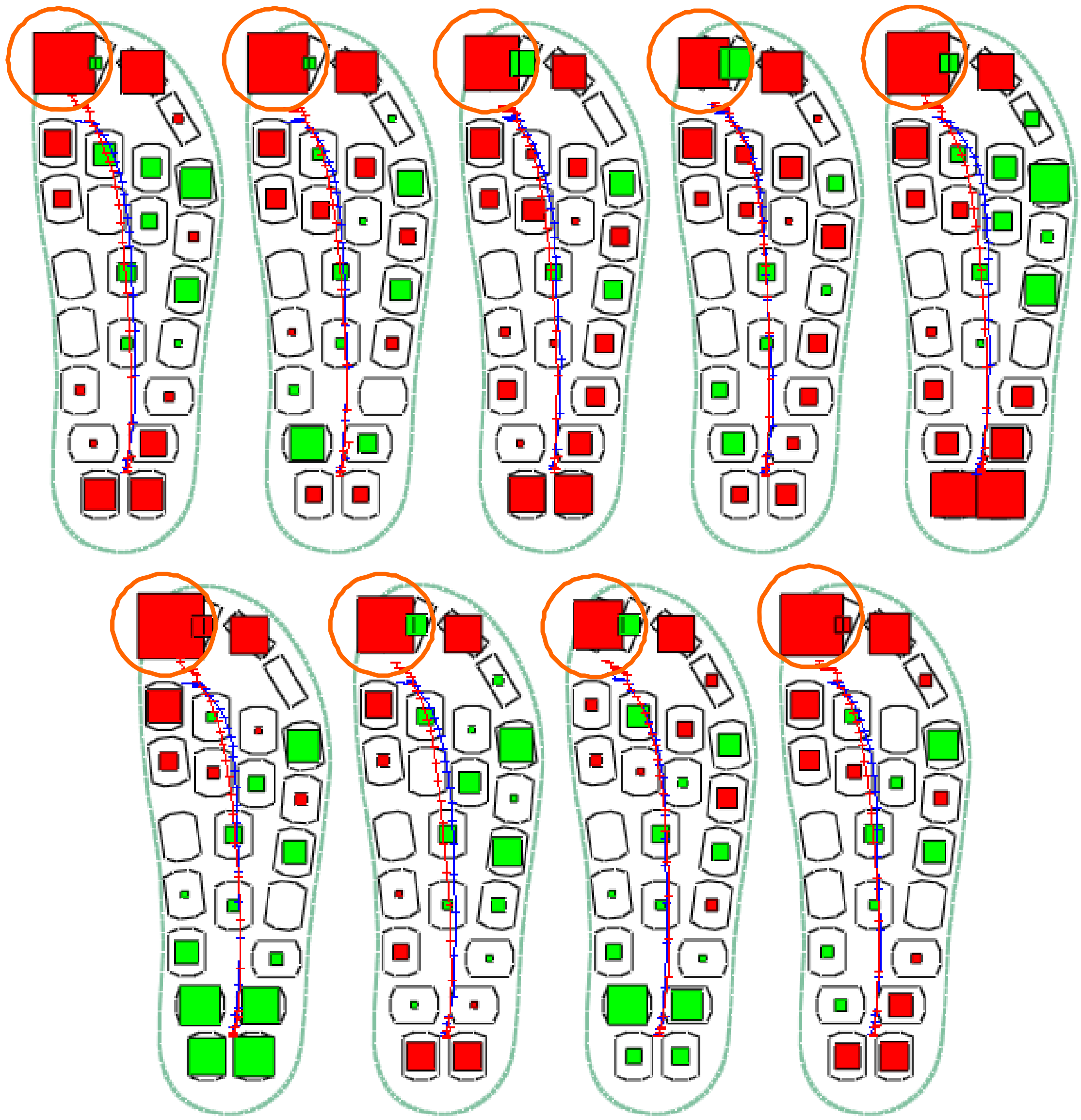

Figure A.21 – Subject F1 Data - Shoe 1 vs. Shoe 6

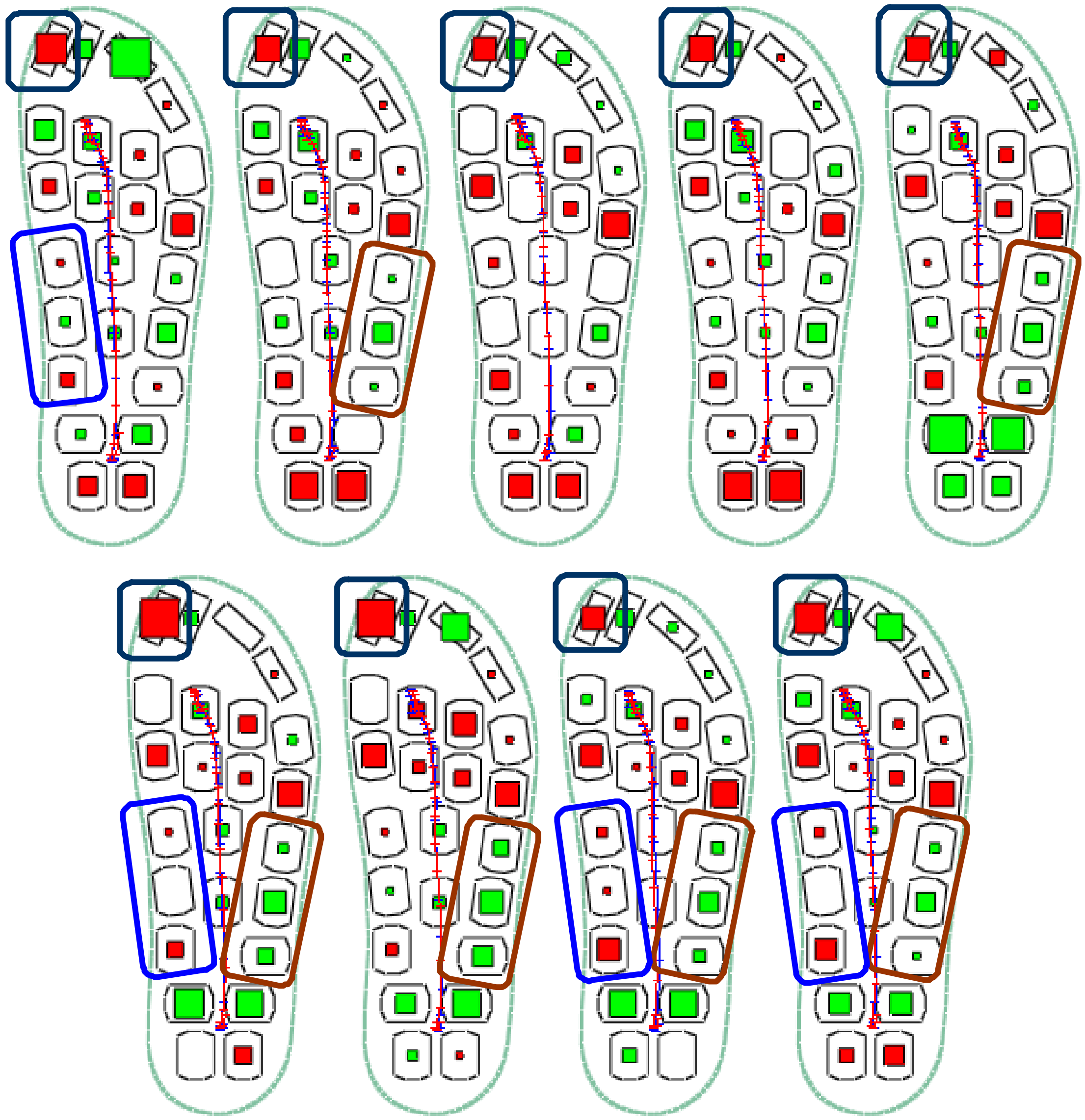

Figure A.22 – Subject F2 Data - Shoe 1 vs. Shoe 2

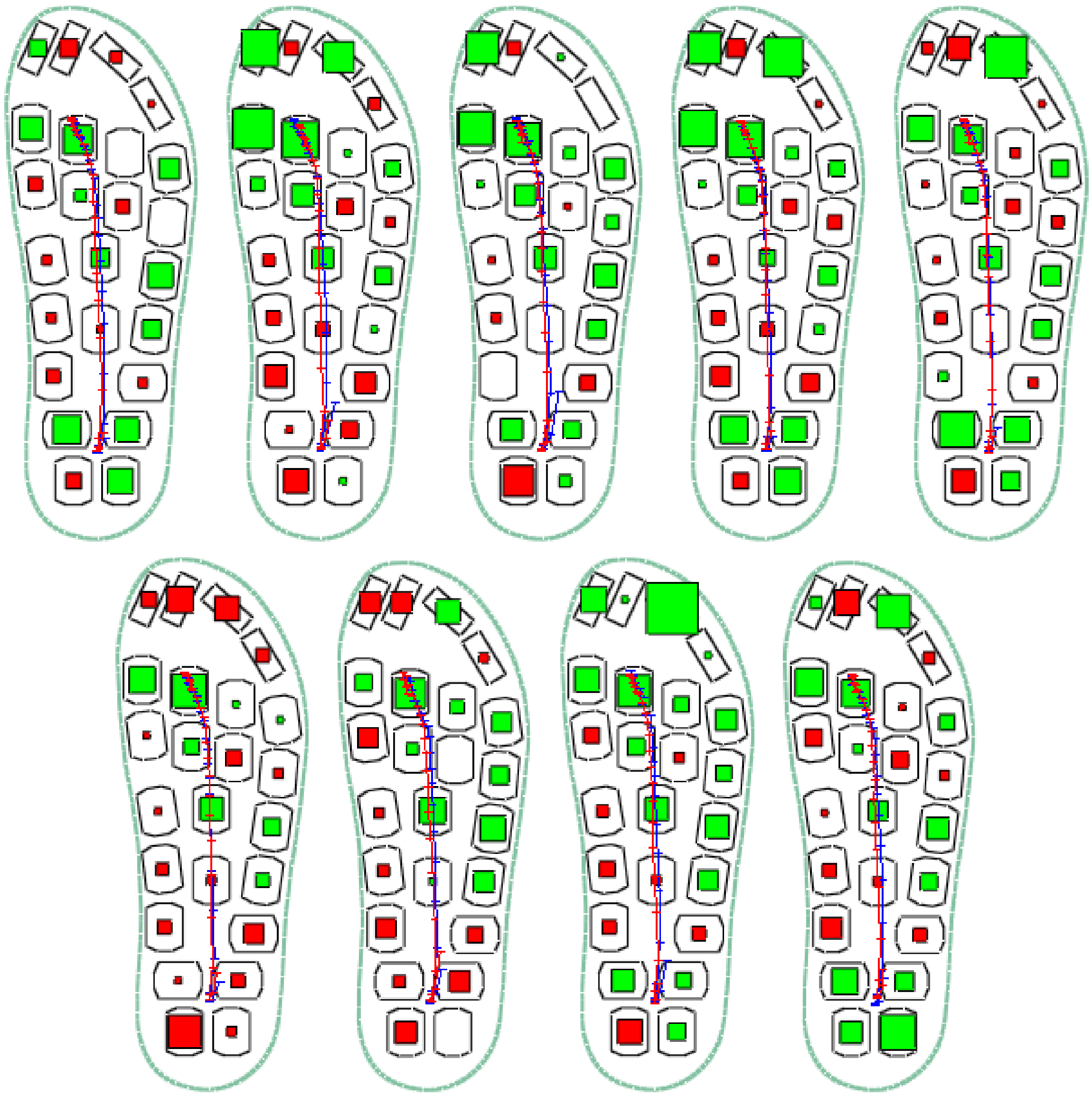

Figure A.23 – Subject F2 Data - Shoe 1 vs. Shoe 3

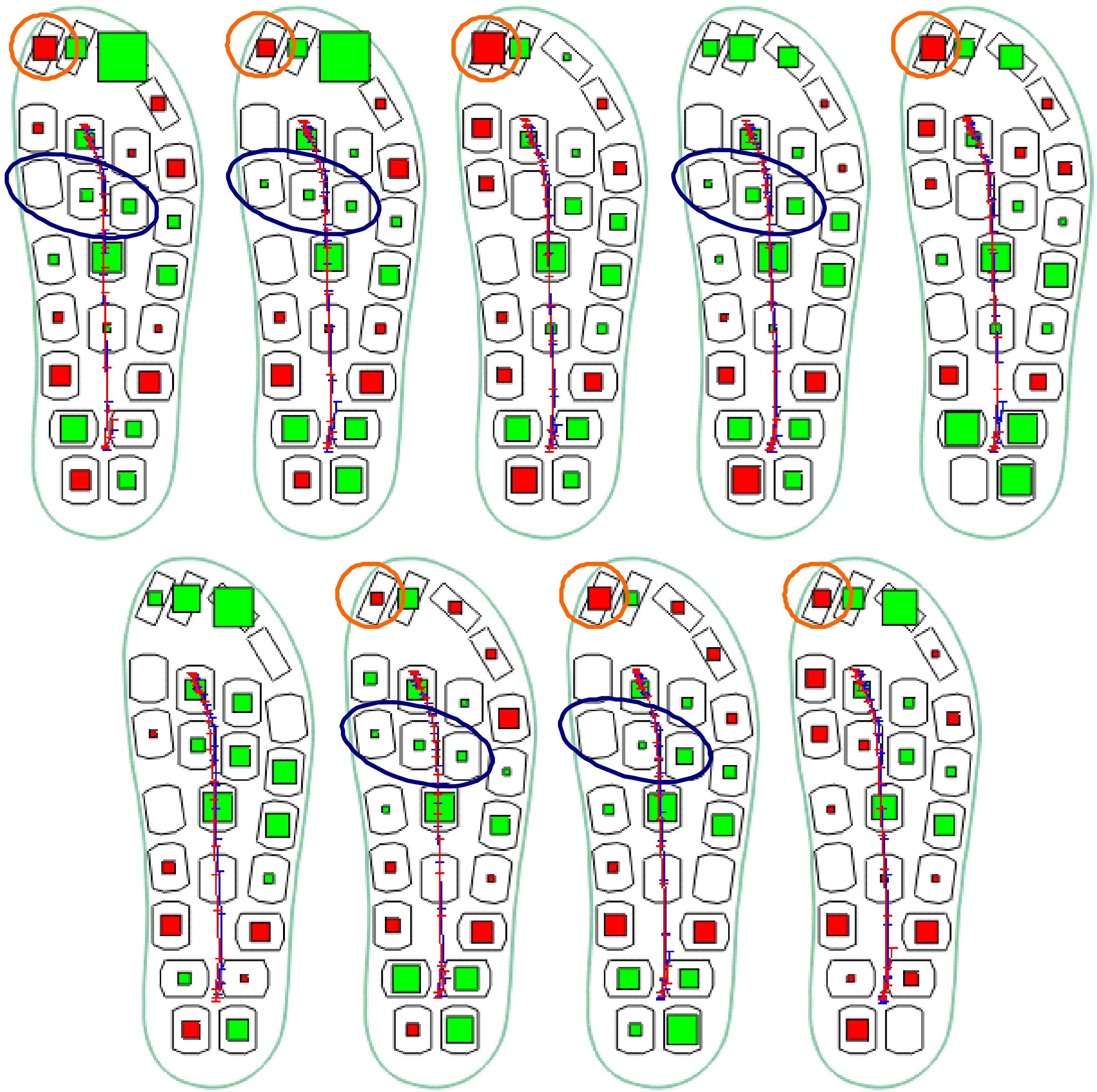

Figure A.24 – Subject F2 Data - Shoe 1 vs. Shoe 4

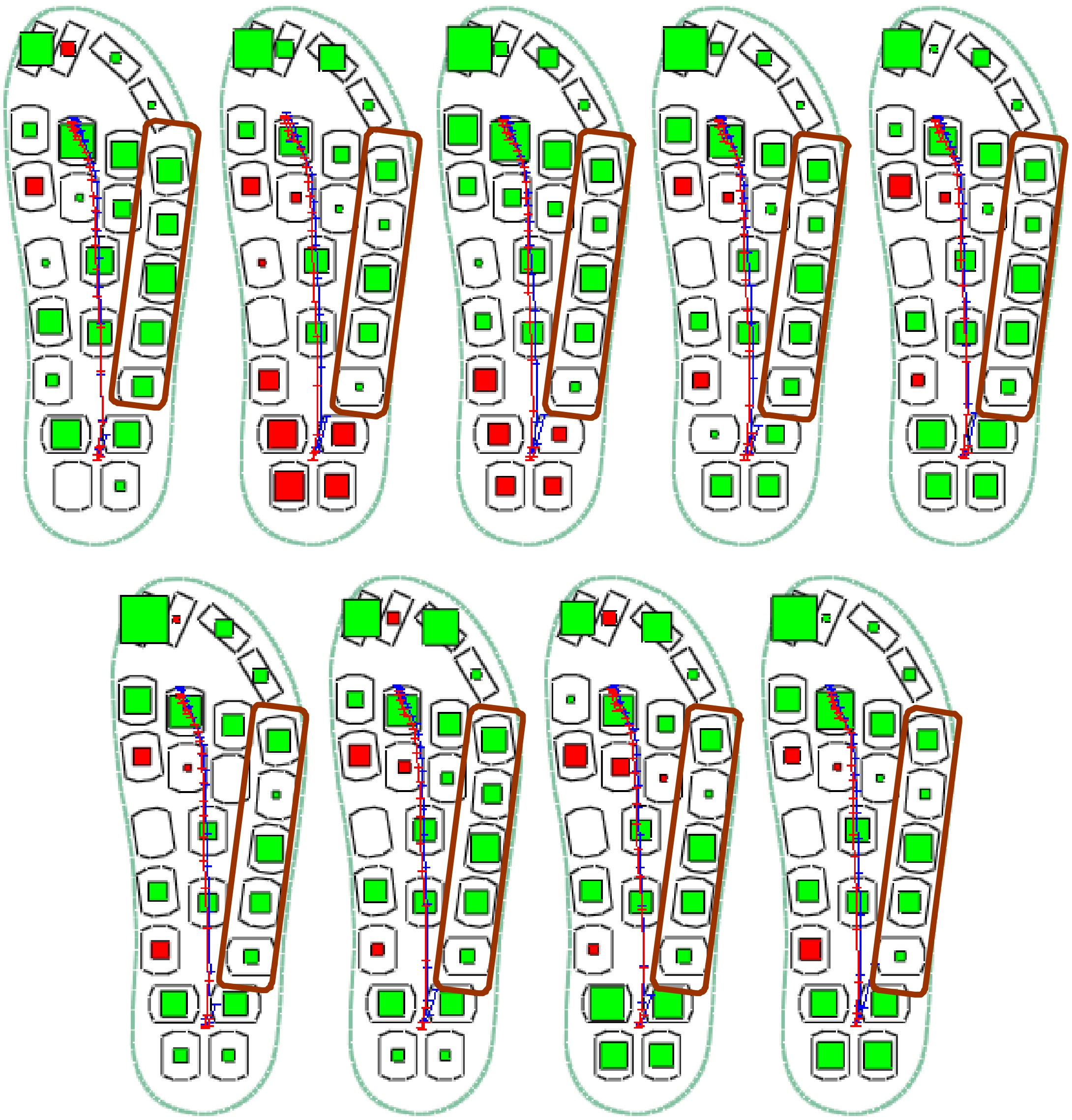

Figure A.25 – Subject F2 Data - Shoe 1 vs. Shoe 5

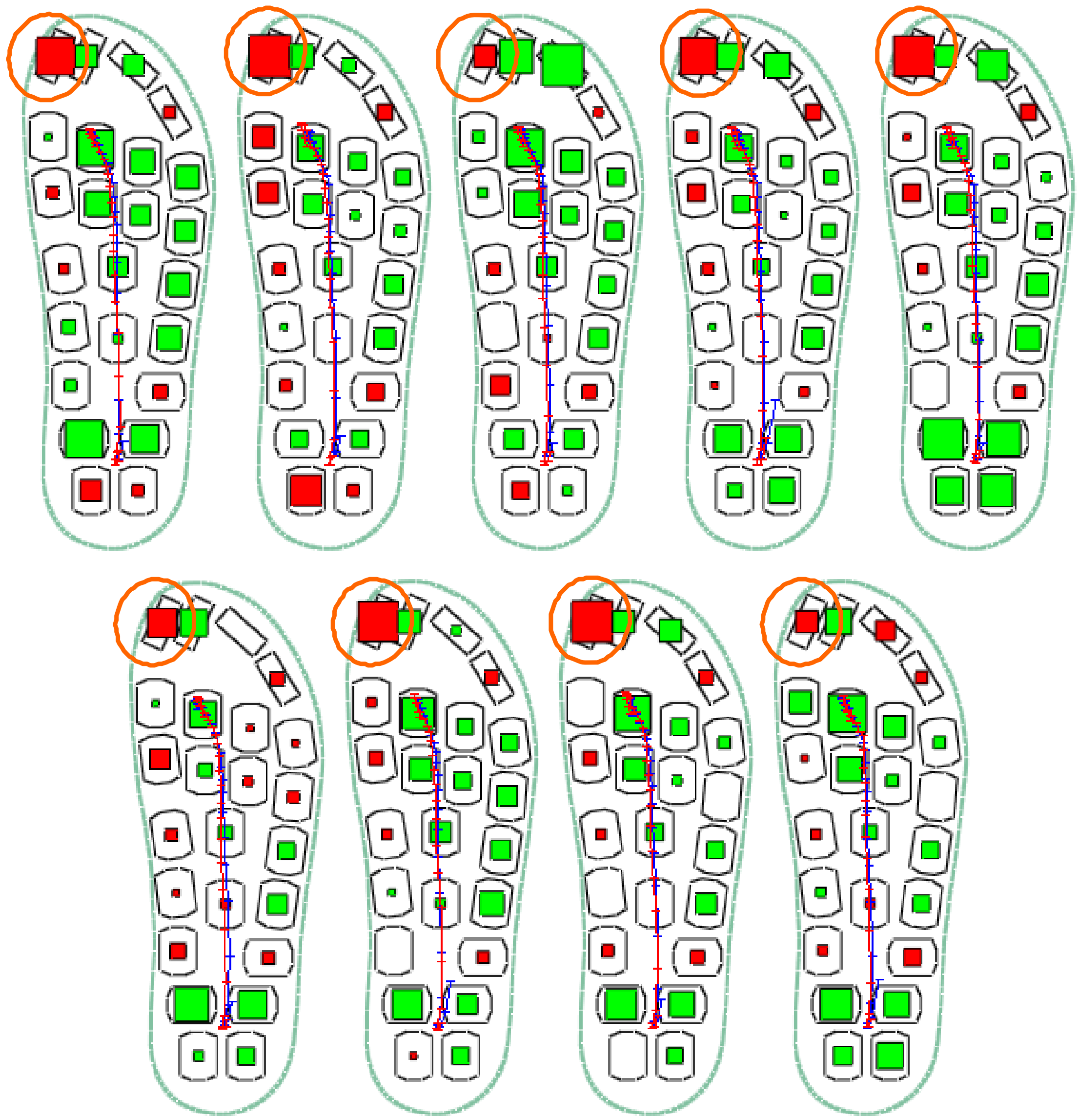

Figure A.26 – Subject F2 Data - Shoe 1 vs. Shoe 6

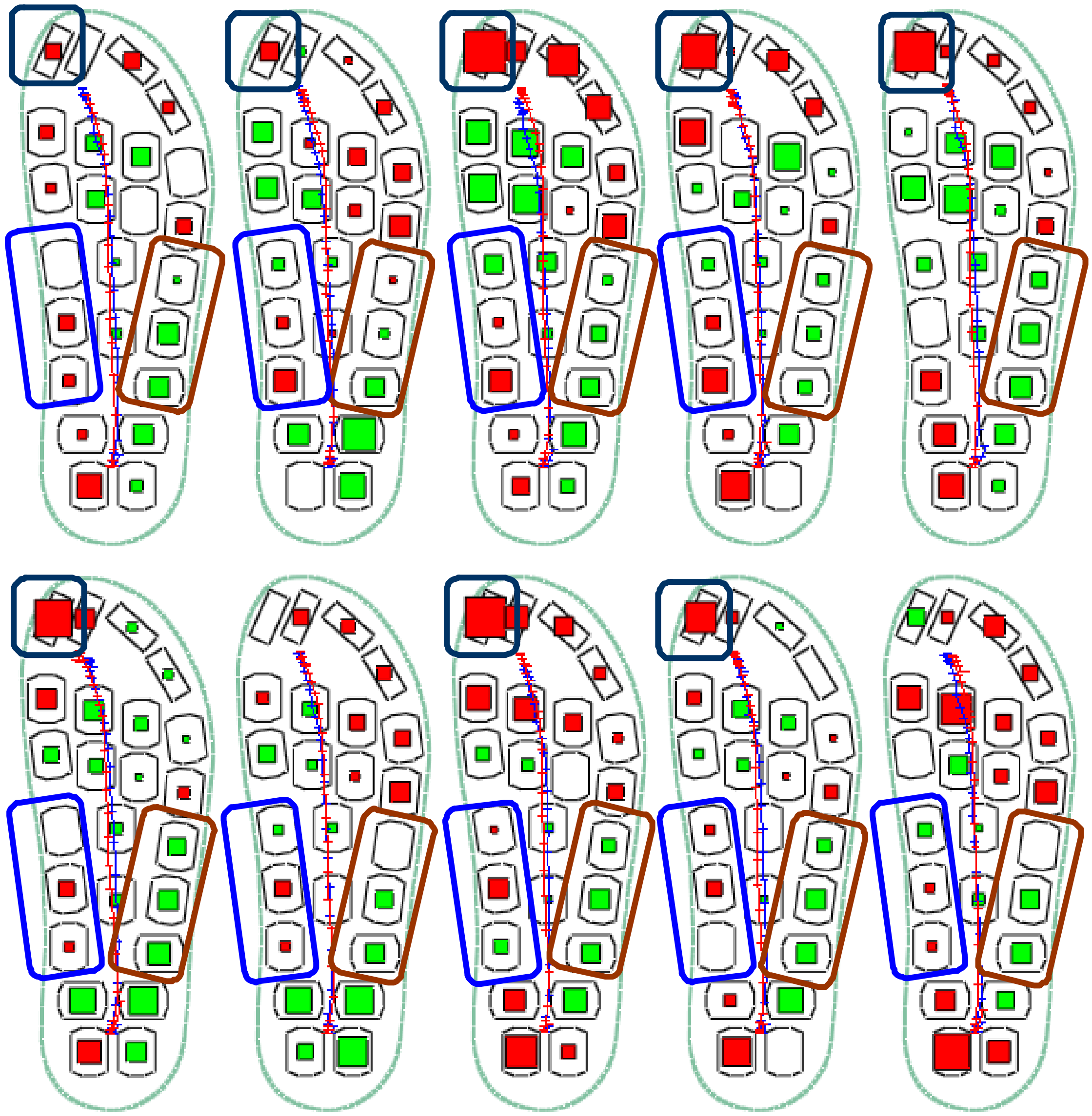

Figure A.27 – Subject F3 Data - Shoe 1 vs. Shoe 2

Figure A.29 – Subject F3 Data - Shoe 1 vs. Shoe 3

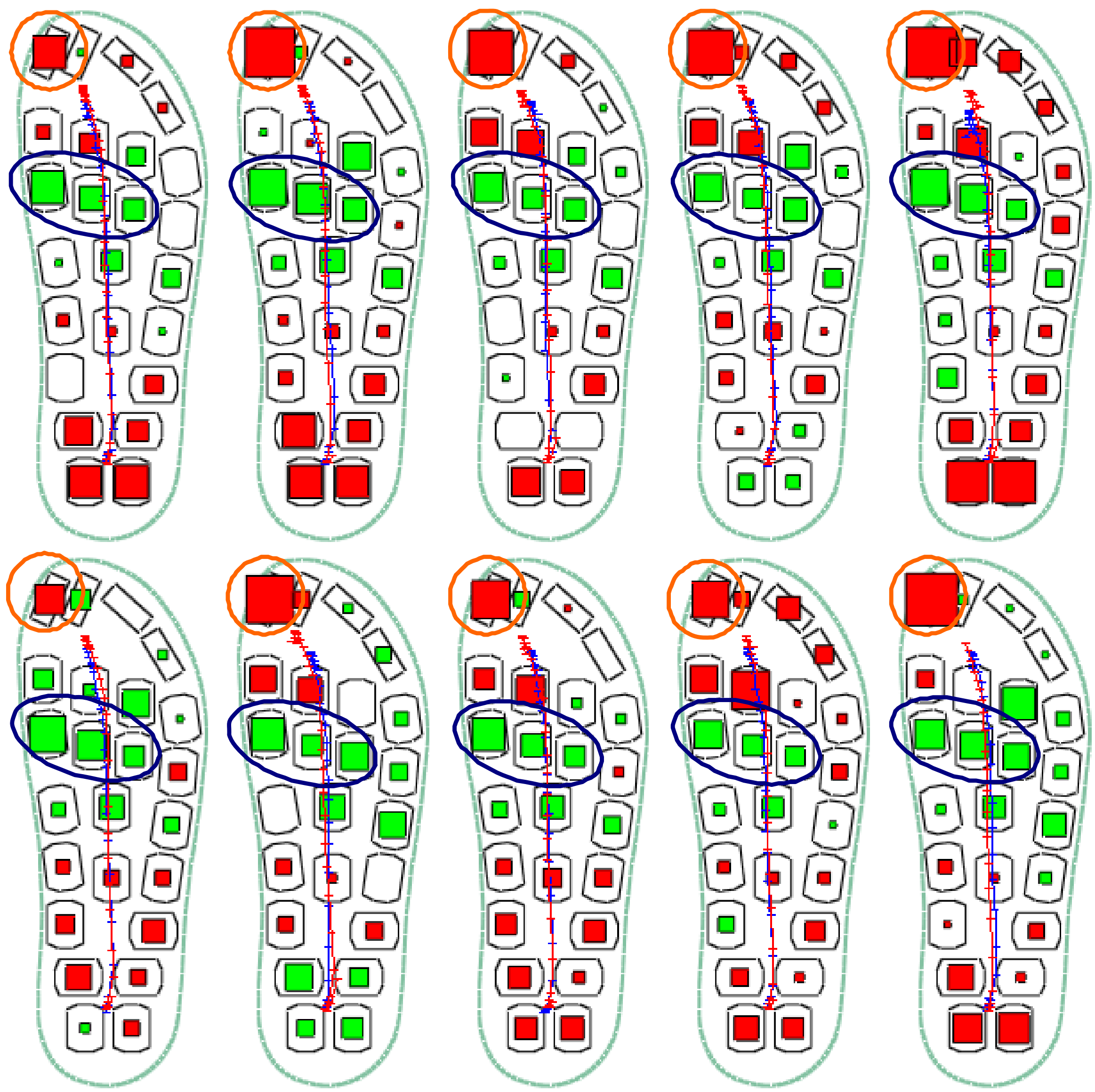

Figure A.29 – Subject F3 Data - Shoe 1 vs. Shoe 4

Figure A.30 – Subject F3 Data - Shoe 1 vs. Shoe 5

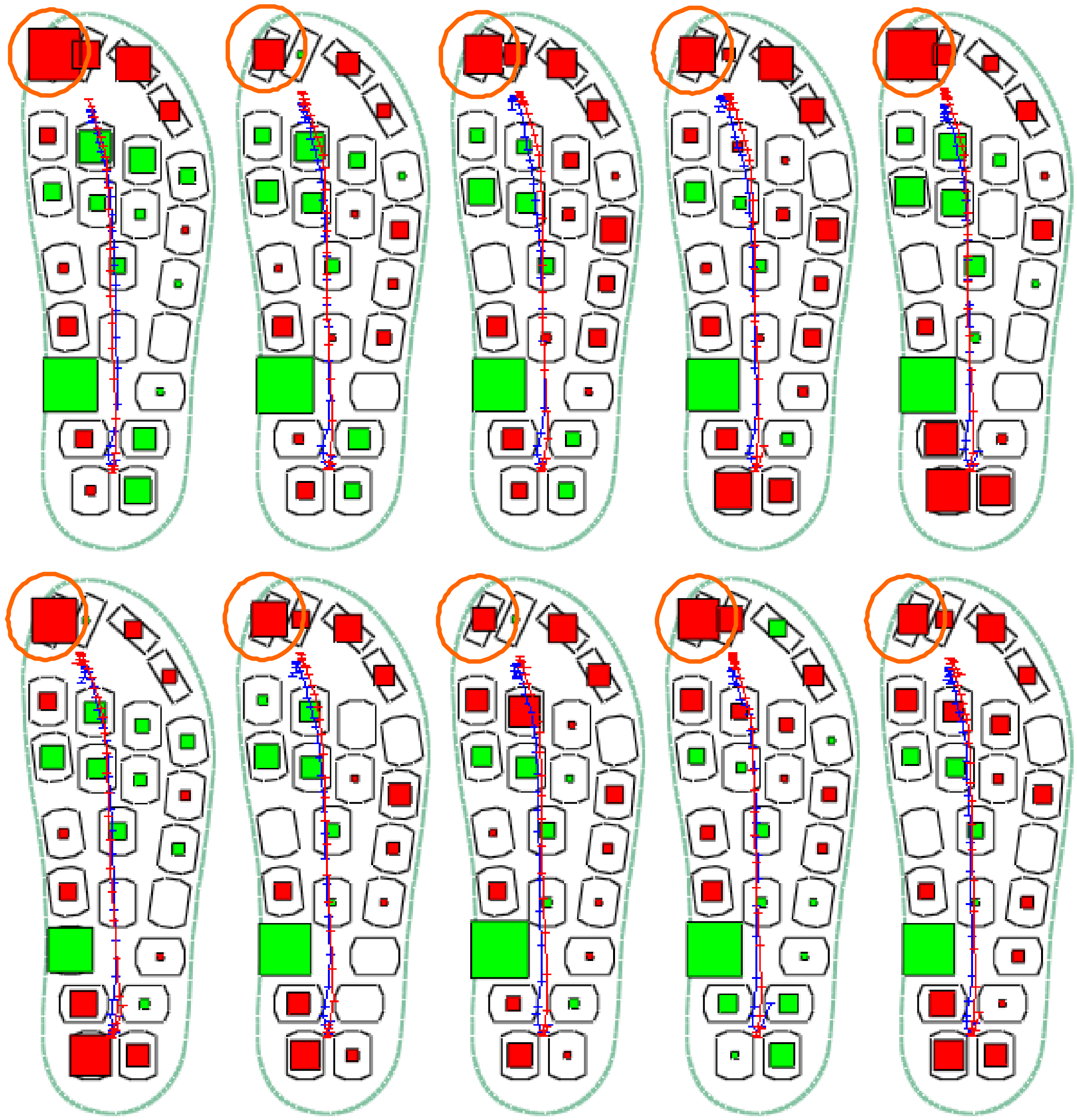

Figure A.31 – Subject F3 Data - Shoe 1 vs. Shoe 6

APPENDIX B
DATA FROM CHAPTER 3

Table B.1 – Knee Moment Data for Subject F1

Subject F1	Knee Adduction/Abduction Moment			
Shoe	Trial #	Normalized Joint Moment (Nm/kg)	Average	Standard Deviation
Neutral	1	0.29	0.29	0.01
Neutral	2	0.28		
Neutral	3	0.29		
Lateral Stiff	1	0.32	0.31	0.01
Lateral Stiff	2	0.30		
Lateral Stiff	3	0.31		
T-Form 1	1	0.35	0.35	0.01
T-Form 1	2	0.34		
T-Form 2	1	0.33	0.32	0.01
T-Form 2	2	0.32		
T-Form 2	3	0.32		
T-Form 3	1	0.32	0.32	0.01
T-Form 3	2	0.33		
T-Form 3	3	0.31		
T-Form 4	1	0.31	0.32	0.04
T-Form 4	2	0.37		
T-Form 4	3	0.29		
T-Form 5	1	0.28	0.30	0.03
T-Form 5	2	0.30		
T-Form 5	3	0.33		

Table B.2 – Knee Moment Data for Subject F2

Subject F2	Knee Adduction/Abduction Moment			
Shoe	Trial #	Normalized Joint Moment (Nm/kg)	Average	Standard Deviation
Neutral	1	0.40	0.35	0.06
Neutral	2	0.36		
Neutral	3	0.29		
Lateral Stiff	1	0.43	0.46	0.04
Lateral Stiff	2	0.46		
Lateral Stiff	3	0.50		
T-Form 1	1	0.40	0.38	0.03
T-Form 1	2	0.39		
T-Form 1	4	0.35		
T-Form 2	1	0.36	0.35	0.02
T-Form 2	2	0.35		
T-Form 2	3	0.33		
T-Form 3	1	0.30	0.29	0.03
T-Form 3	2	0.31		
T-Form 3	3	0.25		
T-Form 4	1	0.45	0.38	0.06
T-Form 4	2	0.33		
T-Form 4	3	0.35		
T-Form 5	1	0.16	0.25	0.09
T-Form 5	2	0.27		
T-Form 5	3	0.33		

Table B.3 – Knee Moment Data for Subject F3

Subject F3	Knee Adduction/Abduction Moment			
Shoe	Trial #	Normalized Joint Moment (Nm/kg)	Average	Standard Deviation
Neutral	1	0.42	0.45	0.03
Neutral	2	0.47		
Neutral	3	0.46		
Lateral Stiff	1	0.45	0.47	0.06
Lateral Stiff	2	0.54		
Lateral Stiff	3	0.43		
T-Form 1	1	0.51	0.48	0.04
T-Form 1	2	0.49		
T-Form 1	3	0.43		
T-Form 2	1	0.49	0.45	0.04
T-Form 2	2	0.45		
T-Form 2	3	0.42		
T-Form 3	1	0.40	0.44	0.04
T-Form 3	2	0.48		
T-Form 3	3	0.45		
T-Form 4	1	0.44	0.44	0.03
T-Form 4	2	0.46		
T-Form 4	3	0.41		
T-Form 5	1	0.48	0.46	0.03
T-Form 5	2	0.43		
T-Form 5	3	0.46		

Table B.4 – Knee Moment Data for Subject F4

Subject F4	Knee Adduction/Abduction Moment			
Shoe	Trial #	Normalized Joint Moment (Nm/kg)	Average	Standard Deviation
Neutral	1	0.35	0.36	0.01
Neutral	2	0.37		
Neutral	3	0.37		
Lateral Stiff	1	0.39	0.38	0.01
Lateral Stiff	2	0.38		
Lateral Stiff	3	0.37		
T-Form 1	1	0.41	0.40	0.06
T-Form 1	2	0.45		
T-Form 1	3	0.34		
T-Form 2	1	0.47	0.44	0.03
T-Form 2	2	0.41		
T-Form 2	3	0.45		
T-Form 3	1	0.51	0.48	0.04
T-Form 3	2	0.50		
T-Form 3	3	0.43		
T-Form 4	1	0.42	0.39	0.03
T-Form 4	2	0.39		
T-Form 4	3	0.37		
T-Form 5	1	0.42	0.44	0.02
T-Form 5	2	0.46		
T-Form 5	3	0.44		

Table B.5 – Knee Moment Data for Subject M1

Subject M1	Knee Adduction/Abduction Moment			
Shoe	Trial #	Normalized Joint Moment (Nm/kg)	Average	Standard Deviation
Neutral	1	0.72	0.75	0.04
Neutral	2	0.79		
Neutral	3	0.73		
Lateral Stiff	2	0.50	0.57	0.08
Lateral Stiff	3	0.56		
Lateral Stiff	4	0.66		
T-Form 1	2	0.71	0.73	0.03
T-Form 1	4	0.73		
T-Form 1	5	0.76		
T-Form 2	1	0.76	0.76	0.05
T-Form 2	2	0.81		
T-Form 2	3	0.71		
T-Form 3	1	0.86	0.81	0.06
T-Form 3	2	0.74		
T-Form 3	3	0.83		
T-Form 4	1	0.74	0.75	0.07
T-Form 4	2	0.83		
T-Form 4	3	0.69		
T-Form 5	2	0.78	0.80	0.02
T-Form 5	3	0.82		
T-Form 5	4	0.81		

Table B.6 – Knee Moment Data for Subject M2

Subject M2	Knee Adduction/Abduction Moment			
Shoe	Trial #	Normalized Joint Moment (Nm/kg)	Average	Standard Deviation
Neutral	1	0.42	0.37	0.08
Neutral	2	0.31		
Lateral Stiff	1	0.28	0.28	0.00
Lateral Stiff	3	0.28		
T-Form 1	1	0.28	0.27	0.08
T-Form 1	2	0.19		
T-Form 1	3	0.34		
T-Form 2	2	0.16	0.21	0.07
T-Form 2	3	0.26		
T-Form 3	1	0.18	0.22	0.06
T-Form 3	2	0.28		
T-Form 3	3	0.19		
T-Form 4	1	0.28	0.28	0.01
T-Form 4	2	0.27		
T-Form 4	3	0.29		
T-Form 5	1	0.20	0.25	0.11
T-Form 5	2	0.18		
T-Form 5	3	0.38		

Table B.7 – Knee Moment Data for Subject M3

Subject M3	Knee Adduction/Abduction Moment			
Shoe	Trial #	Normalized Joint Moment (Nm/kg)	Average	Standard Deviation
Neutral	1	0.13	0.17	0.03
Neutral	2	0.19		
Neutral	3	0.18		
Lateral Stiff	1	0.22	0.24	0.02
Lateral Stiff	2	0.26		
Lateral Stiff	3	0.24		
T-Form 1	1	0.25	0.25	0.01
T-Form 1	2	0.26		
T-Form 1	3	0.24		
T-Form 2	1	0.21	0.20	0.02
T-Form 2	2	0.20		
T-Form 2	3	0.18		
T-Form 3	1	0.26	0.24	0.02
T-Form 3	2	0.23		
T-Form 3	4	0.23		
T-Form 4	1	0.30	0.29	0.01
T-Form 4	2	0.29		
T-Form 4	5	0.29		
T-Form 5	1	0.26	0.27	0.03
T-Form 5	2	0.30		
T-Form 5	3	0.25		

Table B.8 – Knee Moment Data for Subject M4

Subject M4	Knee Adduction/Abduction Moment			
Shoe	Trial #	Normalized Joint Moment (Nm/kg)	Average	Standard Deviation
Neutral	1	0.30	0.38	0.07
Neutral	2	0.43		
Neutral	3	0.42		
Lateral Stiff	1	0.28	0.31	0.03
Lateral Stiff	2	0.32		
Lateral Stiff	3	0.34		
T-Form 1	1	0.32	0.37	0.05
T-Form 1	2	0.38		
T-Form 1	3	0.42		
T-Form 2	1	0.35	0.39	0.03
T-Form 2	2	0.41		
T-Form 2	3	0.41		
T-Form 3	1	0.31	0.35	0.03
T-Form 3	2	0.36		
T-Form 3	3	0.37		
T-Form 4	1	0.37	0.35	0.03
T-Form 4	2	0.32		
T-Form 4	3	0.37		
T-Form 5	1	0.34	0.35	0.02
T-Form 5	2	0.37		
T-Form 5	3	0.35		

APPENDIX C

BODYBUIDLER CODE FOR CHAPTER 3

Model Parameter File (.mp)
(Used for all models)
$HipOffset and $BodyMass were manually measured and input into the file
$KneeOffset and $Ankle Offset were measured and input by processing the static trial

```
{*T-Form.mp*}
{*Written by Jerrod Braman*}

{*For use with T-Form.mod and T-Form.mkr*}

{*All Distance measurements in millimeters*}
{*All angles in degrees*}
{*All mass in kilograms*}

{*General Parameters*}
{*==================*}

        $HipOffset =
        $MarkerDiameter = 14
        $BodyMass =



{*Static Trial Parameters*}
$KneeOffset =
$AnkleOffset =
```

Marker Set File (.mkr)
(Used for all models)

```
!MKR#2


[Markers]

ASIS        Anterior Superior Iliac Spine
RGTR        Right Greater Trochanter
RPOT        Right Posterior Thigh
RMKJ        Right Medial Knee Joint Line
RLKJ        Right Lateral Knee Joint Line
RPOC        Right Posterior Calf
RMMA                Right Medial Malleolus
RLMA        Right Lateral Malleolus
RLCA        Right Lateral Calcaneous
R5MH        Right 5th Metatarsal Head
R2MH
```

Force1	Force Value of Forceplate
Plate1	COP Value
CenterPlate	Center of the Force Plate
RCKJ	Right Center of the Knee Joint
RANK	Right Ankle Center
RGTRHead	Right Greater Trochanter Head

R2MH,RANK
RANK,RCKJ
RCKJ,RGTRHead
Force1,Plate1

[Segments]

[Force Vectors]

P_ForcePlate1 Base of Plate 1 Vector
F_ForcePlate1 Tip of Plate 1 Vector

[Angles]

RKneeAngles Right Knee Rotation
RAnkleAngles Right Ankle Rotation

[Forces]

RKneeForce Right Knee Resultant Force
RAnkleForce Right Ankle Resultant Force

[Moments]

RKneeMoment Right Knee Resultant Moment
RAnkleMoment Right Ankle Resultant Moment

Massless Model

axislength = 100

{*Start of macro section*}

```
{*=======================*}
Macro REPLACE4(p1,p2,p3,p4)
{*Replaces any point missing from set of four fixed in a

segment*}
s234 = [p3,p2-p3,p3-p4]        {*Defines a segment s234 using

all points except p1*}
p1V = Average(p1/s234)*s234          {*Finds the average position

of p1 in the s234 local Co-ord system and creates virtual

point p1V from this reference system*}
s341 = [p4,p3-p4,p4-p1]                  {*Defines a segment s341 using

all points except p2*}
p2V = Average(p2/s341)*s341          {*Finds the average position

of p2 in the s341 local Co-ord system and creates virtual

point p2V from this reference system*}
s412 = [p1,p4-p1,p1-p2]                  {*Defines a segment s412 using

all points except p3*}
p3V = Average(p3/s412)*s412          {*Finds the average position

of p3 in the s412 local Co-ord system and creates virtual

point p3V from this reference system*}
s123 = [p2,p1-p2,p2-p3]                  {*Defines a segment s123 using

all points except p4*}
p4V = Average(p4/s123)*s123          {*Finds the average position

of p4 in the s123 local Co-ord system and creates virtual

point p4V from this reference system*}
{* Now only replaces if original is missing  11-99 *}
p1 = p1 ? p1V
p2 = p2 ? p2V
p3 = p3 ? p3V
p4 = p4 ? p4V
endmacro

Macro Axes(segment,axislength)
{* This macro creates segment axes for display purposes*}
```

```
segment#o={0,0,0}*segment
segment#x={axislength,0,0}*segment
segment#y={0,axislength,0}*segment
segment#z={0,0,axislength}*segment

output (segment#o,segment#x,segment#y,segment#z)

endmacro

{*Forceplate Data*}
{*===============*}
if EXIST( ForcePlate1 )
        Force1 = ForcePlate1(1)
        Moment1 = ForcePlate1(2)
        Centre1 = ForcePlate1(3)
if ( ABS ( Force1 ) > 10 )
        Point1 = Centre1 + {-Moment1(2)/Force1(3),

                Moment1(1)/Force1(3), -Centre1(3) }
        else
                Point1 = Centre1
        endif
Force1 = Force1 + Point1
        OUTPUT ( Point1, Force1, Centre1 , Moment1 )
endif

{*Define Optional Points*}
{*======================*}
OptionalPoints(RMKJ,RMMA)


{*Define Offset Points*}
{*====================*}
RANK = RLMA+{0,$AnkleOffset,0}
RCKJ = RLKJ+{0,$KneeOffset,0}
RGTRHead = RGTR+{0,$HipOffset,0}

Output(RANK,RCKJ,RGTRHead)

If $Static == 1 Then
        $KneeOffset = DIST(RLKJ,RMKJ)/2
        $AnkleOffset = DIST(RLMA,RMMA)/2
        Param($KneeOffset)
        Param($AnkleOffset)
EndIf
```

```
{*Define Segments*}
{*================*}

{*Foot Segment*}
{*============*}
RFoot = [R5MH,R5MH-RLCA,RCKJ-RANK,xyz]

{*Knee Segment*}
{*============*}
RShank = [RANK,RANK-RLMA,RCKJ-RANK,yxz]

{*Thigh Segment*}
{*============*}
RThigh = [RCKJ,RCKJ-RLKJ,RCKJ-RGTRHead,yxz]

Axes(RThigh,100)
Axes(RShank,100)
Axes(RFoot,100)

{*Anthropometric Data*}
AnthropometricData
RFootAnthro   .0    .0    .0    0
RShankAnthro        .0    .0    .0    0
RThighAnthro  .0    .0    .0    0
EndAnthropometricData

{*Kinetic Hierarchy and Associated Data*}

RThigh=[RThigh,RThighAnthro]
RShank=[RShank,RThigh,RCKJ,RShankAnthro]
RFoot=[RFoot,RShank,RANK,RFootAnthro]

AF=REACTION(RFoot)
KF=REACTION(RShank)
OUTPUT(AF,KF)
GAF=AF*RFoot
GKF=KF*RShank
AnkleForce=GAF(1)
AnkleMoment=GAF(2)
KneeForce=GKF(1)
KneeMoment=GKF(2)
OUTPUT(AnkleForce,AnkleMoment,KneeForce,KneeMoment)
```

Quasi-static Model

```
axislength = 100

{*Start of macro section*}
{*======================*}
Macro REPLACE4(p1,p2,p3,p4)
{*Replaces any point missing from set of four fixed in a segment*}
s234 = [p3,p2-p3,p3-p4]        {*Defines a segment s234 using all points except p1*}
p1V = Average(p1/s234)*s234          {*Finds the average position of p1 in the s234 local Co-ord
system and creates virtual point p1V from this reference system*}
s341 = [p4,p3-p4,p4-p1]              {*Defines a segment s341 using all points except p2*}
p2V = Average(p2/s341)*s341          {*Finds the average position of p2 in the s341 local Co-ord
system and creates virtual point p2V from this reference system*}
s412 = [p1,p4-p1,p1-p2]              {*Defines a segment s412 using all points except p3*}
p3V = Average(p3/s412)*s412          {*Finds the average position of p3 in the s412 local Co-ord
system and creates virtual point p3V from this reference system*}
s123 = [p2,p1-p2,p2-p3]              {*Defines a segment s123 using all points except p4*}
p4V = Average(p4/s123)*s123          {*Finds the average position of p4 in the s123 local Co-ord
system and creates virtual point p4V from this reference system*}
{* Now only replaces if original is missing  11-99 *}
p1 = p1 ? p1V
p2 = p2 ? p2V
p3 = p3 ? p3V
p4 = p4 ? p4V
endmacro

Macro Axes(segment,axislength)
{* This macro creates segment axes for display purposes*}

segment#o={0,0,0}*segment
segment#x={axislength,0,0}*segment
segment#y={0,axislength,0}*segment
segment#z={0,0,axislength}*segment

output (segment#o,segment#x,segment#y,segment#z)

endmacro

{*Forceplate Data*}
{*===============*}
if EXIST( ForcePlate1 )
        Force1 = ForcePlate1(1)
        Moment1 = ForcePlate1(2)
        Centre1 = ForcePlate1(3)
if ( ABS ( Force1 ) > 10 )
        Point1 = Centre1 + {-Moment1(2)/Force1(3),
```

```
                Moment1(1)/Force1(3), -Centre1(3) }
        else
                Point1 = Centre1
        endif
Force1 = Force1 + Point1
        OUTPUT ( Point1, Force1, Centre1 , Moment1 )
endif

{*Define Optional Points*}
{*======================*}
OptionalPoints(RMKJ,RMMA)


{*Define Offset Points*}
{*====================*}
RANK = RLMA+{0,$AnkleOffset,0}
RCKJ = RLKJ+{0,$KneeOffset,0}
R2MH ={R5MH(1),RANK(2),R5MH(3)}

RGTRHead = RGTR+{0,$HipOffset,0}

{*COM for segments*}
comf=(RANK+R2MH)/2
coms=RANK+(RCKJ-RANK)*.567

Output(RANK,RCKJ,RGTRHead,comf,coms)

If $Static == 1 Then
        $KneeOffset = DIST(RLKJ,RMKJ)/2
        $AnkleOffset = DIST(RLMA,RMMA)/2
        Param($KneeOffset)
        Param($AnkleOffset)
EndIf

{*Define Segments*}
{*===============*}

{*Foot Segment*}
{*============*}
RFoot = [R5MH,R5MH-RLCA,RCKJ-RANK,xyz]

{*Knee Segment*}
{*============*}
RShank = [RANK,RANK-RLMA,RCKJ-RANK,yxz]

{*Thigh Segment*}
```

```
{*============*}
RThigh = [RCKJ,RCKJ-RLKJ,RCKJ-RGTRHead,yxz]

Axes(RThigh,100)
Axes(RShank,100)
Axes(RFoot,100)

{*Anthropometric Data*}
AnthropometricData
RFootAnthro   .0   .0   .0   0
RShankAnthro       .0   .0   .0   0
RThighAnthro .0    .0   .0   0
EndAnthropometricData

{*Kinetic Hierarchy and Associated Data*}


footforce=$BodyMass*.0146*9.8
dummyforce={0,0,-footforce}
dummymoment={0,0,0}
dummyapplication={comf(1),comf(2),comf(3)}

reactionforce=|dummyforce,dummymoment,dummyapplication|
LRF=reactionforce/RFOOT
CONNECT(RFOOT,reactionforce,1)


shankforce=$BodyMass*.0465*9.8
dummyforce2={0,0,-shankforce}
dummymoment2={0,0,0}
dummyapplication2={coms(1),coms(2),coms(3)}

reactionforce2=|dummyforce2,dummymoment2,dummyapplication2|
CONNECT(RSHANK,reactionforce2,1)

RThigh=[RThigh,RThighAnthro]
RShank=[RShank,RThigh,RCKJ,RShankAnthro]
RFoot=[RFoot,RShank,RANK,RFootAnthro]

AF=REACTION(RFoot)
KF=REACTION(RShank)
OUTPUT(AF,KF)
GAF=AF*RFoot
GKF=KF*RShank
AnkleForce=GAF(1)
AnkleMoment=GAF(2)
```

```
KneeForce=GKF(1)
KneeMoment=GKF(2)
OUTPUT(AnkleForce,AnkleMoment,KneeForce,KneeMoment)
```

Full Dynamic Model

```
axislength = 100

{*Start of macro section*}
{*======================*}
Macro REPLACE4(p1,p2,p3,p4)
{*Replaces any point missing from set of four fixed in a

segment*}
s234 = [p3,p2-p3,p3-p4]         {*Defines a segment s234 using

all points except p1*}
p1V = Average(p1/s234)*s234           {*Finds the average position

of p1 in the s234 local Co-ord system and creates virtual

point p1V from this reference system*}
s341 = [p4,p3-p4,p4-p1]                   {*Defines a segment s341 using

all points except p2*}
p2V = Average(p2/s341)*s341           {*Finds the average position

of p2 in the s341 local Co-ord system and creates virtual

point p2V from this reference system*}
s412 = [p1,p4-p1,p1-p2]                   {*Defines a segment s412 using

all points except p3*}
p3V = Average(p3/s412)*s412           {*Finds the average position

of p3 in the s412 local Co-ord system and creates virtual

point p3V from this reference system*}
s123 = [p2,p1-p2,p2-p3]                   {*Defines a segment s123 using

all points except p4*}
p4V = Average(p4/s123)*s123           {*Finds the average position

of p4 in the s123 local Co-ord system and creates virtual
```

```
point p4V from this reference system*}
{* Now only replaces if original is missing  11-99 *}
p1 = p1 ? p1V
p2 = p2 ? p2V
p3 = p3 ? p3V
p4 = p4 ? p4V
endmacro

Macro Axes(segment,axislength)
{* This macro creates segment axes for display purposes*}

segment#o={0,0,0}*segment
segment#x={axislength,0,0}*segment
segment#y={0,axislength,0}*segment
segment#z={0,0,axislength}*segment

output (segment#o,segment#x,segment#y,segment#z)

endmacro

{*Forceplate Data*}
{*================*}
if EXIST( ForcePlate1 )
        Force1 = ForcePlate1(1)
        Moment1 = ForcePlate1(2)
        Centre1 = ForcePlate1(3)
if ( ABS ( Force1 ) > 10 )
        Point1 = Centre1 + {-Moment1(2)/Force1(3),

                Moment1(1)/Force1(3), -Centre1(3) }
        else
                Point1 = Centre1
        endif
Force1 = Force1 + Point1
        OUTPUT ( Point1, Force1, Centre1 , Moment1 )
endif

{*Define Optional Points*}
{*======================*}
OptionalPoints(RMKJ,RMMA)


{*Define Offset Points*}
{*====================*}
RANK = RLMA+{0,$AnkleOffset,0}
RCKJ = RLKJ+{0,$KneeOffset,0}
```

```
R2MH ={R5MH(1),RANK(2),R5MH(3)}

RGTRHead = RGTR+{0,$HipOffset,0}

{*COM for segments*}
comf=(RANK+R2MH)/2
coms=RANK+(RCKJ-RANK)*.567

Output(RANK,RCKJ,RGTRHead,R2MH,comf,coms)

If $Static == 1 Then
        $KneeOffset = DIST(RLKJ,RMKJ)/2
        $AnkleOffset = DIST(RLMA,RMMA)/2
        Param($KneeOffset)
        Param($AnkleOffset)
EndIf


{*Define Segments*}
{*===============*}

{*Foot Segment*}
{*============*}
RFoot = [R5MH,R5MH-RLCA,RCKJ-RANK,xyz]

{*Knee Segment*}
{*============*}
RShank = [RANK,RANK-RLMA,RCKJ-RANK,yxz]

{*Thigh Segment*}
{*============*}
RThigh = [RCKJ,RCKJ-RLKJ,RCKJ-RGTRHead,yxz]

Axes(RThigh,100)
Axes(RShank,100)
Axes(RFoot,100)

{*Anthropometric Data*}
AnthropometricData
RFootAnthro  .0145  .50    .475   0
RShankAnthro        .0465  .567   .302   0
RThighAnthro .100   .567   .323   0
EndAnthropometricData

{*Kinetic Hierarchy and Associated Data*}
```

```
RThigh=[RThigh,RThighAnthro]
RShank=[RShank,RThigh,RCKJ,RShankAnthro]
RFoot=[RFoot,RShank,RANK,RFootAnthro]

AF=REACTION(RFoot)
KF=REACTION(RShank)
OUTPUT(AF,KF)
GAF=AF*RFoot
GKF=KF*RShank
AnkleMoment=GAF(2)
KneeMoment=GKF(2)
OUTPUT(AnkleMoment,KneeMoment)
```

APPENDIX D

BODYBUILDER CODE FOR CHAPTER 4

Model Parameter File (.mp)

```
{*WaveDisk.mp*}
{*Written by Jerrod Braman*}

{*For use with WaveDisk.mod and WaveDisk.mkr*}

{*All Distance measurements in millimeters*}
{*All angles in degrees*}
{*All mass in kilograms*}

{*General Parameters*}
{*==================*}
```

Marker Set File (.mkr)

```
!MKR#2

[Markers]

Heel1   Top Heel
Heel2   Center Heel
Heel3   Right Heel

Toe1    Top Toe
Toe2    Center Toe
Toe3    Right Toe

Heel1,Heel2
Heel2,Heel3
Toe1,Toe2
Toe2,Toe3
```

Biomechanical Model File (.mod)

```
{*WaveDisk Analysis Model*}
{*Orthopaedic Biomechanics Laboratories -- Gait Analysis Laboratory*}
{*Written by Jerrod Braman*}

{*Use with BodyBuilder*}
{*Use with WaveDisk.mkr*}
{*Use with WaveDisk.mp*}

axislength = 100

Macro Axes(segment,axislength)
```

```
{* This macro creates segment axes for display purposes*}

segment#o={0,0,0}*segment
segment#x={axislength,0,0}*segment
segment#y={0,axislength,0}*segment
segment#z={0,0,axislength}*segment

output (segment#o,segment#x,segment#y,segment#z)

endmacro

{*Define Segments*}
{*================*}

{*Heel Segment*}
{*=============*}
Heel = [Heel2,Heel3-Heel2,Heel1-Heel2,yxz]

{*Toe Segment*}
{*=============*}
Toe = [Toe2,Toe3-Toe2,Toe1-Toe2,yxz]

{*Global Segment*}
GlobalO={0,0,0}
Globalx={100,0,0}
Globaly={0,100,0}
Global=[GlobalO,Globalx-GlobalO,GlobalO-Globaly,xzy]

OUTPUT(GlobalO,Globalx,Globaly)

Axes(Heel,100)
Axes(Toe,100)
Axes(Global,100)

{*Angle Calculations*}

ToeAngle=<Toe,Global,xyz>
HeelAngle=<Heel,Global,xyz>

OUTPUT(ToeAngle,HeelAngle)
```

APPENDIX F

OTHER BIOMECHANICAL PROJECTS

Ph.D. Project

Biomechanical comparison of three methods of back squatting
Adam Bruenger, Ph.D. – 2009

M.S. Projects

An analysis of pressure distribution with a prefabricated foot orthotic on a symptomatic population
B.J. Vascik, M.S. – 2006

The difference in immediate changes in dorsiflexion range of motion using an ultrasound heat treatment, followed by two different stretching techniques
Gregory Hawthorne, Jr., M.S., ATC – 2008

A comparison of the effects of joint mobilizations versus muscle energy on increasing shoulder range of motion in healthy individuals
Anna Leyland, M.S. – 2009

Assisted in designing and manufacturing data collection device and data collection

Wolverine World Wide, Incorporated Projects

Parotec In-shoe Pressure Measurement System

Thermal Footwear Characteristics (Subject and Mechanical Testing)

Compression Testing (Instron)

Impact Testing (ASTM Drop Test)

Flexion Testing

Force Plate Testing

Vicon Motion Analysis

Wound Healing Shoe Project

Evaluated a would healing shoe using the Parotec In-shoe Pressure Measurement System